Mechanisms and factors determining DSB repair pathway choice in G2

Vom Fachbereich Biologie der Technischen Universität Darmstadt

zur

Erlangung des akademischen Grades

eines Doctor rerum naturalium

(Dr. rer. nat.)

genehmigte Dissertation von

Dipl.-Biol. Christian Reul

aus Frankfurt am Main

Darmstadt 2014

D17

Referent: Prof. Dr. Markus Löbrich
Koreferent: Prof. Dr. Bodo Laube

Tag der Einreichung: 06.02.2014
Tag der mündlichen Prüfung: 23.04.2014

Ehrenwörtliche Erklärung

Ich erkläre hiermit ehrenwörtlich, dass ich die vorliegende Arbeit entsprechend den Regeln guter wissenschaftlicher Praxis selbstständig und ohne unzulässige Hilfe Dritter angefertigt habe.

Sämtliche aus fremden Quellen direkt oder indirekt übernommenen Gedanken sowie sämtliche von Anderen direkt oder indirekt übernommenen Daten, Techniken und Materialien sind als solche kenntlich gemacht. Die Arbeit wurde bisher bei keiner anderen Hochschule zu Prüfungszwecken eingereicht.

Darmstadt, den 24. April 2014

Index

1 List of abbreviations

53BP1	p53 binding protein 1
ATM	Ataxia telangiectasia mutated
ATMi	specific ATM inhibitor
ATR	ATM and Rad3 related
bp	basepair
BrdU	5-Bromo-2‘-desoxy-uridine
BSA	bovine serum albumine
CDK	cyclin-dependent kinase
CHK	checkpoint kinase
CK2	caseine kinase 2
CoIP	coimmunprecitpitation
DMEM	Dulbecco´s minimal essential medium
DMSO	dimethyl sulfoxide
DNA	desoxyribonucleic acid
DNA-PK	DNA-dependent Protein kinase
DNA-PK$_{cs}$	catalytic subunit of DNA-PK
DNA-PKi	specific DNA-PK$_{cs}$ inhibitor
DSB	DNA double strand break
dsDNA	double stranded DNA
EDTA	Ethylenediaminetetraacetic acid
EdU	5-Ethylene-2’-desoxy-uridine
ERCC	excision repair cross complementation group
FACS	fluorescence activated cell scanner
FCS	fetal calf serum
Gy	Gray
HR	homologous recombination
HP1	heterochromatin protein 1
IP	immunoprecipitation
IR	ionizing radiation
KAP-1	KRAB associated protein 1

kDa	kilodalton
MDC1	mediator of DNA damage checkpoint protein 1
MNase	micrococcal nuclease
Mre11	meiotic recombination 11
MRN	MRE11/RAD50/NBS1-complex
NBS1	Nijmegen breakage syndrome 1
NEAA	non essential amino acids
NHEJ	non homologous end-joining
PAGE	polyacrylamide gel electrophoresis
PBS	phosphate buffered saline
PIKK	Phosphatidylinositol 3-kinase-related kinases
RAD	radiation repair protein
RMI	RecQ-mediated genome instability
RNA	ribonucleic acid
RNF	RING-finger-containing nuclear factor
RPA	Replication protein A
rpm	rounds per minute
RT	room temperature
SDS	sodium dodecyl sulfate
ssDNA	single-stranded DNA
SUMO	small ubiquitin-related modifier
U	unit
UV	ultraviolet
V(D)J	variable (diversity) joining
WB	Western Blot
WT	wildtype
XLF	XRCC4 like factor
XPF	xermoderma pigmentosum complementation group F
XRCC	X-ray repair cross-complementing protein

2 Summary

Aim of this work was to investigate the interplay between the different DNA double-strand break (DSB) repair pathways during the G2 phase of the cell cycle. In G2, DSBs which are located in euchromatic regions are repaired with fast kinetics via canonical NHEJ (c-NHEJ), whereas heterochromatic DSBs are repaired with slow kinetics via homologous recombination (HR). C-NHEJ comprises a ligation of both DSB ends without the requirement of sequence homology. HR is a repair pathway, where the DSB ends are resected to produce ssDNA that invades the sister chromatid and uses the sequence as a template for error-free repair. If cells are deficient in the HR core factors BRCA2 or RAD51, the DSBs are resected but remain unrepaired. This can lead to genomic instability, less cell survival and cancer.

The presence of ssDNA itself might explain why c-NHEJ does not repair resected DSBs in a BRCA2 deficient cell to prevent an accumulation of unrepaired DSBs. But an alternative NHEJ (alt-NHEJ) process is described, which uses microhomologies within the ssDNA to ligate both resected DSB ends. Therefore we sought to further characterize resected DSBs in G2 and observed an ATM release at resected DSBs. In G1, ATM is assembled at DSBs and facilitates the repair of heterochromatic DSBs by heterochromatin relaxation due to the phosphorylation of the heterochromatin building factor KAP-1. Contrary to G1, in G2 is ATM needed to initiate resection but is dispensable for later stages of HR. A permanent heterochromatin relaxation by downregulation of KAP-1 or expression of a phosphomimic form of KAP-1 allows the repair of resected DSBs in BRCA2- or RAD51-deficient cells by error-prone alt-NHEJ. Moreover, in HR proficient cells a KAP-1 depletion causes a switch from HR to alt-NHEJ repair, too.

We support a model, where the heterochromatin is initially relaxed, but after extended resection, the heterochromatin is reconstituted due to the release of ATM and the dephosphorylation of KAP-1. The restored heterochromatin structure now facilitates error-free HR and prevents the usage of error-prone alt-NHEJ.

Secondarily, we investigated the mechanistic reason of the ATM release at resected DSBs. The cascade of the assembly of ATM at DSBs involves first the phosphorylation of H2AX by ATM itself and the binding of MDC1 to this phosphorylation. ATM phosphorylates MDC1 to allow the binding of the ubiquitin ligase RNF8, which together with RNF168, ubiquitinates

the histone H2A/H2AX and the demethylase JMJD2A. JMJD2A is bound at H4K20me2 and degraded after its ubiquitination. After the degradation of JMJD2A, 53BP1 has the ability to bind H4K20me2 that in turn allows the assembly of ATM at the DSB site.

We were able to show that at resected DSBs, 53BP1 is released and RNF8/168 actity is decreased, whereas H2AX phosphorylation and MDC1 binding are not affected. A switch from ATM to ATR activity at resected DSBs allows H2AX phosphorylation and MDC1 binding. But ATR cannot phosphorylate MDC1, so RNF8/168 activation is impaired. Without the RNF8/168 activity, 53BP1 cannot bind H4K20me2 and assemble ATM at the resected break. This leads to a heterochromatin reconstitution, which facilitates HR and prevents alt-NHEJ.

A co-depletion of JMJD2A and JMJD2B is described to allow 53BP1 binding in RNF8/168 deficient cells. This co-depletion or using a phosphomimic form of MDC1, which mimics a permanent phoshporylation to allow RNF8/168 activity at resected DSBs, allows the repair of heterochromatic DSBs in BRCA2-deficient cells. We suggest that under such conditions cells switch to alt-NHEJ instead of using HR, equal to a KAP-1 knockdown.

In summary, our results provide a model where the resection is the most important step of the HR process, which determines the repair of a heterochromatic DSB to HR and exclude end-joining repair: not the resection *per se*, but rather the heterochromatin reconstitution in consequence of ATM release at resected DSBs. ATM is released due to the inability of ATR to phosphorylate MDC1to trigger RNF8/168 activition. We suggest that without RNF8/168 activity, JMJD2A replaces 53BP1 at resected DSBs. Without 53BP1, ATM is released and the heterochromatin structure is reconstituted.

Ziel dieser Arbeit war es, das Zusammenspiel der verschiedenen DSB-Reparaturwege in der G2-Phase des Zellzykluses zu untersuchen. In der G2-Phase werden euchromatische DSBs mit schneller Kinetik über das kanonische NHEJ (c-NHEJ) repariert, während heterochromatische DSBs mit langsamer Kinetik über HR repariert werden. Das c-NHEJ beinhaltet eine sequenzunabhängige Ligation der DSB-Enden. Die HR hingegen ist ein Reparaturweg, bei dem die DSB-Enden erst resektiert werden, um einzelsträngige DNA-Bereiche freizulegen, welche dann im Anschluss in das Schwesterchromatid einwandern und dessen homologe Sequenz als Vorlage für eine fehlerfreie Reparatur verwende wirdt.

In Zellen, welche in den HR-Kernfaktoren BRCA2 oder RAD51 defizient sind, verbleiben die resektierten DSBs unrepariert. Dies kann zu genomischer Instabilität, geringerem Zellüberleben bis hin zur Krebsentstehung führen.

Die Präsenz einzelsträngiger DNA an sich könnte erklären, warum resektierte DSBs in BRCA2-defizienten Zellen nicht über c-NHEJ reparieren werden, um eine Akkumulation unreparierter DSBs zu verhindern. Es ist allerdings ein alternativer NHEJ (alt-NHEJ)-Reparaturweg beschrieben, welcher Mikrohomologien innerhalb einzelsträngiger DNA nutzen kann, um die resektierten DSB-Enden zu ligieren. Daher wurden diese resektierten DSBs in der G2-Phase von uns genauer untersucht und wir konnten ein Ablösen von ATM an diesen resektierten DSBs beobachten. In der G1-Phase akkumuliert ATM an DSBs und fördert die Reparatur heterochromatischer DSBs durch eine Relaxation des Heterochromatins aufgrund einer Phosphorylierung des Heterochromatin-bildenden Faktors KAP-1. Im Gegensatz zur G1-Phase wird in der G2-Phase ATM benötigt, um die Resektion zu initiieren, während es für spätere Schritte der HR verzichtbar ist. Eine permanente Heterochromatin-Relaxation mit Hilfe einer KAP-1-Depletion oder der Expression einer dauerhaft phosphorylierten Form von KAP-1 erlaubt die Reparatur resektierter DSBs in BRCA2- oder RAD51-defizienten Zellen über das alt-NHEJ. Desweiteren führt eine KAP-1-Depletion in HR-profizienten Zellen ebenfalls zu einem Wechsel von HR zu alt-NHEJ.

Wir schlagen ein Modell vor, in dem das Heterochromatin initial relaxiert wird, aber nach einer ausgedehnten Resektion die Heterochromatinstruktur als Folge der ATM-Ablösung vom Chromatin und der darauf folgenden KAP-1-Dephosphorylierung wiederhergestellt wird.

Desweiteren wurde der mechanistische Grund für das Ablösen von ATM an resektierten DSBs untersucht. Die Kaskade der ATM-Akkumulierung an DSBs beinhaltet zuerst eine

Phosphorylierung von H2AX durch ATM und der Bindung von MDC1 an diese Phosphorylierung. Danach phosphoryliert ATM MDC1, um die Bindung der Ubiquitinligase RNF8 zu erlauben, welche zusammen mit RNF168 die Histone H2A/H2AX und die Demethylase JMJD2A ubiquitiniert. JMJD2A bindet normalerweise an H4K20me2 und wird nach seiner Ubiquitinierung abgebaut. Nach dem Abbau von JMJD2A kann 53BP1 an H4K20me2 binden, was wiederum die Akkumulierung von ATM am DSB fördert.

Es konnte gezeigt werden, dass an resektierten Brüchen 53BP1 abgelöst wird und die Aktivität von RNF8/168 verringert ist, während die H2AX-Phoshporylierung und MDC1-Bindung nicht beeinträchtigt ist. Ein Wechsel von einer ATM- zu einer ATR-Aktivität an resektierten DSBs erlaubt weiterhin eine H2AX-Phosphorylierung und MDC1-Bindung. Allerdings kann ATR MDC1 nicht phosphorylieren, wodurch die RNF8/168-Aktivität beeinträchtigt wird. Ohne RNF8/168-Aktivität kann 53BP1 nicht an H4K20me2 binden, um ATM an resektierten DSBs zu akkumulieren. Dies führt zu einer Rekonstitution der Heterochromatinstruktur, welche HR fördert und dadurch die Reparatur über alt-NHEJ verhindert.

Es ist bekannt, dass eine Co-Depletion von JMJD2A und JMJD2B die 53BP1-Bindung in RNF8/168 defizienten Zellen erlaubt. Diese Depletion oder das Verwenden einer dauerhaft phosphorylierten Formvon MDC1, was eine RNF8/168-Aktivität an resektierten DSBs ermöglicht, erlaubt die Reparatur heterochromatischer DSBs in BRCA2-defizienten Zellen. Unter diesen Umständen scheinen die Zellen anstatt HR zu verwenden, in alt-NHEJ zu wechseln, ähnlich wie nach einer KAP-1-Depletion.

Zusammengefasst unterstützen unsere Ergebnisse ein Modell, in dem die Resektion der wichtigste Schritt des HR-Prozesses ist, welcher die Reparatur heterochromatischer DSBs für HR determiniert und alt-NHEJ ausschließt: nicht die Resektion *per se*, sondern die Rekonstitution des Heterochromatins als Konsequenz des Ablösens von ATM an resektierten DSBs. ATM wird abgelöst, da ATR nicht in der Lage ist MDC1 zu phosphorylieren, um RNF8/168 zu aktivieren. Vermutlich wird ohne RNF8/168-Aktivität JMJD2A das gebundene 53BP1 an resektierten DSBs ersetzen. Ohne diese 53BP1-Bindung wird ATM abgelöst und die Heterochromatinstruktur wiederhergestellt.

3 Introduction

The genetic information of all organisms is encoded in the deoxyribonucleic acid (DNA), but endogenous and exogenous factors can harm the genomic integrity. Reactive oxygen species, a side product of the respiratory chain, replication errors or mistakes in meiosis are endogenous factors which can damage the DNA. Exogenous factors are ultraviolet (UV) radiation, ionizing radiation (IR), different chemicals or chemotherapeutic agents like methylmethanulfonate. Depending on the inducing agent, the quality of DNA damage differs. Nucleobases can become lost or chemically altered, or the phosphate backbone can be broken, which leads to single-strand breaks (SSBs) or the most severe DNA damage, the DNA double-strand break (DSB). All DNA damages can cause cell death or degeneration, which in turn can lead to cancer or other severe diseases. To protect themselves from degeneration, mammalian cells have developed different mechanisms to handle DNA damage. The important mechanisms are DNA damage recognition and repair, cell cycle control and programmed cell death (apoptosis).

3.1 Physical basics of DSB induction

In our laboratory, DSBs were induced by X-ray irradiation. X-rays are electromagnetic waves which consist of packages of energy, called photons. Photons can interact with electrons in the electron shell of the molecules, whereby the energy of a photon is transferred to the interacting electron in form of kinetic energy. The electron leaves the electron shell and the molecule is ionized. If the full energy of the photon is transferred to the electron, the effect is called Photo-effect. The effect is called Compton-effect, if the photon deposits only a part of its energy. Appearance of both effects depends on the energy of the photon, whereas lower energetic photons preferably interact via Photo-effect and higher energetic photons preferably interact via Compton-effect (Hall and Giccia 2006).

IR can interact with DNA directly and indirectly. A photon can ionize the DNA molecule directly, if the phosphate backbone is ionized by the photon, which causes a SSB. More common is the ionization of a water molecule by a photon. A product of this ionization is a

hydroxyl radical which can react with the phosphate backbone of the DNA and cause a SSB. Two SSBs in spatial proximity result in one DSB.

The number of DNA damage events is dose dependent. 1 Gy X-ray causes 1000-2000 base damages, 600-1000 SSBs and 16-40 DSBs (Ward 1988).

3.2 Cellular response to DSBs

Cells developed various mechanisms to respond to DSBs which include DSB recognition and repair and cell cycle checkpoints. To regulate the different mechanisms, the involved factors are modified. The most common modifications are phosphorylation, acetylation, methylation and ubiquitination. During the DNA damage response (DDR) phophorylation is the favored modification and mostly mediated by the phosphatidylinositol 3-kinase-related kinases (PIKK) ATM, ATR and DNA-PK_{cs}.

Many repair factors and mediators, which accumulate at the damage sites, can form IR induced foci (IRIF). These foci can be detected and analyzed by microscopic analyses.

3.2.1 DSB recognition and signal amplification

After DSB induction, a complex of MRE11, NBS1, and RAD50 (MRN) recognizes free DNA ends and binds to them (de Jager et al. 2001). The major DDR kinase ATM is activated by an interaction with NBS1, but it is also described, that an activation of ATM can occur by chromatin changes due to the presence of a DSB (You et al. 2005; Kaidi and Jackson 2013). The inactive ATM forms a dimer in unirradiated cells and is activated by an autophosphorylation at serine 1981, which causes dissociation and monomerization and initiates intracellular ATM activity (Bakkenist and Kastan 2003). The function of active ATM can be divided in two interlinked sets of responses: on the one hand the diffusible function within the nucleus and the cytoplasm, for example cell cycle control. On the other hand ATM has a chromatin-based function at the DSB site to promote the DDR (Panier and Durocher 2013). Therefore, ATM phosphorylates the histone variant H2AX on serine 139 to form γH2AX within a region of megabasepairs surrounding the DSB site (Rogakou et al. 1998). In

ATM deficient cells DNA-PK_{cs} can take on the task of ATM in phosphorylating H2AX, but DNA-PK_{cs} is not as efficient as ATM (Savic et al. 2009). Thereafter, the mediator protein MDC1 binds directly at the phosphorylated serine 139 of γH2AX (Stucki et al. 2005). MDC1 itself is constitutively phosphorylated by CK2 at serine-aspartate-threonine (SDT) repeats within its N-terminus to allow binding of NBS1 (Melander et al. 2008). The result of this interaction is a simultaneous recruitment of MDC1 and the MRN complex. The MDC1 bound MRN complex activates additional ATM, which phosphorylates neighboring H2AX to expand the γH2AX focus at the DSB site.

Beside the γH2AX focus expansion, ATM also phosphorylates MDC1 on its T-Q-X-F cluster to enhance the binding of the E3-ubiquitin ligase RNF8 (Kolas et al. 2007; Mailand et al. 2007). RNF8 ubiquitinates H2A and H2AX, amongst others, on lysine 63 (K63) and this ubiquitin is recognized and expanded by another E3-ubiquitin ligase, named RNF168 (Mailand et al. 2007; Doil et al. 2009; Mattiroli et al. 2012). Additionally to the H2A/H2AX ubiquitination, RNF8 and RNF168 ubiquitinate the factors JMJD2A and L3MBTL1 so that these factors are degraded by the proteasome.(Acs et al. 2011; Mallette et al. 2012). JMJD2A and L3MBTL1 normally bind to the mono- or dimethylated lysine 20 on histone 4(H4K20me1/2), but after their removal the DSB repair mediator 53BP1 can bind to H4K20me1/2 (Botuyan et al. 2006; Lee et al. 2010). However, the H2A/H2AX ubiquitination by RNF8 and RNF168 is also essential for 53BP1 recruitment to DSB sites (Mattiroli et al. 2012). It is still unclear how both mechanisms are balancend and regulated.

After 53BP1 recruitment to DSB sites it interacts with the MRN complex to bind and fix ATM to the chromatin, because 53BP1 is essential for pATM focus formation in G1-phase cells (Lee et al. 2010; Noon et al. 2010). The chromatin bound ATM facilitates repair by phosphorylation of repair factors and chromatin remodelers.

Recent publications have shown, that during repair the recruitment and retention of repair factors and mediators, for example 53BP1, change at the DSB site (Chapman et al. 2012; Geuting et al. 2013; Kakarougkas et al. 2013).

3.2.2 Repair of IR-induced DSBs

DSBs are the most severe DNA lesion. Therefore the repair of the DSBs has a high priority within the cell. The two main DSB repair pathways are canonical non-homologous end-joining (c-NHEJ) and homologous recombination (HR) (van Gent and van der Burg 2007; Mazon et al. 2010). For IR induced DSBs in mammalian cells, c-NHEJ represents the major repair pathway, which acts in all cell cycle phases (Rothkamm et al. 2003). HR acts only in late S- and G2-phase of the cell cycle, because HR needs a homologous template for repair (Rothkamm et al. 2003). If cells are deficient in core factors of c-NHEJ, DSBs can also be repaired by an alternative end-joining pathway (Mladenov and Iliakis 2011).

The repair of IR induced DSBs exhibits a biphasic kinetic in G1 and G2: a fast component, where the majority of the DSBs are repaired in the first hours and a slow component, where the breaks are repaired up to days (Riballo et al. 2004; Beucher et al. 2009). It is also described, that the fast component represents the repair of euchromatic DSBs, which are repaired by c-NHEJ in G1 and G2 (Goodarzi et al. 2008; Beucher et al. 2009). The slow component represents the repair of heterochromatic DSBs, which are repaired by c-NHEJ in G1 and HR in G2 (Goodarzi et al. 2008; Beucher et al. 2009; Noon et al. 2010). One reason for the different kinetics of c-NHEJ in G1 is that heterochromatic DSBs need additional chromatin modifications to allow repair, which are not required for the repair of euchromatic DSBs (Goodarzi et al. 2008; Noon et al. 2010).

3.2.2.1 Canonical-NHEJ

In principle, c-NHEJ is a ligation of two DSB ends without the necessity of homologous areas (Fig. 1). C-NHEJ is initiated by the binding of a heterodimer of KU70 and Ku80 (Ku70/80), which forms a ring structure to thread on dsDNA without sequence specifity (Walker et al. 2001). The two major roles of the Ku70/80 heterodimer are protecting the dsDNA ends against nucleolytic degradation and recruiting DNA-PK_{cs} to form an active DNA-PK holoenzyme (Gell and Jackson 1999; Singleton et al. 1999; Goodarzi and Jeggo 2013). The DNA-PK_{cs} tethers the DNA ends to avoid misrejoining events (DeFazio et al. 2002). Moreover, an DNA-PK_{cs} autophosphorylation *in trans* brings the two sides of a DSB together

and facilitates DNA-PK dissociation to allow ligation (Meek et al. 2007; van Gent and van der Burg 2007). The final step is the ligation of DNA ends by the c-NHEJ specific DNA ligase IV (Wilson et al. 1997). DNA ligase IV forms a complex with XRCC4 and XLF, where XRCC4 and XLF are proposed to align DNA ends to promote ligation (Hammel et al. 2011). An absence or defect of DNA ligase IV or XRCC4 leads to minimal c-NHEJ efficiency and is embryonic lethal in mice (Barnes et al. 1998; Frank et al. 1998). XLF deficiency leads to minimal c-NHEJ efficiency and radiosensitivity, but is not embryonic lethal (Zha et al. 2007).

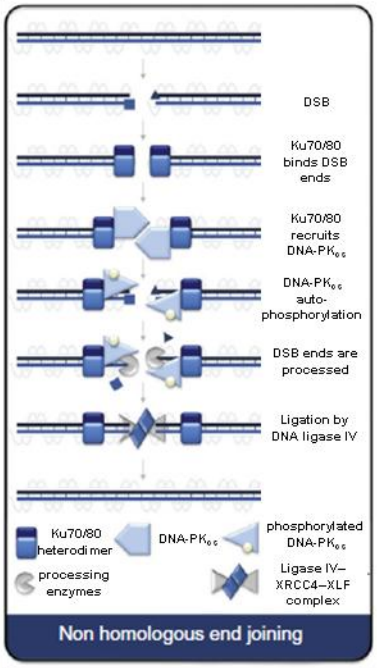

Figure 1: canonical-NHEJ

Ku70/80 heterodimer binds DNA ends, recruits DNA-PK_{cs} to generate the DNA-PK holoenzyme. After DNA-PK autophosphorylation a complex involving DNA ligase IV, XRCC4 an XLF ligates the DNA ends.

(modified from Goodarzi and Jeggo 2013)

3.2.2.2 Homologous Recombination

HR is an error-free repair process and can be divided into three well described steps: DSB end-resection to generate ssDNA, formation of heteroduplex DNA to copy the missing sequences and resolution of the generated Holliday junctions (Fig. 2).

DSB end-resection comprises two steps: an initial resection mediated by MRE11 and CtIP and an elongation step involving EXO1 and BLM (Mimitou and Symington 2009). The initiation of DSB end-resection is controlled by ATM, which phosphorylates and activates CtIP after DSB induction (Sartori et al. 2007; Shibata et al. 2011). RPA immidiately binds to ssDNA to prevent formation of secondary structures and it is replaced by RAD51 in a

BRCA2 dependent manner (Chen et al. 2013; Daley et al. 2013). The RAD51-nucleoproteinfilament invades the sister chromatid and searches for homologous sequences. Using the sister chromatid as a template, the DNA strand is elongated by DNA polymerases. At last, the formed Holliday junctions, generated by strand invasion, are dissolved. This occurs either by dissolution, which does not create sister chromatid exchanges and is mediated by the BTR-complex (BLM, Top3α, RMI) and resolution, which can potentially lead to sister chromatid exchanges and is mediated by different resolvases (Wu and Hickson 2003; Wyatt et al. 2013).

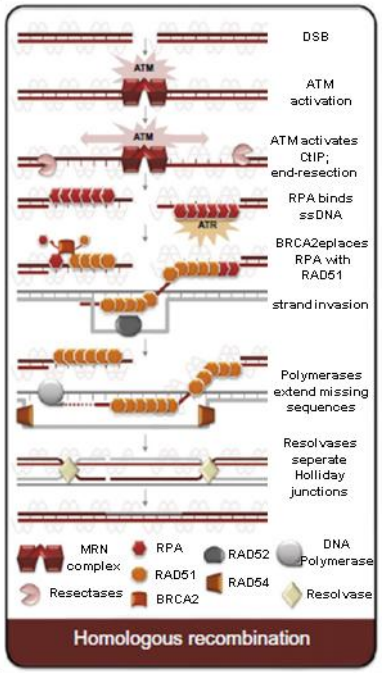

Figure 2: Homologous recombination

Resection is initiated by MRN and CtIP and elongated by Exo1 and BLM. The generated ssDNA is bound by RPA and replaced by RAD51. The RAD51-nucleoproteinfilament invades the sister chromatid and DNA polymerases extend missing sequences. Finally, Holliday junctions are resolved, which can potentially lead to sister chromatid exchanges.

(modified from Goodarzi and Jeggo 2013)

A deficiency in one of the HR factors RAD51 or BRCA2 leads to unrepaired DSBs, whereas a deficiency of one of the end-resection factors, like CtIP, does not lead to unrepaired DSBs (Beucher et al. 2009).

3.2.2.3 Alternative end-joining

DSB repair in cell extracts of cells deficient in the c-NHEJ core factor Ku80 provided evidence of an alternative end-joining (alt-NHEJ) process (Feldmann et al. 2000). But the

classification of this pathway or different subpathways is not clear and confusing. In general, alt-NHEJ, which is also called backup-NHEJ (B-NHEJ), because wiltype cells prevent this repair pathway, does not use c-NHEJ factors. But it involves the factors PARP1, XRCC1, DNA ligase I or III (Wang et al. 2006; Corneo et al. 2007; Iliakis 2009; Della-Maria et al. 2011; Mladenov and Iliakis 2011; Simsek et al. 2011). It was also shown, that Ku70 deficient cells show an elevated level of chromosomal translocations and repair junctions display nucleotide deletions and overlapping microhomologies of 3-16 nucleotides (Boulton and Jackson 1996; Weinstock et al. 2007). Thus, it is supposed, that these DSBs are repaired by using microhomologies from the same or a different chromosome to tether the ends. This repair pathway is called microhomolgy mediated end-joining (MMEJ), which is sometimes used equal to alt-NHEJ (McVey and Lee 2008). Mechanistically, MMEJ starts with a resection step via the MRN complex, CtIP and EXO1 (Decottignies 2007; Bennardo et al. 2008; Della-Maria et al. 2011). After the resection, the exposed microhomolgies anneal and form an intermediate, which tethers both DNA ends (McVey and Lee 2008). Overhanging DNA is removed by the specific endonuclease XPF-ERCC1 and DNA strands are ligated by DNA ligase III (Ahmad et al. 2008; Simsek et al. 2011). Contradictory to the declaration, MMEJ and alt-NHEJ are identical.

Another mechanism of DSB annealing independent of pre-existing microhomolgies by alt-NHEJ is described (Simsek et al. 2011). This mechanism comprises an elongation of the 3’ end of one DSB site to the ssDNA on the other site by a polymerase to generate microhomolgies to tether the ends. After filling of the gaps, the ligation is performed by the DNA ligase I (Simsek et al. 2011). The different pathways and nomenclatures of alt-NHEJ are subject of current research and scientific discussion.

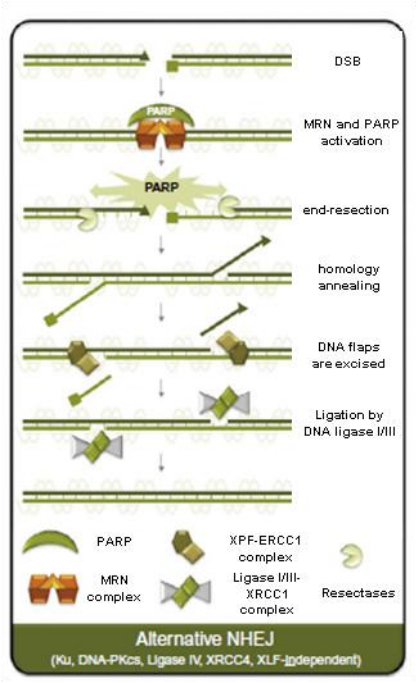

Figure 2: alternative-NHEJ

Alt-NHEJ is used in the absence of Ku, DNA ligase IV or XRCC4. Resection is initiated by MRN, CtIP and Exo1. By using microhomologies both DNA sites are annealed, overhanging DNA is removed by XPF-XRCC1, and the DNA strands are ligated by DNA ligase III or I.

(modified from Goodarzi and Jeggo 2013)

We were recently able to show that alt-NHEJ can back-up for HR after resection has taken place (Geuting et al. 2013). The requirement of this back-up function of alt-NHEJ is a relaxed heterochromatin structure, which is suppressed in wild type cells.

3.2.3 Heterochromatin and DSB repair

15-20 % of the chromatin within a nucleus is heterochromatic. DSBs induced by IR are randomly distributed in the nucleus, so that also 15-20 % of the DSBs are located in heterochromatic regions (Goodarzi et al. 2008). In G1 and G2, these DSBs are repaired with slow kinetics in an ATM-dependent manner (Goodarzi et al. 2008; Beucher et al. 2009). ATM is needed to allow efficient repair by modifying the heterochromatin structure (Ziv et al. 2006; Goodarzi et al. 2008). In G2, ATM is also needed to modify the chromatin but it has a secondary role in the initiation of the resection step of HR (Beucher et al. 2009).

Heterochromatin is a highly condensed structure , containing repetitious sequences and is mainly located at centromeric or telomeric regions (Grewal and Elgin 2007). An important player in heterochromatin organization is the heterochromatin building factor KAP-1, which acts as a scaffold for different chromatin remodelers (Xiao et al. 2011). On the one side,

KAP-1 interacts with HP1 which interacts with trimethylated lysine 9 on histone 3 (H3K9me3) to link HP1 and KAP1 to the chromatin. On the other side, it interacts via a sumoylation on lysine 804 with CHD3, a subunit of the nuclear remodeling and deacetylase (NuRD) complex (Ryan et al. 1999; Goodarzi et al. 2011). The NuRD complex has been described to be involved in chromatin organization, regulation of gene transpriction, genomic stability and developmental signaling. The NuRD complex consists 4 noncatalytic two catalytic active subunits: a ATPase (CHD3) for nucleosome repositioning and a histone deacetylase (HDAC1 or HDAC2) (Allen et al. 2013).

ATM phosphorylates KAP-1 on serine 824 after DSB induction and this phosphorylation competes with the sumyolation on lysine 804 and causes a removal of the CHD3/NuRD complex (Goodarzi et al. 2011). A result of the KAP-1 phosphorylation on serine 824 and the following CHD3/NuRD complex removal is a relaxation of the heterochromatin structure (Ziv et al. 2006; Goodarzi et al. 2011). This relaxation has been shown to be a prerequisite to the repair of heterochromatic DSBs by c-NHEJ in G1 cells (Goodarzi et al. 2008). In our study, we were able to show that in G2-phase cells, the heterochromatin is also relaxed due to ATM dependent KAP-1 phosphorylation after irradiation, but it is recondensed after the resection, due to an ATM release from chromatin. This facilitates DSB repair by HR and excludes error-prone alt-NHEJ (Geuting et al. 2013).

3.2.4 Cell cycle checkpoints

Cells have evolved different checkpoints within the cell cycle to stop cell cycle progression after DNA damage and allow the cell to complete DNA repair. The most important are the G1/S checkpoint, to prevent transition into S-Phase with DNA damage, and the G2/M checkpoint, to prevent a cell division with unrepaired DSBs.

The transition from G1- into S-phase is regulated by CyclinD/CDK4/6 and CyclinE/CDK2 complexes (Koff et al. 1992; Blomen and Boonstra 2007). Two different pathways are described to prevent S-phase entry. After DSB induction, ATM phosphorylates and activates CHK2 (Kastan and Lim 2000). In one of the two pathways ATM and CHK2 phosphorylate and activate p53. Active p53 stimulates a p21-dependent inhibition of the CDKs 2, 4 and 6. In

the other pathway, CHK2 phosphorylates and deactivates the phosphatase CDC25A, which normally removes inhibitory phosphates from CDK2 (Iliakis et al. 2003; Deckbar et al. 2011).

Mitosis is initiated by a complex of CyclinB1 and CDK1. In G2, ATM is activated from "blunt" DSBs and ATR from resected DSB ends (Shiotani and Zou 2009). ATM phosphorylates mainly CHK2 and ATR phosphorylates mainly CHK1. Activated CHK1 and CHK2 phosphorylate CDC25 to prevent the removal of the inhibitory phosphate on CDK1 by CDC25. By this removal, the G2 checkpoint is activated with very fast kinetics (Deckbar et al. 2011). One limitation of the G2/M checkpoint is that cells are released from the G2/M checkpoint with incomplete repair and enter mitosis with up to 20 DSBs (Deckbar et al. 2007). The mechanistic reason of this limitation is still unclear.

4 Manuscript: ATM release at resected double-strand breaks provides heterochromatin reconstitution to facilitate homologous recombination (published on 1st of August 2013 in PLOS Genetics)

ATM release at resected double-strand breaks provides heterochromatin reconstitution to facilitate homologous recombination

Verena Geuting[1,2], Christian Reul[1,2] and Markus Löbrich[1]

[1]Darmstadt University of Technology, Radiation Biology and DNA Repair,
64287 Darmstadt, Germany

[2]These authors contributed equally

Running title:
Heterochromatin promotes homologous recombination
Keywords:
KAP-1; heterochromatin; double-strand break repair; pathway choice; homologous recombination; non-homologous end-joining; ATM

4.1 Abstract

Non-homologous end-joining (NHEJ) and homologous recombination (HR) represent the two main pathways for repairing DNA double-strand breaks (DSBs). During the G2 phase of the mammalian cell cycle, both processes can operate and chromatin structure is one important factor which determines DSB repair pathway choice. ATM facilitates the repair of heterochromatic DSBs by phosphorylating and inactivating the heterochromatin building factor KAP-1, leading to local chromatin relaxation. Here, we show that ATM accumulation and activity is strongly diminished at DSBs undergoing end-resection during HR. Such DSBs remain unrepaired in cells devoid of the HR factors BRCA2, XRCC3 or RAD51. Strikingly, depletion of KAP-1 or expression of phospho-mimic KAP-1 allows repair of resected DSBs in the absence of BRCA2, XRCC3 or RAD51 by an erroneous PARP-dependent alt-NHEJ process. We suggest that DSBs in heterochromatin elicit initial local heterochromatin relaxation which is reversed during HR due to the release of ATM from resection break ends. The restored heterochromatic structure facilitates HR and prevents usage of error-prone alternative processes.

4.2 Author summary

Double-strand breaks (DSBs) are critical DNA lesions because they can lead to cell death or, which is even more devastating, to the formation of genomic rearrangements. Cells are equipped with two main pathways to repair such lesions, homologous recombination (HR) and non-homologous end-joining (NHEJ). HR is an error-free process and completely restores the genetic information, whereas NHEJ has the potential to form genomic rearrangements. We have previously shown that the structure of the chromatin is one important factor which determines the choice between these two pathways, such that DSBs localizing to highly condensed heterochromatic regions are mainly repaired by HR and breaks in more open euchromatic DNA undergo repair by NHEJ. Here, we investigate this aspect of DSB repair pathway choice. We show that DSB end-resection, which channels DSB repair into the process of HR, counteracts the profound local relaxation which initially takes place at the break site and reconstitutes the heterochromatic structure. Cells which are genetically modified such that they cannot reconstitute the heterochromatic structure at resected DSBs

fail to employ HR and instead repair heterochromatic DSBs by alternative NHEJ mechanisms. Thus, chromatin modifications which occur during the process of end-resection prevent error-prone repair pathways from generating genomic rearrangements.

4.3 Introduction

DNA double-strand breaks (DSBs) are among the most deleterious cellular lesions since they threaten genomic integrity and cell viability. To counteract cell degeneration and to preserve genomic integrity, a complex network of DSB repair and signaling processes has evolved [1–4].

Two main DSB repair pathways exist, canonical non-homologous end-joining (c-NHEJ) and homologous recombination (HR) [5,6]. In mammalian cells, c-NHEJ represents the major repair pathway for ionizing radiation (IR)-induced DSBs [7]. C-NHEJ repairs unresected break ends without the need for sequence homologies and can function throughout the cell cycle [8]. The key factors in c-NHEJ involve the KU70/80 heterodimer, which binds to the DSB end, and the DNA-dependent protein kinase catalytic subunit (DNA-PKcs), which, together with KU70/80, constitutes the DNA-PK holoenzyme. The repair process is completed by a complex of DNA ligase IV, XRCC4 and XLF/Cernunnos [5]. In contrast to c-NHEJ, HR is restricted to the S and G2 phases of the cell cycle where break ends undergo extensive resection and homologous DNA sequences on the sister chromatid serve as a template for repair. In addition to the repair of DSBs, HR functions during the S-phase to restart stalled or collapsed replication forks [9]. HR is initiated by CtIP-dependent resection to create 3'-overhangs at the DSB ends [10,11]. Following extended resection by EXO1 or BLM/DNA2, loading of RAD51 onto single-stranded DNA (ssDNA) is facilitated by BRCA2, XRCC2 and XRCC3. RAD54-mediated homology search then promotes strand exchange and Holliday junction formation [6]. HR is completed after repair synthesis by Holliday junction resolution and DNA end ligation. In the absence of c-NHEJ factors, DSB repair can also occur by an alternative end-joining mechanism, termed alt-NHEJ [12,13]. In contrast to c-NHEJ but similar to HR, alt-NHEJ involves CtIP-dependent resection. The resected break ends are subsequently rejoined by a process involving micro-homologies and various repair factors, such as poly (ADP-ribose) polymerase (PARP), DNA ligase I or III and

XRCC1 [14–17]. Although alt-NHEJ can efficiently operate in cells devoid of c-NHEJ factors, little is known about its ability to compensate for HR defects.

It has become clear over the last years that higher order chromatin structure impacts on the response to DSBs [18]. Thus, IR-induced DSBs in densely compacted heterochromatin (HC) are more difficult to repair than euchromatic (EC) DSBs and require additional structural changes in the surrounding chromatin [19,20]. One example are ATM-mediated chromatin changes due to KAP-1 phosphorylation [21]. In undamaged cells, KAP-1 forms HC by recruiting HP1, CHD3 and other remodeling factors [22,23]. DSB-induced KAP-1 phosphorylation leads to release of CHD3 which locally relaxes HC and facilitates repair [23]. Other studies involving HP-1 mobilization have observed either a release from [24] or a recruitment to damaged chromatin [25–27]. These apparently conflicting findings have led to the suggestion that a transient release might be followed by an accumulation of HP1 at sites of DNA damage [19,28]. It is, however, often unclear how the various processes of chromatin modification impact on DSB repair and if different repair pathways are differentially affected.

Repair kinetics for IR-induced DSBs are biphasic, exhibiting a fast and a slow component [29]. The slow component accounts for the repair of a subset (15-20%) of IR-induced DSBs that are localized to HC DNA regions, whereas DSBs induced in EC regions are typically repaired with fast kinetics. In G1 phase, the fast and the slow component of DSB repair comprise a c-NHEJ mechanism [29]. ATM-dependent phosphorylation of KAP-1 on serine 824 (S824) is specifically required for the slow component [30,31]. In G2 phase, in contrast, c-NHEJ accounts only for the fast DSB repair process, while the slow ATM-dependent HC component represents HR [32]. Thus, in G2, defined DSB populations, EC vs. HC breaks, are repaired by either c-NHEJ or HR, respectively. Despite the existence of two repair pathways in G2, a mutation in one of them leads to elevated unrepaired DSBs. Thus, c-NHEJ and HR cannot compensate for each other which might be attributed to the fact that c-NHEJ is unable to repair DSBs which have undergone extensive resection. Consistent with this notion, c-NHEJ can compensate for HR if resection is prevented by CtIP depletion [33]. What remains unclear is why alt-NHEJ, which is in principal able to rejoin resected break ends, cannot compensate for a loss of down-stream HR factors such as BRCA2 or RAD51.

In the present study, we analyzed the process of HR at HC DSBs in G2 phase. We show that the intensity of phosphorylated ATM at DSBs decreases during the process of resection, suggesting that ATM initially binds to but is then released from DSBs which undergo repair by HR. Consistent with this notion, chemical inhibition of ATM prior to but not after

resection causes a repair defect. Thus, ATM has an early role during HR but is dispensable for later stages. This contrasts to the situation in G1 where continuous ATM activity is required for HC DSB repair by c-NHEJ [34]. In G1, ATM functions to phosphorylate KAP-1, leading to its inactivation and local relaxation of the HC structure [30]. Moreover, depletion of KAP-1 by siRNA overcomes the requirement for ATM in G1 but leads to reduced HR usage in G2. Finally, following KAP-1 siRNA or expression of a phospho-mimic form of KAP-1, both of which cause HC relaxation, resected DSBs can be repaired by a PARP-dependent alt-NHEJ process. Together, these data show that the HC structure represents a barrier to repair by c-NHEJ and alt-NHEJ but facilitates usage of HR. ATM, which initially binds to DSBs, is released from break ends during the process of resection. This prevents usage of c-NHEJ and alt-NHEJ and commits resected DSBs to repair by HR.

4.4 Results

PhosphoATM (pATM) accumulation and activity is diminished at resected DSBs

We have previously demonstrated that BRCA2-deficient cells exhibit elevated γH2AX foci levels at 8 h post irradiation in G2 [1,32]. These unrepaired DSBs have undergone efficient end-resection as evidenced by RPA loading (Figure 1A) which might explain why they cannot be repaired by NHEJ. We sought to further characterize these breaks and observed that the pATM focal intensity in G2- but not in G1-phase cells is greatly diminished at 8 h compared with 30 min time points (Figure 1A and Figure S1A). In contrast, the γH2AX focal signal is equally intensive at 30 min and 8 h in G1 and G2 (Figure S1B). We also measured the pATM focal intensity at 2 h post IR, a time point when resected and unresected DSBs are present in G2-phase cells. Of note, the pATM focal intensity of RAD51-foci-positive resected breaks is reduced compared with RAD51-foci-negative unresected breaks. In contrast, the γH2AX focal intensity is similar or even slightly increased at resected versus unresected DSBs (Figure 1B). These findings suggest that the pATM focal intensity decreases during resection in G2. pATM contributes, together with DNA-PKcs and ATR, to the phosphorylation of H2AX [35,36]. To test if the loss of pATM intensity at the break site leads to reduced ATM activity, we measured the γH2AX focal intensity in cells with strongly diminished levels of ATR, a kinase which is activated by ssDNA regions [37]. Significantly, although ATR-deficient cells show γH2AX focal intensities at unresected DSBs similar to

wildtype (wt) cells, they exhibit greatly diminished intensities at resected breaks (Figure 1C). Consistent with the notion that ATM is active at unresected but not at resected DSBs, chemical inhibition of ATM only affects γH2AX foci intensities at unresected but not at resected DSBs (Figure 1D and Figure S1C).

We next sought to confirm the immunofluorescence (IF) measurements by Western blotting. We used A549 tumor cells which can be efficiently synchronized in G1 by serum starvation and moderately enriched in G2 by double thymidine blocking (Figure S2A). The level of chromatin-bound pATM decreases with time after IR due to ongoing repair in G1 and in G2 but, importantly, at later times the pATM level per γH2AX level is smaller in G2-enriched than in G1-synchronized cells (Figure 2A). We also measured pKAP-1 (S824) levels as a specific read-out for ATM activity [21] and obtained similar results (Figure 2A). We next wished to measure pATM bound to DSBs and employed immunoprecipitation (IP) experiments. For this, we used HeLa tumor cells which can be efficiently synchronized in G2 (Figure S2B). Strikingly, pATM bound to γH2AX is readily detected at 30 min but nearly absent at 8 h post IR in G2 (Figure 2B). To directly show that the diminished pATM activity in G2 is a result of resection, we inhibited resection by depleting CtIP or BLM [38] and measured pKAP-1 levels. G2-synchronized HeLa tumor cells show a strongly reduced pKAP-1 level at 4 h post IR compared with unsynchronized cells which is fully or partly restored after CtIP or BLM depletion (Figure 2C and Figure S2C). To provide evidence for the restoration of chromatin condensation at resected DSBs, we performed IP experiments as in Figure 2B. We observed that the level of KAP-1 bound to γH2AX continuously increases with repair time (Figure 2D), possibly due to an enrichment of HC DSBs at longer times and the recruitment of KAP-1 to damaged sites as previously reported [25]. Importantly, □H2AX-bound KAP-1 is substantially phosphorylated at early times post IR but largely unphosphorylated at later times (Figure 2D). Together, these biochemical approaches confirm the IF data above and provide strong evidence that ATM accumulation and activity is strongly reduced at DSBs which undergo resection. This leads to KAP-1 dephosphorylation and possibly the restoration of HC. The observed diminished ATM activity at resected DSBs is consistent with studies using a human cell extract-based assay in which ATM is activated by blunt DSB ends and ends with short ss overhangs but not by extended ssDNA regions which arise during the process of resection [39].

ATM is dispensable for later stages of HR

ATM has been implicated in early steps of HR [33,40,41]. A prediction of our findings above is that ATM is no longer required for HR after resection has occurred. To test this, we inactivated ATM either before or at 2 h post IR, a time point when resection has occurred (Figure S1C), and investigated the efficiency of DSB repair. γH2AX foci numbers at 8 h post IR were substantially elevated both in G1- and G2-phase cells treated with ATM inhibitor (ATMi) before IR but only in G1-phase and not in G2-phase cells if ATMi was added 2 h post IR (Figure 3A). We also analyzed mitotic chromatid breakage in G2-irradiated cells and observed substantially elevated break levels if ATMi is administered before irradiation but not if it is added 2 h post IR (Figure 3B). HR in G2 leads to sister chromatid exchanges (SCEs) [42] which are diminished if ATM is inhibited before but not at 2 h after IR (Figure 3C). Together, these data show that ATM is dispensable for HR stages that occur after resection has taken place.

KAP-1 depletion overcomes the BRCA2 repair defect

It was previously shown that ATM operates in G1 by continuously phosphorylating KAP-1 at heterochromatic DSBs and that KAP-1 depletion overcomes the requirement for this ATM function [34]. Since ATM accumulation and activity is reduced at resected DSBs we next asked if KAP-1 depletion might affect DSB repair in G2. KAP-1 siRNA did not alter γH2AX foci numbers in wt cells but, strikingly, rescued the repair defect in BRCA2 mutants and cells treated with BRCA2 siRNA (Figure 4A and Figure S3A). The same effect was observed in CHO cells deficient for the HR factor XRCC3 as well as in RAD51-depleted CHO cells (Figures S3B and S3C). Moreover, KAP-1 siRNA reduced the elevated level of chromatid breaks in BRCA2-deficient cells to that of wt cells (Figure 4A). We also measured the formation of SCEs and did not observe any IR-induced SCE formation in BRCA2/KAP-1-depleted cells (Figure S3D). Finally, we investigated cells containing an integrated HR reporter with two differentially mutated GFP genes [43]. Expression of the endonuclease I-SceI generates a DSB in one of the two genes which can be repaired by HR (gene conversion) with the second gene copy as a template, resulting in a cell with functional GFP. HR frequencies assessed by the fraction of GFP-positive cells are significantly decreased after BRCA2 depletion and dual depletion of BRCA2 and KAP-1, confirming that the repair events occurring in BRCA2/KAP-1-depleted cells do not represent HR (Figure S3E). A pathway switch from HR to c-NHEJ has recently been demonstrated for heterochromatic DSBs after the inhibition of resection by CtIP siRNA consistent with the idea that resection determines

DSB repair pathway choice [33]. We, therefore, asked if RPA foci formation, as a read-out for resection, is affected by KAP-1 depletion. Significantly, wt and BRCA2-depleted cells show the same initial level of RPA foci at 2 h post IR which is unaffected by KAP-1 siRNA. These RPA foci persist in BRCA2-depleted cells up to 8 h post IR consistent with their elevated γH2AX foci level. In contrast, RPA foci numbers decrease with time due to ongoing repair both in wt and BRCA2-depleted cells treated with KAP-1 siRNA (Figure 4B and Figure S3F). We also investigated RAD51 loading at resected DSBs and observed normal RAD51 foci numbers after KAP-1 siRNA in wt but not in BRCA2-depleted cells (Figure 4B).

The finding that a BRCA2-independent process repairs resected DSBs after combined BRCA2 and KAP-1 siRNA suggests that the commitment for HR results from the loss of pATM at resected DSBs which is overcome by KAP-1 depletion. To consolidate this finding, we investigated DSB repair in cells treated with KAP-1 siRNA and complemented with siRNA-resistant KAP-1 constructs which were mutated at the ATM-dependent phosphorylation site on S824 [30]. The BRCA2 repair defect, which is rescued after KAP-1 siRNA, is restored after complementation with wt KAP-1 or with KAP-1 rendered unphosphorylatable by mutating serine at position 824 to alanine (S824A). Significantly, however, KAP-1 mutated to a phospho-mimic aspartate at position 824 (S824D) fails to restore the BRCA2 repair defect (Figure 4C). Thus, KAP-1 phosphorylation at the established ATM site 824 overcomes the commitment for HR, and DSB repair in the absence of BRCA2 can proceed by an HR-independent process.

Alt-NHEJ can function as a back-up pathway for HR

We next wanted to investigate the process which is employed in BRCA2-deficient cells for the repair of resected DSBs. For this, we depleted BRCA2 and/or KAP-1 in cells deficient in the c-NHEJ factor XLF. XLF-defective cells show greatly elevated γH2AX foci and chromatid breaks consistent with the notion that c-NHEJ represents the predominant repair pathway in G2 [32]. Interestingly, depletion of BRCA2 leads to a similar increase in γH2AX foci/chromatid break numbers in wt cells and XLF mutants, demonstrating additivity of the two major repair pathways in G2, c-NHEJ and HR (Figure 5A). But most importantly in the present context, dual depletion of BRCA2 and KAP-1 did not affect γH2AX foci/chromatid break numbers in XLF mutants demonstrating that the HR defect is rescued by KAP-1 depletion even in the absence of the c-NHEJ factor XLF (Figure 5A). The same effect was observed in CHO cells deficient for the c-NHEJ factor KU80 (Figure S4A).

We then tested if an alt-NHEJ pathway repairs DSBs in BRCA2/KAP-1 depleted cells and employed chemical inhibition of PARP (PARPi), a factor which has been implicated in alt-NHEJ [14,17]. γH2AX foci and chromatid breaks were not significantly affected in wt cells treated with PARPi, demonstrating that alt-NHEJ processes do not contribute substantially to IR-induced DSB repair in normal cells. However, the elevated level of γH2AX foci/chromatid breaks in BRCA2-deficient cells, which is rescued after KAP-1 siRNA, is restored by PARPi (Figures 5B and 5C). Thus, PARPi precluded the repair events which arose in BRCA2-deficient cells after KAP-1 siRNA, demonstrating that a PARP-dependent process can function as a back-up pathway for HR. We also investigated other factors which have been described to function in alt-NHEJ. In CHO mutants deficient in XRCC1 as well as in cells deficient for DNA ligase I and III, KAP-1 failed to rescue the elevated γH2AX foci level which is conferred by a deficiency in BRCA2 or RAD51 (Figure 5D and Figure S4B). Consistent with the notion that alt-NHEJ can function as a back-up pathway for HR, we observed greatly increased levels of chromatid fusions in BRCA2/KAP-1 depleted cells (Figure 5E). To characterize the nature of these chromatid fusion events, we employed *fluorescence-in-situ-hybridization* (FISH) analysis with chromosome-specific probes. In one set of experiments, we used probes for chromosomes 1, 2 and 4 and observed that all fusion events (~40 fusions from the analysis of ~800 cells) occurred between heterologous chromosomes, that is, between a stained and an unstained chromosome or between two differently stained chromosomes (Figure 5F). Further, we employed probes for chromosome 19 which is exceptionally rich in KAP-1 binding sites and for the similar-sized chromosome 18 which is largely devoid of these sites [44]. Following BRCA2 depletion, we observed significantly higher breakage levels in chromosome 19 compared with chromosome 18, confirming that HR in G2 occurs mainly in KAP-1-dependent HC (Figure 5G). Importantly, following dual depletion of BRCA2 and KAP-1, chromosome fusions occur more often in chromosome 19 than in chromosome 18 confirming the notion that they arise from the misrejoining of chromatid breaks in KAP-1-dependent HC (Figure 5G).

HR requires KAP-1-dependent heterochromatin

The data above show that KAP-1 depletion allows heterochromatic DSBs to be repaired by an alt-NHEJ pathway in the absence of BRCA2, XRCC3 or RAD51. It is, however, unclear how the efficiency of HR in wt cells is affected by KAP-1-mediated chromatin changes. As shown above, γH2AX foci and chromatid breaks are repaired with similar kinetics with and without

KAP-1 siRNA (see Figure 4A) but it is not known if repair after KAP-1 siRNA involves HR or, as in the case of HR mutants, an alt-NHEJ pathway. To address this question, we investigated the formation of SCEs in mitotic cells and observed greatly diminished SCE levels after KAP-1 siRNA in wt cells (Figure 6A). We also employed the HR reporter assay described above (Figure S3E) and observed strongly reduced HR levels following KAP-1 depletion (Figure 6B). Thus, KAP-1-depleted cells do not employ HR although repair occurs efficiently. We also analyzed chromatid fusion events as a read-out for incorrect end-joining. Strikingly, KAP-1-depleted cells show elevated chromosomal fusions, suggesting that the DSBs are repaired by an error-prone alt-NHEJ pathway (Figure 6C). This notion is consolidated by the observation that PARPi increases γH2AX foci and chromatid break numbers in cells depleted for KAP-1 or complemented with phospho-mimic KAP-1 (S824D) (Figures 6D and 6E). Further, cells deficient in DNA ligase I and III or in XRCC1 show elevated γH2AX foci levels following KAP-1 depletion (Figures 6F and 6G). Taken together, this data shows that HR is efficiently used in cells with unphosphorylatable KAP-1 and cannot occur if KAP-1 is depleted.

4.5 Discussion

HR involves resection of DSB ends. Here, we investigated the process of HR at HC DSBs in G2 and showed that pATM, which initially binds to DSB ends, is released from the break sites during the process of resection. This leads to diminished KAP-1 phosphorylation at HC breaks and a commitment to repair such resected DSBs by HR. If the loss of KAP-1 phosphorylation is overcome by KAP-1 depletion or expression of phospho-mimic KAP-1, both of which are known to cause local HC relaxation, this commitment to HR is abolished and resected DSBs are repaired by an alt-NHEJ process. Thus, KAP-1-dependent HC facilitates later stages of HR whereas c-NHEJ and alt-NHEJ both require continuous HC relaxation due to ATM-dependent KAP-1 phosphorylation (see Figure 6H).

ATM is released from resected DSBs

ATM binding and activation at DSB ends occurs within minutes after damage induction and is important for the initiation of various signaling processes [45]. Concomitant with the induction of signaling pathways, a variety of chromatin remodeling processes are initiated.

This involves modifications which either relax or condense the chromatin structure in the surrounding of DSBs. It is, however, currently unclear how these changes are chronologically orchestrated and how they differentially affect different DSB repair pathways in different chromatin compartments. We have, therefore, focused our investigation on chromatin modifications which occur in HC regions due to the process of resection to specifically investigate how such chromatin changes impact on later stages of HR. Thus, we did not examine chromatin remodeling processes at early times which affect the decision to initiate resection.

We have previously shown that ATM is dispensable for the majority of DSB repair in G1 but that HC breaks strictly require ATM [30]. ATM's function during HC DSB repair in G1 involves continuous KAP-1 phosphorylation which leads to local HC relaxation [46]. Our finding here that ATM is released from resected DSBs in G2 was therefore unexpected. However, there is precedence in the literature that ATM changes binding properties upon resection of DSBs. First, ATM's binding affinity to break ends has been reported to be attenuated with the progressive presence of ssDNA at resected DSBs [39]. This ATM attenuation is accompanied by increasing ATR activity [39], consistent with our result that H2AX phosphorylation at RAD51-foci-positive DSBs requires ATR. Second, 53BP1, a damage response factor which localizes to and facilitates pATM accumulation at DSB sites [34], has been reported to show reduced occupancy at resected DSBs in G2 [47]. Although the reported reduction of ATM accumulation and activity at resected breaks is consistent with published data, the functional consequence of this finding was hitherto unclear.

ATM release at resected DSBs commits to HR

In G2 phase, DSB repair can be performed by NHEJ and HR. It is therefore remarkable that cells with mutations in BRCA2, XRCC3 or RAD51 exhibit unrejoined DSBs, which, obviously, are refractory to repair by NHEJ. Thus, it has been suggested that the process of resection commits DSB repair to HR and prevents usage of NHEJ [33]. Here, we provide mechanistic insight into the processes determining pathway usage upon resection. Since ATM is released from resected DSBs we reasoned that the concomitant reduction in KAP-1 phosphorylation prevents repair of resected breaks by NHEJ. Indeed, if loss of ATM-dependent KAP-1 phosphorylation is overcome by KAP-1 depletion or expression of phospho-mimic KAP-1, BRCA2-, XRCC3- or RAD51-deficient cells exhibit normal repair

kinetics. Thus, it is not the resection *per se* but the loss of ATM activity at resected breaks which commits repair to HR.

Alt-NHEJ can function as a back-up pathway for HR

HC DSBs which remain unrepaired in BRCA2-, XRCC3- or RAD51-deficient cells can be repaired if HC relaxation is provided by KAP-1 depletion or expression of phospho-mimic KAP-1. Interestingly, these DSBs undergo resection as evidenced by normal RPA foci formation. Thus, HC repair occurring in the absence of BRCA2, XRCC3 or RAD51 must involve a pathway which is capable of dealing with resected breaks. Consistent with the notion that alt-NHEJ can repair resected DSBs, we show that the HC repair events occurring in the absence of BRCA2, XRCC3 or RAD51 require PARP, XRCC1 and DNA ligase I/III. We also observed that HC repair in the absence of BRCA2 has a significant propensity to lead to chromatid exchanges in G2-irradiated cells. Because alt-NHEJ has been implicated in the formation of genomic exchanges [48–51], this finding supports our contention that HC repair in the absence of BRCA2, XRCC3 or RAD51 involves alt-NHEJ.

KAP-1-dependent heterochromatin facilitates HR

Perhaps surprisingly, we observed that the process of HR is nearly abolished in cells with depleted KAP-1, even in the presence of functional HR factors. This suggests that DSB repair pathway usage is significantly affected by chromatin modifications, favoring HR in condensed genomic regions. This notion is further supported by the observation that PARP inhibition or the loss of XRCC1 or DNA ligase I and III leads to elevated unrepaired breaks in KAP-1-depleted cells, which not only demonstrates that cells use alt-NHEJ but also that they cannot employ HR in the absence of KAP-1-dependent HC. In summary, these findings establish that KAP-1-dependent HC is not only a barrier to repair by c-NHEJ or alt-NHEJ but, unexpectedly, facilitates the process of HR.

Consistent with our results, depletion of HP1α or KAP-1 strongly reduces gene conversion frequencies in a I-SceI-based HR assay [25]. Furthermore, HP1α and KAP-1 is recruited to chromatin damaged by laser- or X-irradiation [26,27], and depletion of HP1α diminishes SCE formation after treatment with camptothecin [52]. One possibility how HC might promote HR is that a reduced spatial distance between sister chromatids in HC regions facilitates homology search [53]. In support of this idea, we have recently obtained preliminary evidence that the average distance between sister chromatids, measured by FISH analysis with locus-

specific probes, is substantially larger in EC versus HC regions (Geuting et al., unpublished data). A similar mechanism has been suggested for cohesin proteins which might promote HR by providing the required proximity of sister chromatids in G2 phase [54]. Finally, another possibility how HC might facilitate HR is by suppressing alt-NHEJ processes. Although it is well established that the presence of KU70/80 at DSB ends prevents repair by alt-NHEJ, KU70/80 is likely released from resected DSB ends. Chromatin condensation occurring due to ATM release at resected DSBs might represent an alternative mechanism to keep error-prone alt-NHEJ processes in check.

Conclusion

In conclusion, our study provides mechanistic insight into sequential events determining DSB repair pathway usage: First, we demonstrate that ATM activity is diminished at DSBs which undergo resection during the process of HR. Second, the concomitant loss of pKAP-1 at resected DSBs leads to local reconstitution of the HC superstructure and prevents repair of resected DSBs by alt-NHEJ. Thus, our study links two seemingly unrelated findings by showing how modifications at DSBs undergoing resection effect chromatin remodeling processes and DSB repair pathway usage.

4.6 Material and Methods

Cell lines and cell culture

Immortalized and transformed cell lines were 82-6 hTert (wt), HSC62 hTert (BRCA2-deficient, kindly provided by Dr. M. Digweed), 2BN hTert (XLF-deficient, kindly provided by Dr. P. Jeggo) and F02-98 hTert (ATR-deficient, kindly provided by Dr. P. Jeggo) human fibroblasts, HeLa-S3, HeLa pGC (kindly provided by Dr. J. Dahm-Daphi) and A549 human tumor cells, and CHO-AA8 (wt), IRS1SF (XRCC3-deficient; kindly provided by Dr. L. Thompson), CHO-K1 (wt), XRS6 (KU80-deficient, kindly provided by Dr. P. Jeggo), CHO-9 (wt) and EMC11 (XRCC1-deficient, kindly provided by Dr. B. Kaina) hamster cells. HeLa-S3 and A549 tumor cells were cultured in DMEM with 10% FCS and 1% NEAA; HeLa pGC cells additionally in 0.3 µg/ml puromycin. Human fibroblasts and CHO cells were cultured in MEM with 20% FCS, 1% NEAA. All cells were maintained at 37°C in a 5% CO_2 incubator.

RNA interference and plasmid transfection

SiRNA transfection was carried out with HiPerFect Transfection Reagent (Qiagen) following the manufacturer's instructions. siRNAs used in the experiments were: BLM (50 nM), Control (10 nM), CtIP (20 nM), KAP-1 (25 nM), RAD51 (20 nM), Lig I (20 nM), Lig III (20 nM) (Qiagen), and BRCA2 (25 nM) (SmartPool, Dharmacon). SiRNA sequences were: BLM (AAG CUA GGA GUC UGC GUG CGA), BRCA2 (GAA ACG GAC UUG CUA UUU A; GUA AAG AAA UGC AGA AUU C; GGU AUC AGA UGC UUC AUU A; GAA GAA UGC AGG UUU AAU A), Control (AAU UCU CCG AAC GUG UCA CGU), CtIP (UCC ACA ACA UAA UCC UAA UUU), KAP-1_A (CAG UGC UGC ACU AGC UGU GAG), KAP-1_B (CAU GAA CCC CUU GUG CUG UUU), RAD51 (AAG GGA AUU AGU GAA GCC AAA), Lig I (AAG GCA UGA UCC UGA AGC AGA), Lig III (AAC CAC AAA AAA AAU CGA GGA). Experiments were performed 48 h following siRNA transfection. For GFP-tagged siRNA-resistant KAP-1 plasmid transfection, HeLa tumor cells were incubated with KAP-1_B or KAP-1_B and BRCA2 siRNA and, 8 h later, transfected with 1 µg plasmid DNA using Lipofectamine LTX Transfection Reagent (Life Technologies). Cells were irradiated with 2 Gy, fixed and stained for □H2AX, EdU and GFP. Only GFP-positive cells were analyzed.

Cell synchronization, X-irradiation and chemical treatment

A549 tumor cells were used for G1 synchronization and G2 enrichment. HeLa tumor cells were only used for G2 enrichment. G1 synchronization was carried out by 48 h serum starvation in DMEM without FCS and NEAA. 0.5 h before irradiation, medium was replaced by DMEM with FCS and NEAA. For G2 enrichment, a double thymidine blocking was used. Cells were blocked 16 h with 2 mM thymidine (Sigma), released in fresh medium for 9 h, blocked again with 2 mM thymidine for 16 h and released in fresh medium for 7-8 h. Synchronization was controlled by FACs analysis as described previously [55]. X-irradiation was performed at 90 kV and 19 mA with an aluminium filter (dose rate: 2 Gy/min). Chemical inhibitors were added 0.5 h prior to IR and maintained during repair incubation. The ATM inhibitor (Tocris KU 60019), the DNA-PK inhibitor Nu7441 (Tocris NU7026) and the PARP inhibitor PJ34 (Calbiochem PARP inhibitor VIII PJ34) were used at concentrations of 5 µM, 10 µM and 20 µM, respectively. Repair incubation was limited to time periods which provided that the majority of G2-irradiated cells remained in G2 (controlled by FACs analysis).

Immunofluorescence

Cells were grown on glass coverslips. EdU (10 µM) was added 0.5 h prior to IR to discriminate between S- and G2-phase cells. In experiments analyzing G1-phase cells, nocodazol (100 ng/ml) was added 0.5 h prior to IR to prevent G2-phase cells progressing into G1 during repair incubation [56]. Cells were fixed and stained as described [57] and additionally stained with Click-it EdU (Life technologies). Antibodies used were: mouse-α-γH2AX at 1:2000 (Millipore); rabbit-α-γH2AX at 1:2000 (Abcam), mouse-α-pATM at 1:1000 (Biomol), rabbit-α-RAD51 at 1:15000 (Abcam), mouse-α-RPA at 1:2000 (Neomarkers) and mouse-α-GFP at 1:200 (Roche). Cells were analyzed with a Zeiss microscope and Metafer software (Metasystems). Samples were evaluated in a blinded manner. Foci intensities were analyzed using ImageJ software (see Figure S1A).

HR reporter assay

HeLa pGC cells were incubated with siRNA and, 24 h later, transfected with 3 µg pBL464-pCBASce plasmid DNA using MaTra transfection (IBA). After 24 h, cells were again siRNA treated and, 48 h later, fixed and stained. 10000 cells per sample were analyzed with a Zeiss microscope and Metafer software (Metasystems).

Protein extracts, chromatin fractionation and chromatin immunoprecipitation

Whole cell extracts were prepared as described [57]. For chromatin fractionation, cells were resuspended two times in NP-40 buffer (10 mM Tris/HCl pH 7.5, 10 mM NaCl, 3 mM $MgCl_2$, 30 mM sucrose, 0.5% NP-40, 0.2 mM sodiumvanadate, 0.5 mM PMSF) and centrifuged for 10 min at 1500 x g. Cell pellet was resuspended in Glycerol buffer (20 mM Tris/HCl pH 7.9, 100 mM KCl, 0.2 mM EDTA, 20% glycerol, 0.2 mM sodiumvanadate, 0.5 mM PMSF) and incubated 10 min on ice. After centrifugation (10 min, 1500 x g) chromatin fraction was lysed and sonicated in RIPA buffer (50 mM Tris/HCl pH 8, 150 mM NaCl, 0.5 Na-deoxycholate, 1% Triton, 0.1% SDS). For immunoprecipitation, cells were fixed with 3% paraformaldehyd containing 2% sucrose for 5 min at 4°C, immediately washed with PBS, scraped in medium and centrifuged for 10 min at 400 x g. Cells were resuspended two times in NP-40 buffer containing 15 mM caffeine and centrifuged for 10 min at 1500 x g. Cell pellet was resuspended in equal volume Nuclease buffer (10 mM HEPES pH 7.5, 10 mM KCl, 1 mM $CaCl_2$, 1.5 mM $MgCl_2$, 0.34 M sucrose, 10% glycerol, 0.1% Triton-X-100, 0.2 mM sodiumvanadate, 0.5 mM PMSF, 15 mM caffeine), micrococcal nuclease (500 U/ml) was added and suspension was incubated for 45 min at 37°C. Equal volume of Solubilization buffer (2% NP-40, 2% Triton-X-100, 600 mM NaCl in Nuclease buffer) was added before mixing, brief sonication and clearifing for 10 min at 8000 x g. Dynabead Protein G (Invitrogen) were blocked 1 h with 100 µg/ml salmon sperm DNA in 0.1% BSA/PBS and antibodies (4 µg) were linked to the beads, washed two times in 0.1% BSA/PBS and then incubated with the cell extract at 4°C over night. Beads were washed three times in Wash buffer (equal volume of Nuclease buffer and Solubilization buffer) and boiled in 2 x Laemmli buffer for 5 min at 95°C.

Immunoblotting

Western blotting was carried out at 300 mA for 1 h or at 80 mA over night. Nitrocellulose membrane (Roth) was blocked for 1 h in 5% low fat milk or 5% BSA in TBS / 0.1% Tween20. Antibody incubation was carried out in TBS / 0.1% Tween20 / 1% low fat milk or 5% BSA over night at 4°C, followed by HRP-conjugated secondary antibody incubation in PBS / 0.1% Tween20 / 1% low fat milk or 5% BSA for 1 h. Immunoblots were developed using ECL (Roche). Signal detection was carried out with a chemi-smart-system (Vilber Lourmat). Primary antibodies used were: rabbit-α-pATM at 1:1000 (Epitomics); rabbit-α-

pKAP-1 (S824) at 1:10000 (Epitomics); rabbit-α-KAP-1 at 1:1000 (abcam); mouse-α-BRCA2 at 1:1000 (Cell signaling); rabbit-α-GAPDH at 1:1000 (Santa Cruz); mouse-α-γH2AX at 1:1000 (Millipore); mouse-α-H3 at 1:1000 (abcam); mouse-α-RPA2 at 1:1000 (Calbiochem); rabbit-α-pRPA2 (S4/8) at 1:10000 (Bethyl).

Chromosomal analysis

EdU (10 μM) was added 0.5 h prior to IR and maintained to discriminate between S- and G2-phase cells. PCCs were harvested at 8 h, mitotic cells for SCE or FISH analysis between 5-8 h after IR as described [32]. Microscope slides were stained with DAPI (0.2 μg/ml) and Click-it EdU. For FISH analysis, whole chromosome probes for chromosomes 1, 2, and 4 or for chromosomes 18 and 19 were used (Metasystems). Chromosome spreads were recorded by Metafer software (Metasystems). Only EdU-negative chromosome spreads were analyzed.

Acknowledgements

We thank Penny Jeggo for critical comments on the manuscript and for providing KAP-1 plasmids, and Bernd Kaina, Larry Thompson, Penny Jeggo, Jochen Dahm-Daphi and Martin Digweed for providing cell lines. We greatly appreciate input from Olivia Barton, who first observed that KAP-1 depletion can overcome a defect in homologous recombination, and from Dorothee Deckbar, who first observed that ATM foci at resected DSBs are less intense.

4.7 References

1. Jeggo PA, Geuting V, Lobrich M (2011) The role of homologous recombination in radiation-induced double-strand break repair. Radiother Oncol 101: 7-12.

2. Thompson LH (2012) Recognition, signaling, and repair of DNA double-strand breaks produced by ionizing radiation in mammalian cells: the molecular choreography. Mutat Res 751: 158-246.

3. Mladenov E, Iliakis G (2011) Induction and repair of DNA double strand breaks: the increasing spectrum of non-homologous end joining pathways. Mutat Res 711: 61-72.

4. Bensimon A, Aebersold R, Shiloh Y (2011) Beyond ATM: the protein kinase landscape of the DNA damage response. FEBS Lett 585: 1625-1639.

5. van Gent DC, van der BM (2007) Non-homologous end-joining, a sticky affair. Oncogene 26: 7731-7740.

6. Mazon G, Mimitou EP, Symington LS (2010) SnapShot: Homologous recombination in DNA double-strand break repair. Cell 142: 646, 646.

7. Weterings E, Chen DJ (2008) The endless tale of non-homologous end-joining. Cell Res 18: 114-124.

8. Rothkamm K, Kruger I, Thompson LH, Lobrich M (2003) Pathways of DNA double-strand break repair during the mammalian cell cycle. Mol Cell Biol 23: 5706-5715.

9. Shrivastav M, De Haro LP, Nickoloff JA (2008) Regulation of DNA double-strand break repair pathway choice. Cell Res 18: 134-147.

10. Takeda S, Nakamura K, Taniguchi Y, Paull TT (2007) Ctp1/CtIP and the MRN complex collaborate in the initial steps of homologous recombination. Mol Cell 28: 351-352.

11. Grabarz A, Barascu A, Guirouilh-Barbat J, Lopez BS (2012) Initiation of DNA double strand break repair: signaling and single-stranded resection dictate the choice between homologous recombination, non-homologous end-joining and alternative end-joining. Am J Cancer Res 2: 249-268.

12. Corneo B, Wendland RL, Deriano L, Cui X, Klein IA, Wong SY, Arnal S, Holub AJ, Weller GR, Pancake BA, Shah S, Brandt VL, Meek K, Roth DB (2007) Rag mutations reveal robust alternative end joining. Nature 449: 483-486.

13. Yan CT, Boboila C, Souza EK, Franco S, Hickernell TR, Murphy M, Gumaste S, Geyer M, Zarrin AA, Manis JP, Rajewsky K, Alt FW (2007) IgH class switching and translocations use a robust non-classical end-joining pathway. Nature 449: 478-482.

14. Audebert M, Salles B, Calsou P (2004) Involvement of poly(ADP-ribose) polymerase-1 and XRCC1/DNA ligase III in an alternative route for DNA double-strand breaks rejoining. J Biol Chem 279: 55117-55126.

15. Mansour WY, Rhein T, Dahm-Daphi J (2010) The alternative end-joining pathway for repair of DNA double-strand breaks requires PARP1 but is not dependent upon microhomologies. Nucleic Acids Res 38: 6065-6077.

16. Wang H, Rosidi B, Perrault R, Wang M, Zhang L, Windhofer F, Iliakis G (2005) DNA ligase III as a candidate component of backup pathways of nonhomologous end joining. Cancer Res 65: 4020-4030.

17. Wang M, Wu W, Wu W, Rosidi B, Zhang L, Wang H, Iliakis G (2006) PARP-1 and Ku compete for repair of DNA double strand breaks by distinct NHEJ pathways. Nucleic Acids Res 34: 6170-6182.

18. Lukas J, Lukas C, Bartek J (2011) More than just a focus: The chromatin response to DNA damage and its role in genome integrity maintenance. Nat Cell Biol 13: 1161-1169.

19. Cann KL, Dellaire G (2011) Heterochromatin and the DNA damage response: the need to relax. Biochem Cell Biol 89: 45-60.

20. Goodarzi AA, Jeggo PA (2012) The heterochromatic barrier to DNA double strand break repair: how to get the entry visa. Int J Mol Sci 13: 11844-11860.

21. Ziv Y, Bielopolski D, Galanty Y, Lukas C, Taya Y, Schultz DC, Lukas J, Bekker-Jensen S, Bartek J, Shiloh Y (2006) Chromatin relaxation in response to DNA double-strand breaks is modulated by a novel ATM- and KAP-1 dependent pathway. Nat Cell Biol 8: 870-876.

22. Ryan RF, Schultz DC, Ayyanathan K, Singh PB, Friedman JR, Fredericks WJ, Rauscher FJ, III (1999) KAP-1 corepressor protein interacts and colocalizes with heterochromatic and euchromatic HP1 proteins: a potential role for Kruppel-associated box-zinc finger proteins in heterochromatin-mediated gene silencing. Mol Cell Biol 19: 4366-4378.

23. Goodarzi AA, Kurka T, Jeggo PA (2011) KAP-1 phosphorylation regulates CHD3 nucleosome remodeling during the DNA double-strand break response. Nat Struct Mol Biol 18: 831-839.

24. Ayoub N, Jeyasekharan AD, Bernal JA, Venkitaraman AR (2008) HP1-beta mobilization promotes chromatin changes that initiate the DNA damage response. Nature 453: 682-686.

25. Baldeyron C, Soria G, Roche D, Cook AJ, Almouzni G (2011) HP1alpha recruitment to DNA damage by p150CAF-1 promotes homologous recombination repair. J Cell Biol 193: 81-95.

26. Luijsterburg MS, Dinant C, Lans H, Stap J, Wiernasz E, Lagerwerf S, Warmerdam DO, Lindh M, Brink MC, Dobrucki JW, Aten JA, Fousteri MI, Jansen G, Dantuma NP, Vermeulen W, Mullenders LH, Houtsmuller AB, Verschure PJ, van Driel R (2009) Heterochromatin protein 1 is recruited to various types of DNA damage. J Cell Biol 185: 577-586.

27. Zarebski M, Wiernasz E, Dobrucki JW (2009) Recruitment of heterochromatin protein 1 to DNA repair sites. Cytometry A 75: 619-625.

28. Dinant C, Luijsterburg MS (2009) The emerging role of HP1 in the DNA damage response. Mol Cell Biol 29: 6335-6340.

29. Riballo E, Kuhne M, Rief N, Doherty A, Smith GC, Recio MJ, Reis C, Dahm K, Fricke A, Krempler A, Parker AR, Jackson SP, Gennery A, Jeggo PA, Lobrich M (2004) A pathway of double-strand break rejoining dependent upon ATM, Artemis, and proteins locating to gamma-H2AX foci. Mol Cell 16: 715-724.

30. Goodarzi AA, Noon AT, Deckbar D, Ziv Y, Shiloh Y, Lobrich M, Jeggo PA (2008) ATM signaling facilitates repair of DNA double-strand breaks associated with heterochromatin. Mol Cell 31: 167-177.

31. Goodarzi AA, Jeggo P, Lobrich M (2010) The influence of heterochromatin on DNA double strand break repair: Getting the strong, silent type to relax. DNA Repair (Amst) 9: 1273-1282.

32. Beucher A, Birraux J, Tchouandong L, Barton O, Shibata A, Conrad S, Goodarzi AA, Krempler A, Jeggo PA, Lobrich M (2009) ATM and Artemis promote homologous recombination of radiation-induced DNA double-strand breaks in G2. EMBO J 28: 3413-3427.

33. Shibata A, Conrad S, Birraux J, Geuting V, Barton O, Ismail A, Kakarougkas A, Meek K, Taucher-Scholz G, Lobrich M, Jeggo PA (2011) Factors determining DNA double-strand break repair pathway choice in G2 phase. EMBO J 30: 1079-1092.

34. Noon AT, Shibata A, Rief N, Lobrich M, Stewart GS, Jeggo PA, Goodarzi AA (2010) 53BP1-dependent robust localized KAP-1 phosphorylation is essential for heterochromatic DNA double-strand break repair. Nat Cell Biol 12: 177-184.

35. Stiff T, O'Driscoll M, Rief N, Iwabuchi K, Lobrich M, Jeggo PA (2004) ATM and DNA-PK function redundantly to phosphorylate H2AX after exposure to ionizing radiation. Cancer Res 64: 2390-2396.

36. Burma S, Chen BP, Murphy M, Kurimasa A, Chen DJ (2001) ATM phosphorylates histone H2AX in response to DNA double-strand breaks. J Biol Chem 276: 42462-42467.

37. Cimprich KA, Cortez D (2008) ATR: an essential regulator of genome integrity. Nat Rev Mol Cell Biol 9: 616-627.

38. Mimitou EP, Symington LS (2008) Sae2, Exo1 and Sgs1 collaborate in DNA double-strand break processing. Nature 455: 770-774.

39. Shiotani B, Zou L (2009) Single-stranded DNA orchestrates an ATM-to-ATR switch at DNA breaks. Mol Cell 33: 547-558.

40. Jazayeri A, Falck J, Lukas C, Bartek J, Smith GC, Lukas J, Jackson SP (2006) ATM- and cell cycle-dependent regulation of ATR in response to DNA double-strand breaks. Nat Cell Biol 8: 37-45.

41. Matsuoka S, Ballif BA, Smogorzewska A, McDonald ER, III, Hurov KE, Luo J, Bakalarski CE, Zhao Z, Solimini N, Lerenthal Y, Shiloh Y, Gygi SP, Elledge SJ (2007) ATM and ATR substrate analysis reveals extensive protein networks responsive to DNA damage. Science 316: 1160-1166.

42. Conrad S, Kunzel J, Lobrich M (2011) Sister chromatid exchanges occur in G2-irradiated cells. Cell Cycle 10: 222-228.

43. Mansour WY, Schumacher S, Rosskopf R, Rhein T, Schmidt-Petersen F, Gatzemeier F, Haag F, Borgmann K, Willers H, Dahm-Daphi J (2008) Hierarchy of nonhomologous end-joining, single-strand annealing and gene conversion at site-directed DNA double-strand breaks. Nucleic Acids Res 36: 4088-4098.

44. O'Geen H, Squazzo SL, Iyengar S, Blahnik K, Rinn JL, Chang HY, Green R, Farnham PJ (2007) Genome-wide analysis of KAP1 binding suggests autoregulation of KRAB-ZNFs. PLoS Genet 3: e89.

45. Lavin MF (2008) Ataxia-telangiectasia: from a rare disorder to a paradigm for cell signalling and cancer. Nat Rev Mol Cell Biol 9: 759-769.

46. Goodarzi AA, Kurka T, Jeggo PA (2011) KAP-1 phosphorylation regulates CHD3 nucleosome remodeling during the DNA double-strand break response. Nat Struct Mol Biol 18: 831-839.

47. Chapman JR, Sossick AJ, Boulton SJ, Jackson SP (2012) BRCA1-associated exclusion of 53BP1 from DNA damage sites underlies temporal control of DNA repair. J Cell Sci 125: 3529-3534.

48. Boboila C, Jankovic M, Yan CT, Wang JH, Wesemann DR, Zhang T, Fazeli A, Feldman L, Nussenzweig A, Nussenzweig M, Alt FW (2010) Alternative end-joining catalyzes robust IgH locus deletions and translocations in the combined absence of ligase 4 and Ku70. Proc Natl Acad Sci U S A 107: 3034-3039.

49. Simsek D, Jasin M (2010) Alternative end-joining is suppressed by the canonical NHEJ component Xrcc4-ligase IV during chromosomal translocation formation. Nat Struct Mol Biol 17: 410-416.

50. Simsek D, Brunet E, Wong SY, Katyal S, Gao Y, McKinnon PJ, Lou J, Zhang L, Li J, Rebar EJ, Gregory PD, Holmes MC, Jasin M (2011) DNA ligase III promotes alternative nonhomologous end-joining during chromosomal translocation formation. PLoS Genet 7: e1002080.

51. Zhang Y, Jasin M (2011) An essential role for CtIP in chromosomal translocation formation through an alternative end-joining pathway. Nat Struct Mol Biol 18: 80-84.

52. Soria G, Almouzni G (2012) Differential contribution of HP1 proteins to DNA end resection and homology-directed repair. Cell Cycle 12.

53. Sonoda E, Hochegger H, Saberi A, Taniguchi Y, Takeda S (2006) Differential usage of non-homologous end-joining and homologous recombination in double strand break repair. DNA Repair (Amst) 5: 1021-1029.

54. Watrin E, Peters JM (2006) Cohesin and DNA damage repair. Experimental Cell Research 312: 2687-2693.

55. Deckbar D, Stiff T, Koch B, Reis C, Lobrich M, Jeggo PA (2010) The Limitations of the G(1)-S Checkpoint. Cancer Research 70: 4412-4421.

56. Lobrich M, Shibata A, Beucher A, Fisher A, Ensminger M, Goodarzi AA, Barton O, Jeggo PA (2010) gammaH2AX foci analysis for monitoring DNA double-strand break repair: strengths, limitations and optimization. Cell Cycle 9: 662-669.

57. Quennet V, Beucher A, Barton O, Takeda S, Lobrich M (2011) CtIP and MRN promote non-homologous end-joining of etoposide-induced DNA double-strand breaks in G1. Nucleic Acids Res 39: 2144-2152.

4.8 Figure legends

Figure 1: phosphoATM focal intensity decreases at DSBs undergoing resection. (A) A549 tumor cells treated with BRCA2 siRNA were irradiated with 1 Gy (0.5 h) or 2 Gy (8 h) and immunostained with the indicated antibodies. Using EdU and cell cycle markers to distinguish G1- from G2-phase cells [32], focal intensities of pATM were measured using ImageJ software (see Figure S1A). BRCA2 siRNA was used in this analysis to accumulate resected DSBs. **(B)** 2BN hTert (XLF-deficient) human fibroblasts were analyzed 2 h post IR with 1 Gy. Cells were stained against γH2AX and RAD51 or pATM and RAD51, and γH2AX or pATM focal intensities were measured at RAD51-foci-positive or RAD51-foci-negative foci. XLF-deficient cells were used in this analysis to prevent repair of EC DSBs during the time needed for resection of HC DSBs. **(C)** 82-6 hTert (wt) and F02-98 hTert (ATR-deficient) human fibroblasts were stained against γH2AX and RAD51 at 2 h post 1 Gy, and γH2AX focal intensities were measured as in (B). **(D)** 2BN hTert (XLF-deficient) human fibroblasts were stained against γH2AX and RAD51 at 2 h post 1 Gy, and γH2AX focal intensities were measured as in (B). Since both DNA-PK and ATM can phosphorylate γH2AX, cells were treated with DNA-PK inhibitor under all conditions. Inhibitors were added 1 h post IR, a time sufficient to allow for ATM-dependent resection and RAD51 loading (see Figure S1C). In (A-D), at least 300 foci from 3 independent experiments were analyzed for each point. Box plots were used with a maximum whisker-length of 1.5-fold the inter-quartile range; the lower and upper "x" indicates the 1% or 99% margin of the data range, respectively.

Figure 2: phosphoATM activity is diminished at resected DSBs. (A) G1-synchronized and G2-enriched A549 tumor cells were irradiated with 10 Gy and harvested at indicated time points. Fractionated chromatin (chromatin) was immunoblotted (left panel), and pATM, pKAP-1 and γH2AX levels of the chromatin fraction from the same blot were quantified using ImageJ. The right panels show the ratio of pATM or pKAP-1 relative to γH2AX for G1 and G2 cells at various time points. The data for G2 was normalized to G1 which was set to 100% (mean ± SEM from ≥2 experiments). **(B)** G2-synchronized HeLa tumor cells were irradiated with 30 Gy, harvested at the indicated time points, immunoprecipitated (IP) with γH2AX antibody and analyzed by immunoblotting. In G2 cells, pATM is co-immuno-

precipitated with γH2AX at 30 min but not at 8 h post IR. The depicted FACs distributions in panels (A) and (B) represent the cell populations at the time of irradiation. How these populations change during repair incubation is shown in Figure S2. **(C)** HeLa tumor cells were treated with siRNA, synchronized in G2, and whole cell extracts were analyzed by immunoblotting 4 h post 10 Gy. pKAP-1 is detected in unsynchronized but not in G2-synchronized cells unless either CtIP or BLM is depleted. Depletion of CtIP or BLM did not affect the cell cycle distribution (see Figure S2C). **(D)** G2-synchronized HeLa tumor cells were irradiated with 30 Gy, harvested at the indicated time points, immunoprecipitated (IP) with γH2AX antibody and analyzed by immunoblotting. The level of KAP-1 co-immuno-precipitated with γH2AX increases with increasing repair time post IR. KAP-1 is substantially phosphorylated at early but not at later times.

Figure 3: ATM is not required for later stages of HR. (A) γH2AX foci were analyzed in G1- and G2-irradiated A549 tumor cells as previously described [32]. Cells were treated with ATMi 0.5 h prior to or 2 h post IR to investigate the impact of ATM inactivation at various stages during repair. Background foci numbers were subtracted. At least 40 cells were analyzed per data point and experiment (mean ± SEM from ≥3 experiments). **(B-C)** Chromatid breaks (B) and SCEs (C) were analyzed in mitotic HeLa tumor cells at 8 h post 2 Gy. Cells were treated with caffeine and colcemid at 5 h post IR to abolish the G2 checkpoint and collect cells in mitosis. The addition of caffeine does not affect homologous recombination levels as assessed by SCE formation [42]. Cells were labeled with EdU, and only EdU-negative cells (i.e. cells in G2 at the time of irradiation) were included in the analysis. Cells were treated with ATMi as in (A). At least 40 metaphases were analyzed per data point and experiment (mean ± SEM from ≥3 experiments). Example of a DAPI-stained metaphase spread with an enlarged SCE (left panel) and chromatid break (right panel). *P* values were obtained by *t*-test and represent a comparison of all cells analyzed in the indicated cell populations (***: $p<0.001$).

Figure 4: KAP-1 depletion allows HC DSB repair in the absence of BRCA2. (A) γH2AX foci and PCC analysis in G2-irradiated 82-6 hTert (wt) and HSC62 hTert (BRCA2-deficient) human fibroblasts. **(B)** RPA and RAD51 foci analysis in G2-irradiated A549 tumor cells. **(C)** Endogenous KAP-1 and BRCA2 was depleted in HeLa tumor cells by siRNA, and cells were transfected with GFP-tagged and siRNA-resistant empty (GFP), wt or mutated

(phospho-mutant S824A or phospho-mimic S824D) KAP-1 plasmids. γH2AX foci were analyzed in GFP-positive G2-irradiated cells. EdU and cell cycle markers were used to distinguish G2- from S- and G1-phase cells [32]. In (A), (B) and (C), foci numbers or PCC breaks from unirradiated cells were subtracted. At least 40 cells or PCC spreads were analyzed per data point and experiment (mean ± SEM from ≥3 experiments). KAP-1 and BRCA2 depletion in this and subsequent experiments was highly efficient (>90% as assessed by Western blotting). *P* values were obtained by *t*-test and represent a comparison of all cells analyzed in the indicated cell populations (***: p<0.001).

Figure 5: Alt-NHEJ can function as a back-up pathway for HR. (A) γH2AX foci and PCC analysis in G2-irradiated 82-6 hTert (wt) and 2BN hTert (XLF-deficient) human fibroblasts. **(B)** γH2AX foci and PCC analysis in G2-irradiated 82-6 hTert (wt) human fibroblasts treated with PARPi 0.5 h prior to IR. **(C)** PCC analysis from G2-irradiated HSC62 hTert (BRCA2-deficient) human fibroblasts treated with PARPi as in (B). **(D)** γH2AX foci analysis in G2-irradiated 82-6 hTert (wt) and HSC62 hTert (BRCA2-deficient) human fibroblasts. **(E-G)** Chromatid fusions and breaks in G2-irradiated mitotic HeLa tumor cells at 8 h post 2 Gy. Cells were treated with caffeine and colcemid at 5 h post IR to abolish the G2 checkpoint and collected in mitosis. Chromosomes were stained with Giemsa (panel E) or analyzed by FISH with probes specific for chromosomes 1 (red), 2 (green) and 4 (yellow) (panel F) or to chromosomes 18 and 19 (panel G). Foci numbers, chromatid breaks and fusions from unirradiated cells were subtracted. For panels A-E, at least 40 cells or 40 PCC/mitotic spreads were analyzed per data point and experiment (mean ± SEM from ≥3 experiments). For panel G, 50 mitotic spreads were analyzed per data point and experiment (mean ± SEM from ≥2 experiments). N.d. indicates that no chromatid fusions were observed under these conditions. *P* values were obtained by *t*-test and represent a comparison of all cells analyzed in the indicated cell populations (***: p<0.001).

Figure 6: HR requires KAP-1-dependent heterochromatin. (A) SCEs in G2-irradiated mitotic HeLa tumor cells at 8 h post 2 Gy. Cells were treated with caffeine and colcemid at 5 h post IR to abolish the G2 checkpoint and collected in mitosis. **(B)** HR frequencies (gene conversion) after I-SceI expression in HeLa pGC cells carrying an integrated GFP reporter system. **(C)** Chromatid fusions analyzed from cells in panel A. **(D)** γH2AX foci and PCC analysis in G2-irradiated 82-6 hTert (wt) human fibroblasts. Cells were treated with PARPi

0.5 h prior to IR. **(E)** Endogenous KAP-1 was depleted in HeLa tumor cells by siRNA, and cells were transfected with GFP-tagged and siRNA-resistant phospho-mimic (S824D) KAP-1 plasmid□□□ γH2AX foci were analyzed in GFP-positive G2-irradiated HeLa tumor cells treated with PARPi 0.5 h prior to IR. **(F)** γH2AX foci analysis in G2-irradiated 82-6 hTert (wt) human fibroblasts. **(G)** γH2AX foci analysis in G2-irradiated CHO9 (wt) and EMC11 (XRCC1-deficient) hamster cells. In (C-G), foci numbers, PCC breaks or chromatid fusions from unirradiated cells were subtracted. At least 40 cells or 40 PCC/mitotic spreads were analyzed per data point and experiment (mean ± SEM from ≥3 experiments). **(H)** Model of heterochromatic IR-induced DSB repair. In wt cells, ATM activates CtIP to initiate resection and phosphorylates KAP-1 to facilitate chromatin decondensation. Following extended resection, ATM is released from chromatin and KAP-1 is dephosphorylated, which likely results in restoration of condensed chromatin and a commitment to HR (left). In the case of decondensed chromatin due to KAP-1 depletion or expression of phospho-mimic KAP-1 (KAP-1 S824D), repair of resected DSBs occurs by alt-NHEJ, which is suppressed by chromatin condensation (right). *P* values were obtained by *t*-test and represent a comparison of all cells analyzed in the indicated cell populations (***: p<0.001).

4.9 Supporting information

Figure S1: (A) Measurement of foci and background intensities in a maximum intensity projection of a cell. Foci were identified by eye and foci shapes were defined by a region of interest (ROI) which was kept constant for all foci of the same experiment (upper panels on the left). The average pixel intensity (grey value) inside an ROI was taken to represent the focus intensity. The background was measured for each cell individually (cell shapes were determined by DAPI staining). For this, the most frequent (modal) grey value of the respective cell was determined which provided nearly identical results to the average grey value of the region without foci (see histogram on the right). The foci intensities were then normalized to the background intensity of the respective cell to account for variations in staining efficiency between different cells and samples. **(B)** A549 tumor cells treated with BRCA2 siRNA were irradiated with 1 Gy (0.5 h) or 2 Gy (8 h), immuno-stained as in Figure 1A, and focal intensities of γH2AX were measured using ImageJ software. **(C)** RAD51 foci were analyzed in G2-irradiated A549 tumor cells. Cells were treated with ATMi 0.5 h prior to

or 1 h post IR. Foci numbers from unirradiated cells were subtracted. At least 40 cells were analyzed per data point and experiment (mean ± SEM from ≥3 experiments). *P* values were obtained by *t*-test and represent a comparison of all cells analyzed in the indicated cell populations (***: p<0.001).

Figure S2: (A) Cell cycle distributions of A549 tumor cells after synchronization in G1-phase by serum starvation (upper panels) or enrichment in G2 phase by double thymidine blocking (lower panels)**. (B)** Cell cycle distributions of HeLa tumor cells after synchronization in G2 phase by double thymidine blocking (upper panels) or without synchronization (lower panels). **(C)** Cell cycle distributions of HeLa tumor cells after treatment with either CtIP or BLM siRNA and synchronization in G2 phase by double thymidine blocking.

Figure S3: (A) γH2AX foci were analyzed in G2-irradiated A549 tumor cells. **(B, C)** γH2AX foci were analyzed in G2-irradiated AA8 (wt) and IRS1SF (XRCC3-deficient) (panel B) or K1 (wt) (panel C) CHO cells. In samples treated with RAD51 siRNA, only RAD51-foci-negative cells were analyzed. **(D)** SCEs in G2-irradiated mitotic HeLa tumor cells at 8 h post 2 Gy. Cells were treated with caffeine and colcemid at 5 h post IR to abolish the G2 checkpoint and collected in mitosis. **(E)** HR frequencies (gene conversion) after I-SceI expression in HeLa pGC cells carrying an integrated GFP reporter system. **(F)** RPA foci were analyzed in G2-irradiated 82-6 hTert (wt) human fibroblasts. Foci numbers from unirradiated cells were subtracted. At least 40 cells were analyzed per data point and experiment (mean ± SEM from ≥3 experiments). *P* values were obtained by *t*-test and represent a comparison of all cells analyzed in the indicated cell populations (***: p<0.001).

Figure S4: (A) γH2AX foci were analyzed in G2-irradiated XRS6 (KU80-deficient) CHO cells. **(B)** γH2AX foci were analyzed in G2-irradiated CHO9 (wt) and EMC11 (XRCC1-deficient) CHO cells. In samples treated with RAD51 siRNA, only RAD51-foci-negative cells were analyzed. Foci numbers from unirradiated cells were subtracted. At least 40 cells were analyzed per data point and experiment (mean ± SEM from ≥3 experiments). *P* values were obtained by *t*-test and represent a comparison of all cells analyzed in the indicated cell populations (***: p<0.001).

4.10 Figures

Figure 1

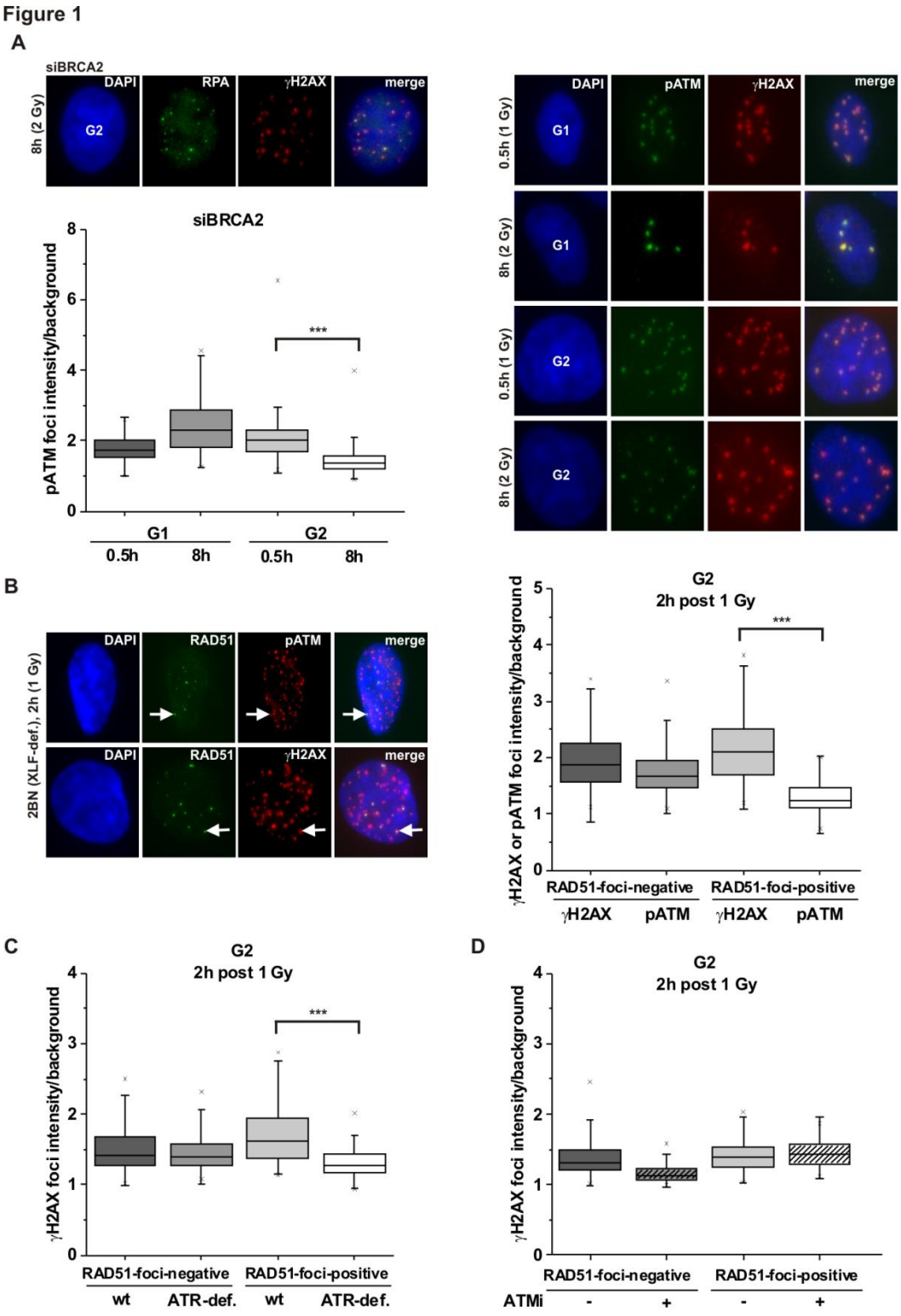

Figure 2

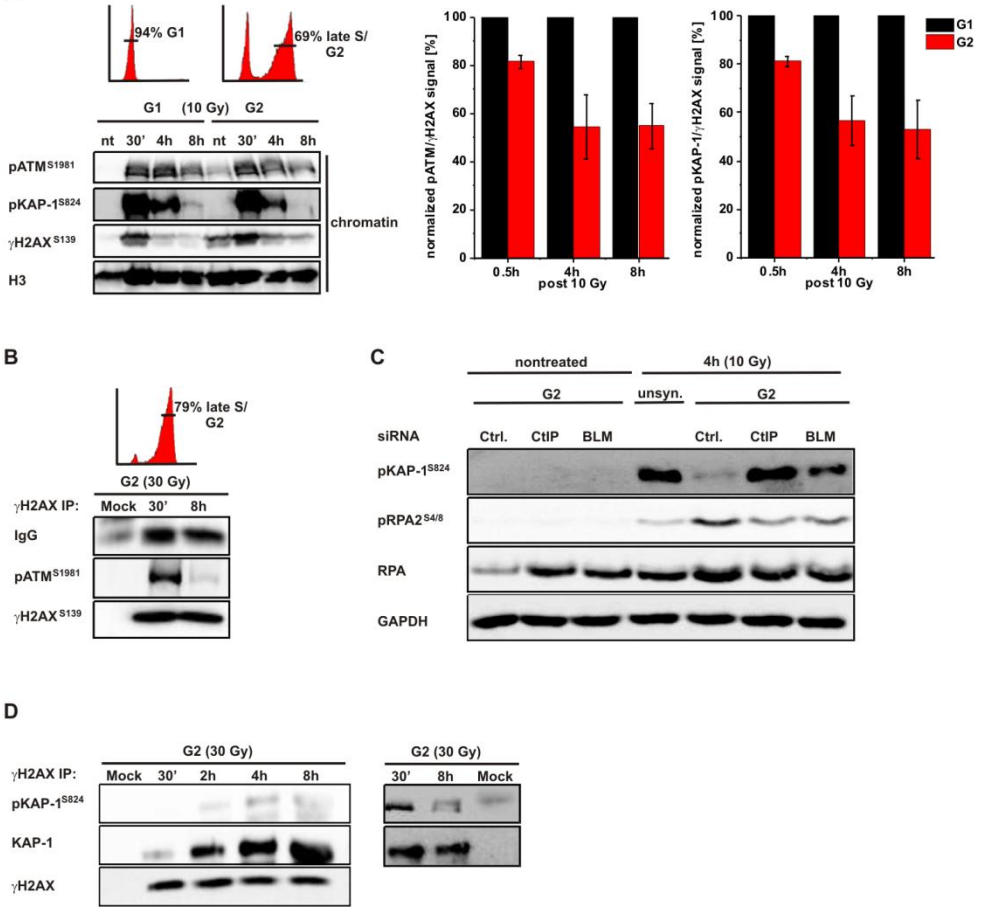
A
94% G1
69% late S/ G2
G1 (10 Gy) G2
nt 30' 4h 8h nt 30' 4h 8h
pATM S1981
pKAP-1 S824
γH2AX S139
H3
chromatin
normalized pATM/γH2AX signal [%]
normalized pKAP-1/γH2AX signal [%]
0.5h
4h post 10 Gy
8h
G1
G2
B
79% late S/ G2
G2 (30 Gy)
γH2AX IP:
Mock 30' 8h
IgG
pATM S1981
γH2AX S139
C
nontreated
4h (10 Gy)
G2
unsyn.
G2
siRNA
Ctrl. CtIP BLM Ctrl. CtIP BLM
pKAP-1 S824
pRPA2 S4/8
RPA
GAPDH
D
G2 (30 Gy)
γH2AX IP:
Mock 30' 2h 4h 8h
pKAP-1 S824
KAP-1
γH2AX
G2 (30 Gy)
30' 8h Mock

Figure 3

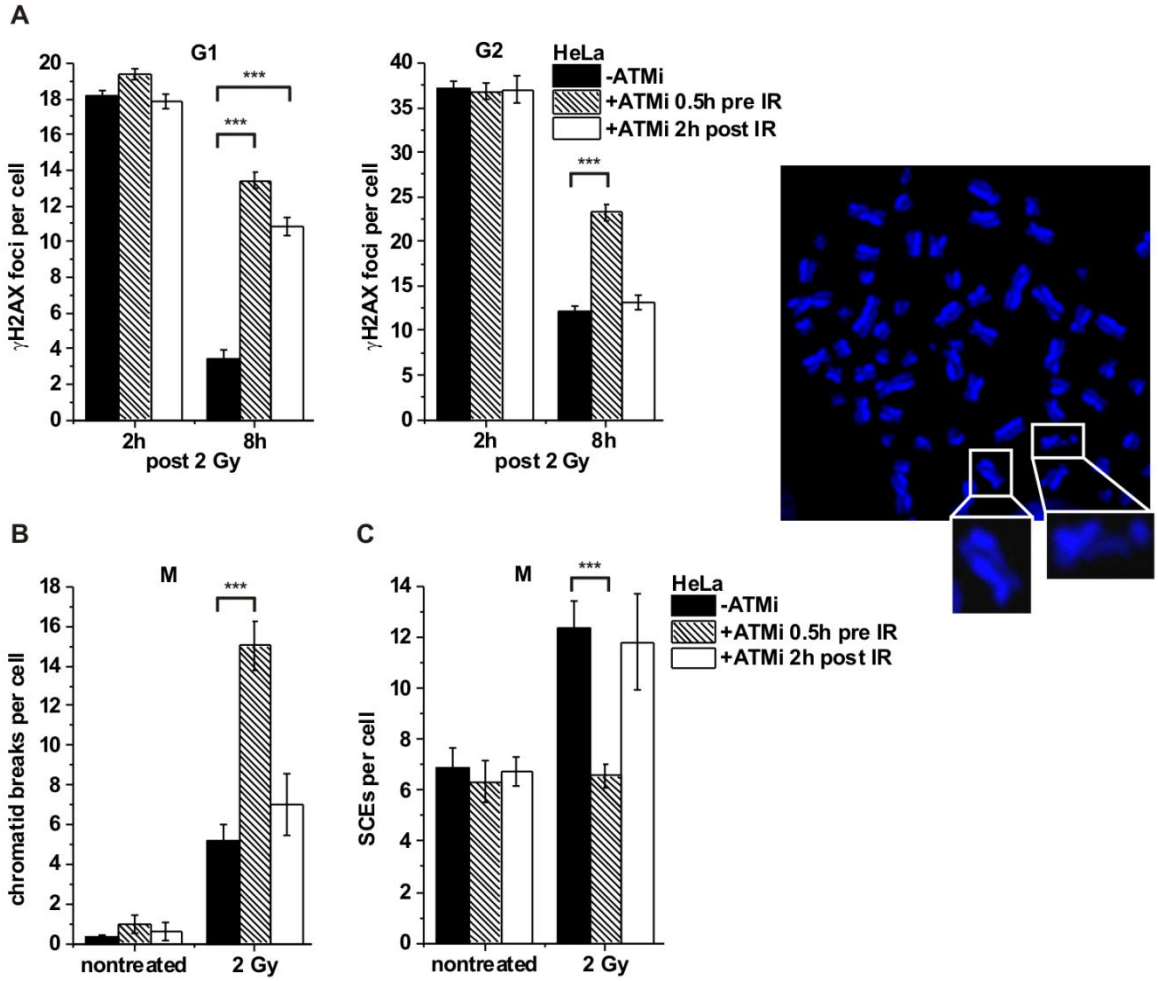
A
G1
G2
HeLa
-ATMi
+ATMi 0.5h pre IR
+ATMi 2h post IR
γH2AX foci per cell
2h
8h
post 2 Gy
***
B
M
chromatid breaks per cell
nontreated
2 Gy
C
SCEs per cell

Figure 4

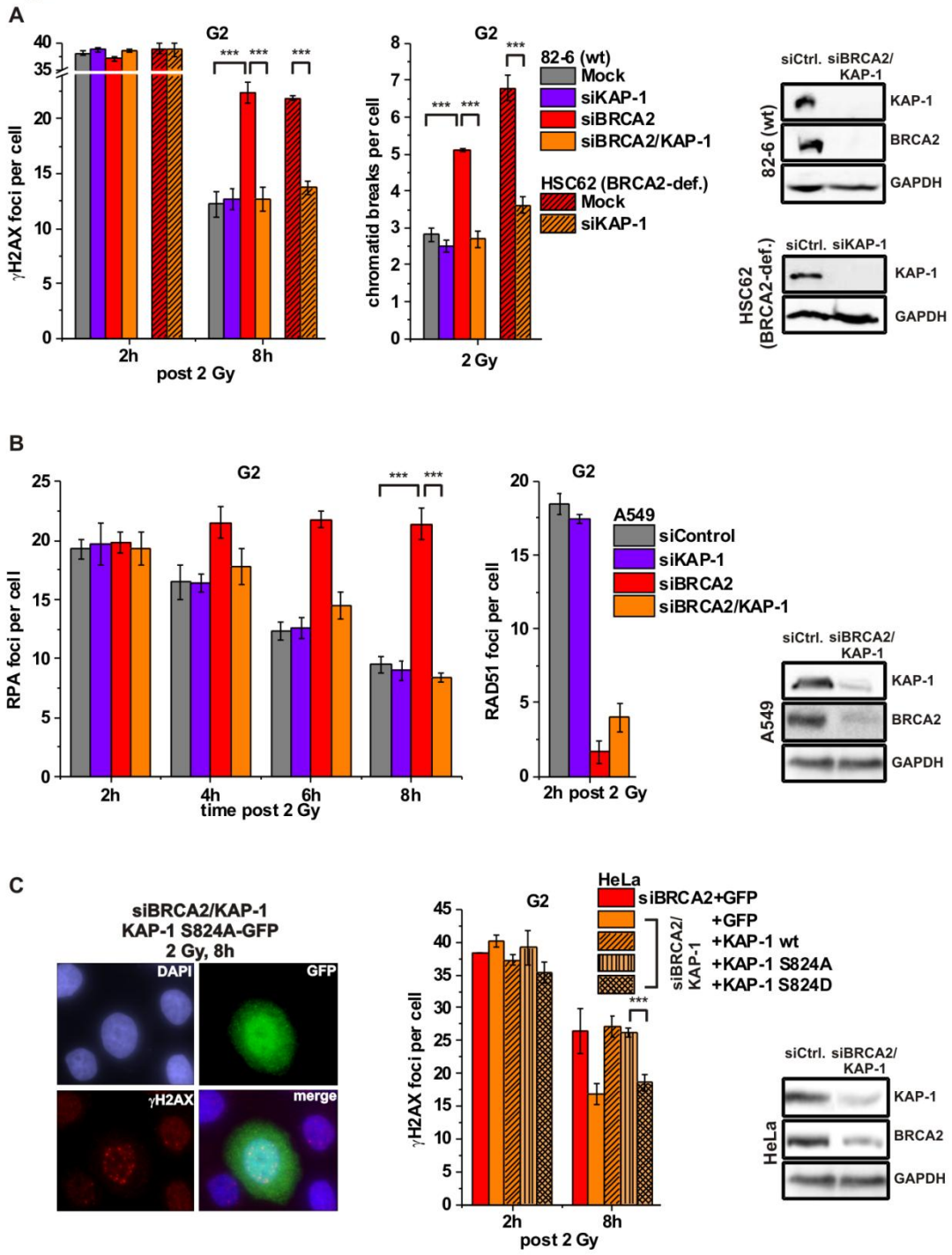
A
G2
γH2AX foci per cell
2h
8h
post 2 Gy
chromatid breaks per cell
2 Gy
82-6 (wt)
Mock
siKAP-1
siBRCA2
siBRCA2/KAP-1
HSC62 (BRCA2-def.)
Mock
siKAP-1
siCtrl. siBRCA2/ KAP-1
KAP-1
BRCA2
GAPDH
82-6 (wt)
siCtrl. siKAP-1
HSC62 (BRCA2-def.)
B
RPA foci per cell
2h
4h
6h
8h
time post 2 Gy
RAD51 foci per cell
2h post 2 Gy
A549
siControl
siKAP-1
siBRCA2
siBRCA2/KAP-1
C
siBRCA2/KAP-1
KAP-1 S824A-GFP
2 Gy, 8h
DAPI
GFP
γH2AX
merge
HeLa
siBRCA2+GFP
+GFP
+KAP-1 wt
+KAP-1 S824A
+KAP-1 S824D
siBRCA2/ KAP-1

Figure 5

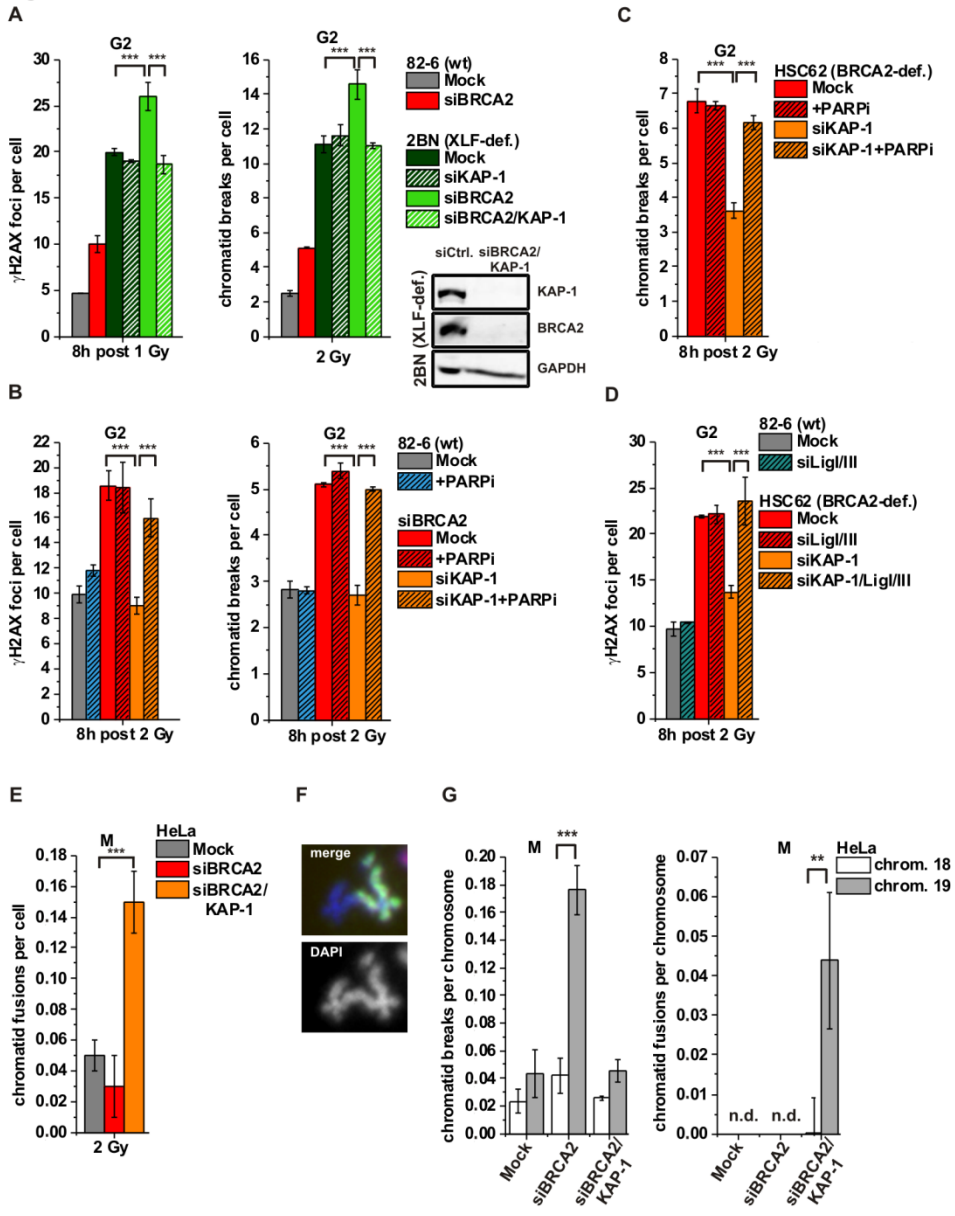
A
G2
γH2AX foci per cell
8h post 1 Gy
chromatid breaks per cell
2 Gy
82-6 (wt)
Mock
siBRCA2
2BN (XLF-def.)
Mock
siKAP-1
siBRCA2
siBRCA2/KAP-1
siCtrl.
siBRCA2/KAP-1
2BN (XLF-def.)
KAP-1
BRCA2
GAPDH
C
HSC62 (BRCA2-def.)
Mock
+PARPi
siKAP-1
siKAP-1+PARPi
8h post 2 Gy
B
82-6 (wt)
Mock
+PARPi
siBRCA2
Mock
+PARPi
siKAP-1
siKAP-1+PARPi
D
82-6 (wt)
Mock
siLigI/III
HSC62 (BRCA2-def.)
Mock
siLigI/III
siKAP-1
siKAP-1/LigI/III
E
HeLa
Mock
siBRCA2
siBRCA2/KAP-1
chromatid fusions per cell
2 Gy
F
merge
DAPI
G
chromatid breaks per chromosome
chromatid fusions per chromosome
HeLa
chrom. 18
chrom. 19
n.d.
Mock
siBRCA2
siBRCA2/KAP-1

Figure 6

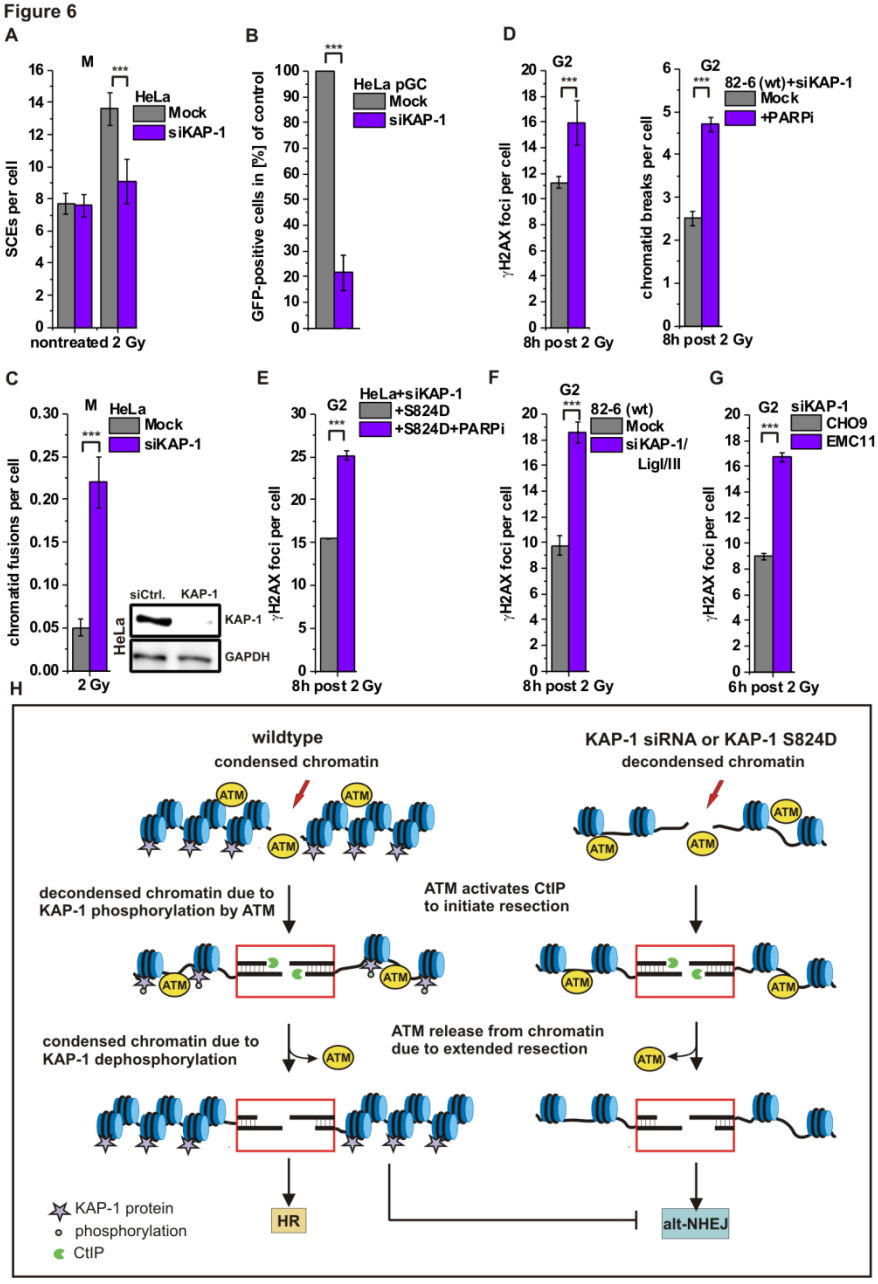
A
M
HeLa
Mock
siKAP-1
SCEs per cell
nontreated 2 Gy
B
HeLa pGC
Mock
siKAP-1
GFP-positive cells in [%] of control
D
G2
γH2AX foci per cell
8h post 2 Gy
82-6 (wt)+siKAP-1
Mock
+PARPi
chromatid breaks per cell
C
chromatid fusions per cell
2 Gy
siCtrl.
KAP-1
GAPDH
E
HeLa+siKAP-1
+S824D
+S824D+PARPi
F
82-6 (wt)
siKAP-1/
LigI/III
G
siKAP-1
CHO9
EMC11
6h post 2 Gy
H
wildtype
condensed chromatin
KAP-1 siRNA or KAP-1 S824D
decondensed chromatin
ATM
decondensed chromatin due to
KAP-1 phosphorylation by ATM
ATM activates CtIP
to initiate resection
condensed chromatin due to
KAP-1 dephosphorylation
ATM release from chromatin
due to extended resection
KAP-1 protein
phosphorylation
CtIP
HR
alt-NHEJ

Supplementary information, Figure S1

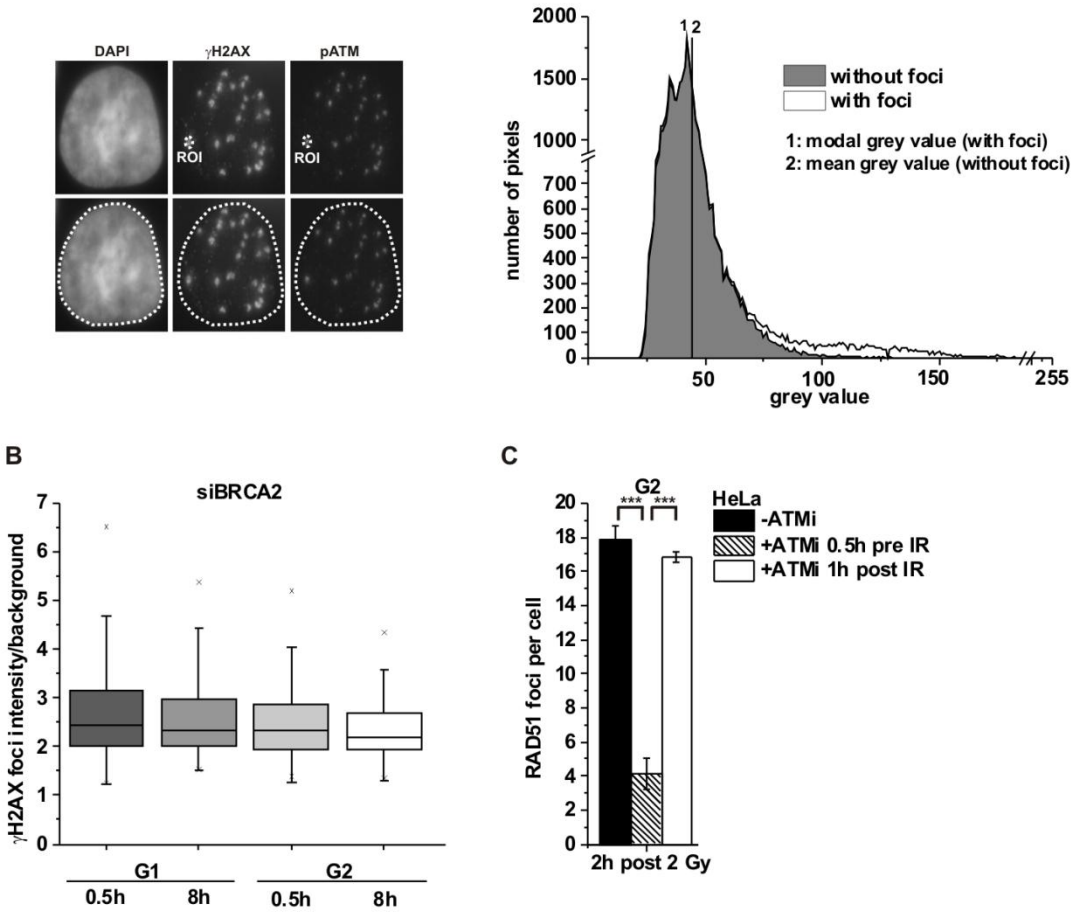

Supplementary information, Figure S2

A

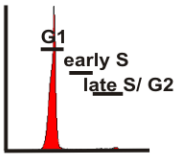

nontreated
G1: 94%
early S: 02%
late S/ G2: 02%

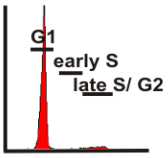

10 Gy, 0.5 h
G1: 89%
early S: 03%
late S/ G2: 08%

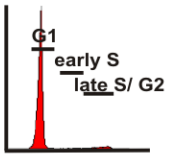

10 Gy, 4 h
G1: 86%
early S: 03%
late S/ G2: 11%

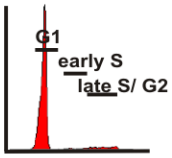

10 Gy, 8 h
G1: 84%
early S: 04%
late S/ G2: 12%

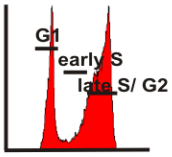

nontreated
G1: 22%
early S: 09%
late S/ G2: 69%

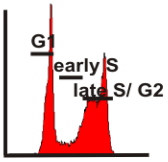

10 Gy, 0.5 h
G1: 30%
early S: 10%
late S/ G2: 60%

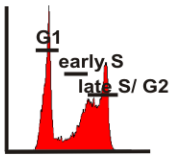

10 Gy, 4 h
G1: 33%
early S: 08%
late S/ G2: 59%

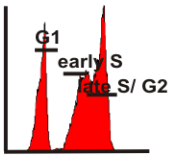

10 Gy, 8 h
G1: 24%
early S: 09%
late S/ G2: 67%

B

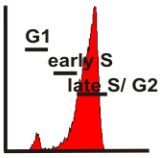

nontreated
G1: 12%
early S: 09%
late S/ G2: 79%

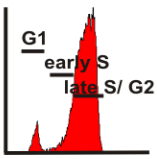

30 Gy, 4 h
G1: 13%
early S: 07%
late S/ G2: 80%

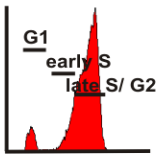

30 Gy, 8 h
G1: 12%
early S: 08%
late S/ G2: 80%

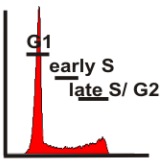

nontreated
G1: 67%
early S: 18%
late S/ G2: 15%

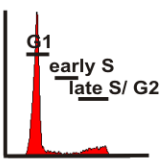

30 Gy, 4 h
G1: 67%
early S: 17%
late S/ G2: 16%

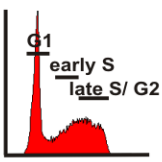

30 Gy, 8 h
G1: 67%
early S: 17%
late S/ G2: 16%

C

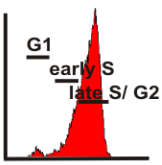

siControl, nt
G1: 03%
early S: 05%
late S/ G2: 92%

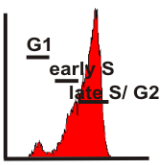

siCtIP, nt
G1: 05%
early S: 07%
late S/ G2: 88%

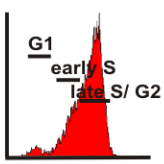

siBLM, nt
G1: 04%
early S: 08%
late S/ G2: 88%

Supplementary information, Figure S3

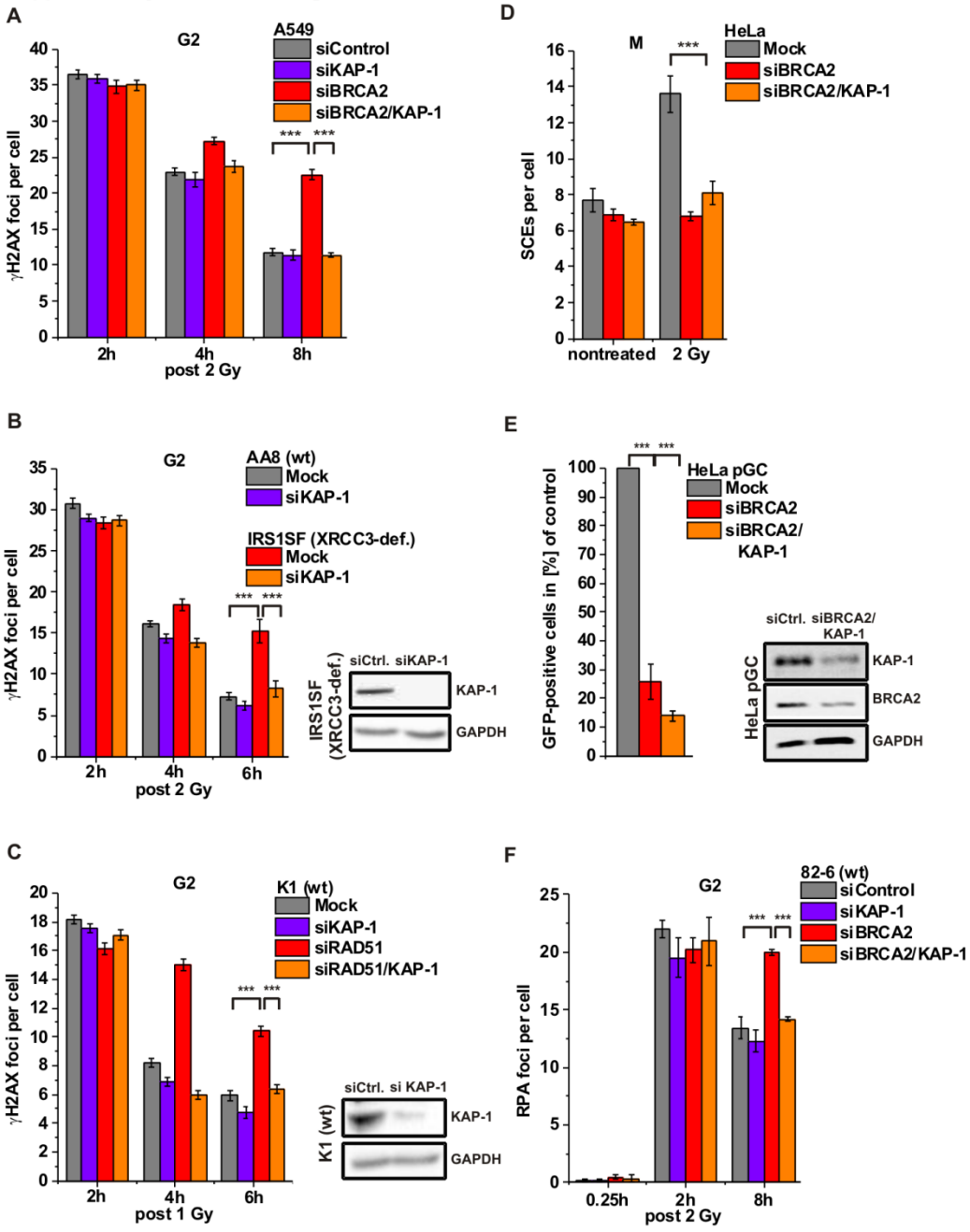

Supplementary information, Figure S4

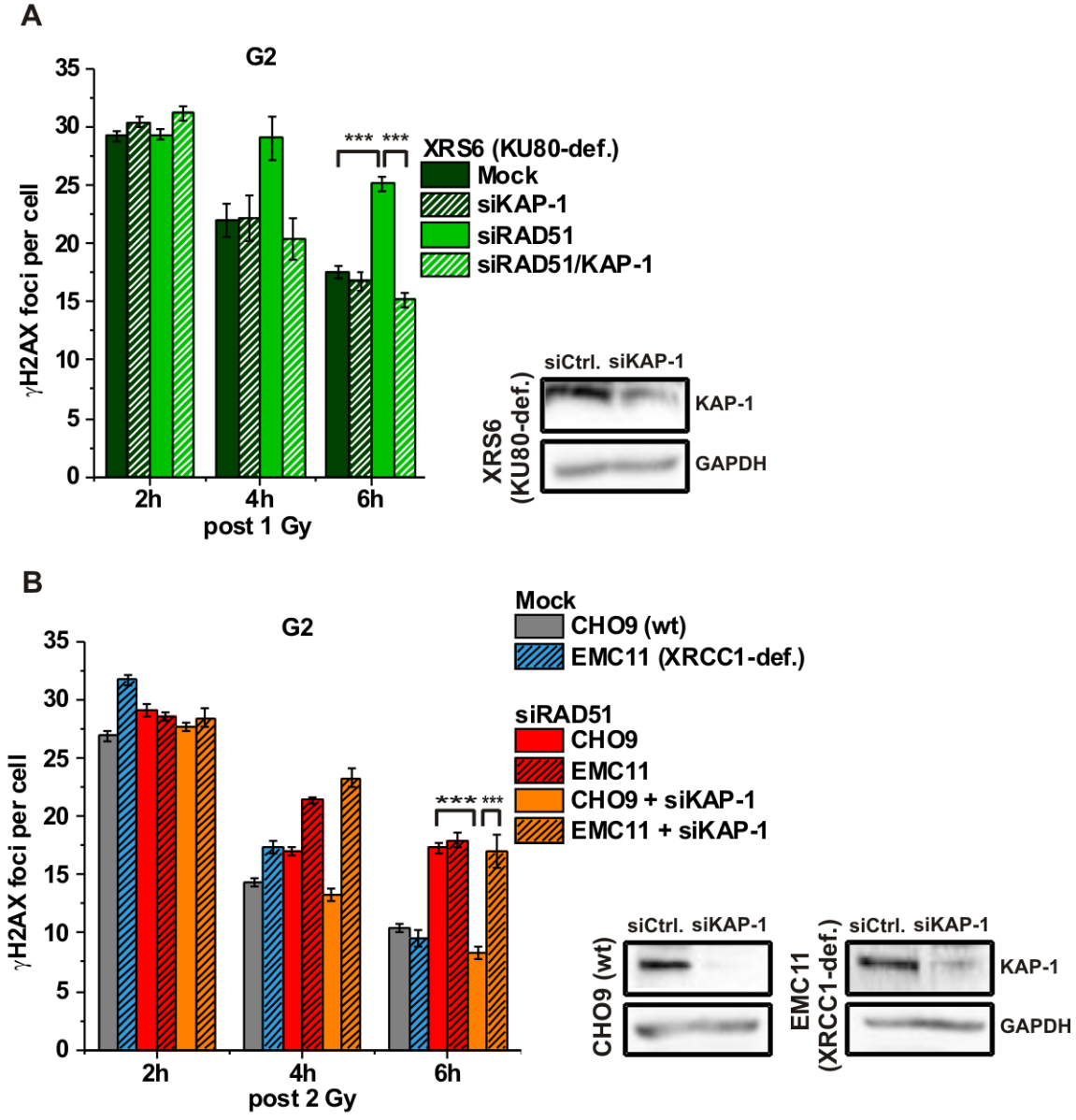

4.11 Declaration of own achievements within the publication

The results of experiments that I designed and performed are represented in the listed figures:

Figure 1: A-D

Figure 2: A-D

Figure 4: A (chromatid breaks and western blot)

Figure 5: A (chromatid breaks and western blot), B (chromatid breaks), C, E, F and G

Figure 6: D (chromatid breaks)

Figure S1: A+B

Figure S2: A-C

Figure S3: B, C+E (western blot)

Figure S4: A+B (western blot)

Furthermore, I analyzed my results and developed the model of heterochromatic IR-induced DSB repair in collaboration with Dr. Verena Geuting and Prof. Markus Löbrich. I did not write the original manuscript, but I was involved in the rewriting-process within the revision. Additionally, I was involved in proofreading the manuscript during the submission- and revision-process.

5 Manuscript: An MDC1-mediated decrease in RNF8/168 activity at resected DSBs facilitates HR

An MDC1-mediated decrease in RNF8/168 activity at resected DSBs facilitates HR

Christian Reul[1], Verena Geuting[1] and Markus Löbrich[1]

[1]Darmstadt University of Technology, Radiation Biology and DNA Repair,
64287 Darmstadt, Germany

Running title:

Resection causes RNF8/168 and 53BP1 release

Keywords:

double-strand break repair; pathway choice; homologous recombination; non-homologous end-joining; MDC1; RNF8; 53BP1; JMJD2A

5.1 Abstract

Non-homologous end-joining (NHEJ) and homologous recombination (HR) represent the major repair pathways in the G2-phase of the mammalian cell cycle. The release of ATM at resected DSBs facilitates HR and prevents the usage of error prone alternative end-joining (alt-NHEJ) processes. Here we could show that the release of ATM is mediated by a release of 53BP1 caused by a decrease in RNF8/168 activity at resected DSBs. A co-depletion of the factors JMJD2A and JMJD2B, which compete with 53BP1 on H4K20me2 binding , or using a phosphomimic MDC1 mutant in the RNF-8 binding site can overcome the determination to HR and allows repair independently of HR.

We support the following model: DSB end-resection causes a switch from ATM to ATR, where ATR phosphorylates H2AX but not MDC1 to facilitate RNF8 binding and activation. The decreased RNF8/168 activity causes a 53BP1 and ATM release, which leads to a heterochromatin reconstitution. This facilitates homologous recombination and prevents usage of error-prone alternative processes.

5.2 Introduction

DNA double-strand breaks (DSBs) are the most severe DNA lesion and they can lead to genomic instability, less cell survival and cancer. The two major repair pathways in mammalian cells for ionizing radiation (IR) induced DSBs are non homologous end-joining (NHEJ) and homologous recombination (HR). NHEJ can function all over the cell cycle, whereas HR is limited to S- and G2-phase.

An important step for the DNA damage response (DDR) is the coordinated assembly of DDR proteins at the DSB, which can be visualized as ionizing radiation induced foci (Jackson and Bartek 2009). H2AX is phosphorylated on serine 139 by ATM and the now called γH2AX is directly bound by the mediator protein MDC1 (Rogakou et al. 1998; Stucki et al. 2005). MDC1 contains a SDT repeat region (also referred as SDTD region), which is constitutively phosphorylated by the caseine kinase 2 (CK2) (Melander et al. 2008). The MRN complex binds the phosphorylated SDT repeat and activates ATM to expand the γH2AX phosphorylation to the neighboring nucleosomes. Additionally, ATM phosphorylates a region of TQ motifs (referred as T-Q-X-F cluster) on MDC1 to enhance the binding of the E3

ubiquitin ligase RNF8 (Kolas et al. 2007; Mailand et al. 2007). RNF8 ubiquitinates H2A/H2AX and these ubuiquitin is recognized and extended by the E3 ubiquitin ligase RNF168 (Doil et al. 2009; Mattiroli et al. 2012). The ubiquination of H2A/H2AX is stated to be essential for the binding and retention of 53BP1 at the DSB site (Huen et al. 2007; Mailand et al. 2007; Doil et al. 2009). Another role of RNF8 and RNF168 is described, where it ubiquitinates the histone demethylase JMJD2A as a signal for its degradation to enhance 53BP1 binding to the chromatin (Mallette et al. 2012). JMJD2A binds normally to dimethylated H4K20 (H4K20me2), but after its degradation the H4K20me2 is accessible for 53BP1 binding (Botuyan et al. 2006; Mallette et al. 2012). 53BP1 itself interacts with the MRN complex, bound by MDC1 at the damage site, to facilitate ATM activation (Lee et al. 2010). Additionally, it is described for G1 phase cells that 53BP1 is needed for the retention of ATM at the DSB site, measured by IR induced foci (IRIF) stained for phosphoATM (pATM) (Lee et al. 2010; Noon et al. 2010). One important role of the retention of ATM is to phosphorylate the heterochromatin building factor KAP-1 to relax the heterochromatin structure to allow successful DSB repair by NHEJ (Ziv et al. 2006; Goodarzi et al. 2008; Noon et al. 2010; Goodarzi et al. 2011).

We could previously show that at resected breaks ATM is released which causes a condensation of the chromatin and by this HR is facilitated (Geuting et al. 2013), whereas the mechanism of this release is still unclear. In this work we could show, that the release of ATM from resected DSBs is due to the fact, that after RNF8/168 activity is diminished and by this also 53BP1 is released. The decrease of RNF8/168 activity is caused by a switch from ATM to ATR activation, where ATR does not phosphorylates MDC1 at its T-Q-X-F cluster to enhance RNF8 binding.

5.3 Results

pATM focus formation in G2 needs MDC1, RNF168 and 53BP1

We have previously shown that pATM is released from resected DSBs (Geuting et al. 2013), whereas the mechanistic reason of this release is still unclear. In G0/G1-phase cells it was demonstrated that 53BP1 and the ubiquitin ligase RNF168 are essential for pATM focus formation (Noon et al. 2010). We confirmed these findings in G2-phase cells, where 53BP1 is obligatory for pATM focus formation (Fig. 1A left panel) and RNF168 is needed for 53BP1

and pATM focus formation (Suppl. Fig.1A). MDC1 is also essential for 53BP1 formation, but forms foci itself independent of RNF168 (Fig. 1A right panel and Suppl. Fig 1A). The formation of γH2AX foci is completely independent of MDC1, RNF168 and 53BP1, but we noticed that, after downregulation of MDC1, the γH2AX foci structure is more diffuse than in control cells (Fig 1A).

RNF8/168 activity and 53BP1 focus formation is diminished at resected DSBs

To investigate the mechanistic reasons of the pATM release at resected breaks, we analyzed the behavior of 53BP1, RNF8/168 dependent ubiquitin chains via FK2 (Mailand et al. 2007; Stewart et al. 2009) and MDC1 focus formation at resected DSBs. We used cells treated with BRCA2 siRNA to accumulate resected breaks in G2 and measured the foci intensities. In G2-phase but not in G1-phase cells 53BP1 focal intensity is diminished 8 h post IR compared to 30 min post IR (Fig. 1B left panel and Fig.1C). FK2 focal intensity is also diminished at 8 h post IR (Fig 1E and Suppl. Fig. 1B). In contrast MDC1 focal intensity is equal or slightly increased in G2-phase cells at an 8 h time point compared to a 30 min time point (Fig. 1B right panel and Fig. 1D). The combined γH2AX focal intensities, measured in Fig 1C-E, are also slightly increased 8 h post IR compared to 30 min post IR in G2-phase cells.

To validate these data, we compared resected and unresected DSBs within the same cell by RAD51 co-staining. 2BN hTert (XLF-deficient) human fibroblasts were used to avoid intensity changes due to repair by NHEJ. RAD51-foci-positive 53BP1 or FK2 foci are less intensive compared to RAD51-foci-negative 53BP1 or FK2 foci (Fig. 2A and 2B). In contrast to 53BP1 and FK2, MDC1 foci are equal intense, both RAD51-foci-positive and RAD51-foci-negative (Fig. 2C). Taken together, 53BP1 foci and RNF8/168 activity is diminished at resected breaks, whereas MDC1 focus formation is not impaired.

Phosphomimic MDC1 overcomes BRCA2 repair defect

We could previously show that the pATM release at resected DSBs comes along with a chromatin condensation and a commitment to HR (Geuting et al. 2013). This chromatin condensation is mediated by a dephosphorylation of KAP-1 at Serine 824, due to the pATM release from chromatin (Ziv et al. 2006; Goodarzi et al. 2011; Geuting et al. 2013). A phosphomimic form of KAP-1 (S824D) can overcome the commitment to HR, because heterochromatic DSBs, which remain unrepaired in HR-deficient cells

(e.g BRCA2-deficient), can now be repaired by alternative end-joining (alt-NHEJ) (Geuting et al. 2013).

A prediction of our findings above is that 53BP1, and thereby pATM, is released at resected breaks due to a lack of RNF8/168 activity. It has been described that an ATM mediated phosphorylation at the T-Q-X-F cluster on MDC1 is essential for RNF8 binding and activation. A triple phosphomutant form of MDC1 (MDC1-3A) within this T-Q-X-F cluster (T699A, T719A and T752A) abolishes completely RNF8 binding (Mailand et al. 2007). So, we assumed a triple phosphomimic from of MDC1 (MDC1-3E: T699E, T719E and T752E) might allow an RNF8 binding independent of ATM and by this overcome the diminished FK2 focal intensity (Fig. 1E and Fig 2B). We were not able to measure focal intensities in MDC1-WT or MDC1-3E transfected cells, due to the high varity in focus size and intensity within the same transfection (data not shown). Therefore we measured the possibility of the MDC1-3E mutant to rescue a BRCA2 defect. A transfection of MDC1-3E causes no enhanced number of γH2AX foci in G1 and G2, furthermore the MDC1-3E mutant can rescue a BRCA2 repair defect in G2 (Fig. 3A and Suppl. Fig. 2D). We assume that under these conditions RNF8/168 activity is not decreased and 53BP1 and pATM are not released at resected DSBs.l

JMJDA2 depletion impairs HR

At resected DSBs is 53BP1 released and the RNF8/168 activity decreased (Fig. 2A and Fig 2B) (Mallette et al. 2012). It was previously shown that 53BP1 foci can be restored in RNF8 or RNF168 deficient cell lines by an additional depletion of JMJD2A and JMJD2B, which compete against 53BP1 to H4K20me2 binding (Botuyan et al. 2006; Mallette et al. 2012). We assume that a depletion of JMJD2A and JMJD2B should prevent the release of 53BP1 and pATM at resected DSB and by this rescue a BRCA2 repair defect like a MDC1-3E mutant.

A depletion of JMJD2A/B itself might not affect DSB repair in G2 due to the same repair kinetics like control cells (Fig. 3B). Furthermore, the JMJD2A and JMJD2B depletion rescues a repair defect caused by a depletion of BRCA2 (Fig. 3B). We could previously show that cells with relaxed heterochromatin (e.g. by KAP-1 knockdown) exhibit repair kinetics like control cells but HR is impaired regardless of the HR proficiency of these cells (Geuting et al. 2013). So we measured HR events by sister chromatid exchanges (SCEs) and gene conversion after depletion of JMJD2A/B and observed a greatly diminished number of SCEs and gene conversions (Fig. 3C and 3D). Furthermore, JMJD2A/B depletion causes no additional

breaks, but a high number of chromatid fusions (Supl Fig. 2B and 2C). A depletion of JMJD2A and JMJD2B impairs HR and the higher number of chromatid fucions are an indication of a repair by an alt-NHEJ process.

5.4 Discussion

Previously we have shown that resection causes a release of pATM which leads to diminished KAP-1 phosphorylation and by this commits heterochromatic DSBs to be repaired by HR (Geuting et al. 2013). Also 53BP1 and the RNF8/168 dependent ubiquitin chains , which are essential for pATM focus formation, are diminished at resected breaks. Consistent to our results, 53BP1 and ubiquitin chains stained by FK2 are excluded to the focus periphery at DSBs which are undergoing resection (Chapman et al. 2012; Kakarougkas et al. 2013). This may lead to an accumulation of pATM at the periphery of a focus at a resected DSB, but this accumulation is not able to relax the chromatin to allow a switch into alternative endjoining like it has been shown for a KAP-1 knockdown (Geuting et al. 2013). However, at resected DSBs γH2AX and MDC1 are not excluded to the periphery and shows similar focal intensity like unresected DSBs (Geuting et al. 2013; Kakarougkas et al. 2013). But MDC1 has been described to enhance the ATM depenent expanding γH2AX focus at the DSB (Lou et al. 2006; Melander et al. 2008), what leads to the question why the γH2AX focal intensitiy is not diminished. It was shown that resected DSBs switch from an ATM to an ATR activation and we could previously show that the γH2AX focus formation at resected DSBs is strongly ATR-dependent (Shiotani and Zou 2009; Geuting et al. 2013). ATR seemed to be hold at MDC1 and does not diffuse free and phosphorylates H2AX , because γH2AX foci at resected DSBs are clearly defined (Geuting et al. 2013), whereas after MDC1 knockdown γH2AX foci are more diffuse. After HU treatment ATR has been described to bind via TOPBP1 to the same phosphorylated SDT repeat on MDC1 like ATM via MRN after IR(Wang et al. 2011). HU causes DSBs in S-Phase cells which are exclusively repaired by HR (*Iloff et al.* unpublished data). So the switch from activation of ATM to ATR at resected breaks might be enhanced by an additional switch of MRN/ATM to a TOPBP1/ATR binding at MDC1.

The largely or completely ATM to ATR switch leads to a lack of ATM dependent phosphorylation of the T-Q-X-F cluster on MDC1 and RNF8/168 binding to MDC1. We confirmed this assumption by measuring diminished FK2 foci at resected DSBs. Furthermore

diminished FK2 foci at resected breaks are an evidence for an impossibility of ATR to phosphorylate the T-Q-X-F cluster on MDC1.

The histone demethylase JMJD2A/B binds to dimethylated H4K20, which is also the binding target of 53BP1 in a damage induced manner (Botuyan et al. 2006; Mallette et al. 2012). MDC1 is phosphorylated by ATM at its T-Q-X-F cluster to enhance the binding of RNF 8 and the recruiting of RNF 168 (Mailand et al. 2007). RNF8 and RNF168 ubiquinate this histone H2A and additionally JMJD2A/B to degrade these proteins and achieve an efficient binding of 53BP1 (Huen et al. 2007; Mallette et al. 2012). If RNF8/168 are not recruited due to a lack of phosphorylated MDC1 at resected breaks, JMJD2A/B is not degraded. We suggest that JMJD2A replaces 53BP1 due to its higher binding affinity to H4K20me2 (Mallette et al. 2012) and causes by this the release of 53BP1.
If a downregulation of JMJD2A/B restores 53BP1focus formation and by this also pATM focus formation, we assumed pATM can phosphorylate KAP-1. This KAP-1 phosphorylation should cause heterochromatin relaxation, like a KAP-1 knockdown or a phosphomimic KAP-1 (S824D) mutant and thereby allow the repair of resected DSBs by alternative endjoining in a BRCA2 deficient cell (Geuting et al. 2013).
Also diminished HR events after JMJD2A/B knockdown in HR-proficient cells indicate, that restoration of 53BP1 leads to a switch from HR to alt-NHEJ, like a KAP-1 knockdown. Together with the finding that ATR cannot phosphorylate the T-Q-X-F cluster, we used a phosphomimic MDC1-3E mutant and measured a rescue of the BRCA2 defect. We assume that the phosphomimic MDC1-3E mutant overcome the loss of FK2 and 53BP1 foci and due to this pATM is not released and can phosphorylate KAP-1, which leads to a switch from HR to alternative end-joining.

Conclusion

In conclusion, this and our previous study (Geuting et al. 2013) provides a mechanistic insight how the cell determines the repair pathway in the G2-phase of the cell cycle. After resection has been taken place, there is a switch from ATM to ATR activation. ATR does not phosphorylate MDC1 at the T-Q-X-F cluster to allow RNF8 binding and activation (Fig. 3E). We suggest that 53BP1 is replaced by JMJD2A and due to this ATM is released from the DSB. The ATM release causes greatly diminished KAP-1 phosphorylation, which leads to a heterochromatin condensation. By this the cell determines for error-free HR as the repair

pathway of heterochromatic DSBs and avoid an interference of error-prone alternative end-joining.

5.5 Material and Methods

Cell lines and cell culture:

Immortalized and transformed cell lines were 2BN hTert (XLF-deficient), RIDDLE syndrome (complemented with HA vector or HA-RNF168, kindly provided by Dr. P. Jeggo) human fibroblast, HeLa-S3, HeLA-pGC (kindly provided by Dr. J. Dahm-Daphi) and A549 human tumor cells. Human fibroblasts were cultured in MEM with 20% FCS, 1% NEAA. HeLa-S3, HeLa-pGC and A549 tumor cells were cultured in DMEM with 10% FCS, 1% NEAA. All cells were maintained at 37 °C in a 5% CO_2 incubator.

RNA interference and plasmid transfection.

SiRNA transfection was carried out with HiPerFect (Qiagen) following the manufacturer's instructions. SiRNAs used in the experiments were: 53BP1 (AAG CCA GGT TCT AGA GGA TGA), MDC1 (CCA GAA ATC TTT ATG AAT AAA), BRCA2 (TTG GAG GAA TAT CGT AGG TAA), JMJD2A (CAC CGA GTT TGT CTT GAA ATA), JMJD2B (CAC CTG ACA AAT CCT AGC GAA)

Experiments were performed 48 h following siRNA transfection.

GFP-MDC1-WT was a gift from Dr. Jiri Lukas. MDC1-3E (T699E, T719E, T752E) were made by site-directed mutagenesis of GFP-MDC1-WT using the primers:

T699E-F, 5'-GGACCTACAAGCTACCGAGTGCTTTCTG-3';

T699E-R, 5'-CCTGGATGTTCGATGGCTCACGAAAGAC-3';

T719E-F, 5'-GGAGGATGAACCTACCGAGGCCTTCATG-3';

T719E-R, 5'-CCTCCTACTTGGATGGCTCCGGAAGTAC-3';

T752E-F, 5'-GAGGTCCTGGCTACAGAGCCATTCTGTC-3';

T752E-R, 5'-CTCCAGGACCGATGTCTCGGTAAGACAG-3'

Hela cells were transfected with MDC1-WT MDC1-3E by Magnet Assistet Transfection (iba) following the manufacturer's instructions. GFP-positive cells were analyzed.

X-irradiation

X-irradiation was performed at 90 kV and 19 mA with an aluminium filter (dose rate 2Gy/min).

Immunofluorescence:

Immunofluorescence was performed as described-in *Geuting et al.2013*

Antibodies used were: mouse-α-γH2AX at 1:2000 (Millipore); rabbit-α-γH2AX at 1:2000 (Epitomics), mouse-α-53BP1 at 1:10000 (Millipore), rabbit-α-53BP1 at 1:1000 (Bethyl) , mouse-α-FK2 at 1:10000 (Calbiochem), mouse-α-pATM at 1:1000 (Biomol),rabbit-α-RAD51 at 1:15000 (Abcam), mouse-α-MDC1 at 1:1000 (Sigma), and mouse-α-GFP at 1:200 (Roche). Cells were analyzed with a Zeiss microscope and Metafer software (Metasystems). Samples were evaluated in a blinded manner. Foci intensities were analyzed using ImageJ software as described in *Geuting et al.2013*.

HR reporter assay and SCE analysis

HR reporter assay and SCE analysis were performed as described in *Geuting et al.2013*.

Protein extract and Immunoblotting

Protein extracts were prepared and Western Blotting was performed as described in *Geuting et al.2013.*

Primary antibodies used in the experiments were: rabbit-α-JMJD2A 1:1000 (Abcam), rabbit-α-JMJD2B 1:1000 (Novus biologicals), mouse-α-BRCA2 at 1:1000 (Cell signaling), rabbit-α-GAPDH at 1:1000 (Santa Cruz)

5.6 References

Botuyan MV, Lee J, Ward IM, Kim JE, Thompson JR et al. (2006) Structural basis for the methylation state-specific recognition of histone H4-K20 by 53BP1 and Crb2 in DNA repair. Cell 127(7): 1361-1373.

Chapman JR, Sossick AJ, Boulton SJ, Jackson SP (2012) BRCA1-associated exclusion of 53BP1 from DNA damage sites underlies temporal control of DNA repair. J Cell Sci 125(Pt 15): 3529-3534.

Conrad S, Kunzel J, Lobrich M (2011) Sister chromatid exchanges occur in G2-irradiated cells. Cell Cycle 10(2): 222-228.

Doil C, Mailand N, Bekker-Jensen S, Menard P, Larsen DH et al. (2009) RNF168 binds and amplifies ubiquitin conjugates on damaged chromosomes to allow accumulation of repair proteins. Cell 136(3): 435-446.

Geuting V, Reul C, Lobrich M (2013) ATM release at resected double-strand breaks provides heterochromatin reconstitution to facilitate homologous recombination. PLoS Genet 9(8): e1003667.

Goodarzi AA, Kurka T, Jeggo PA (2011) KAP-1 phosphorylation regulates CHD3 nucleosome remodeling during the DNA double-strand break response. Nat Struct Mol Biol 18(7): 831-839.

Goodarzi AA, Noon AT, Deckbar D, Ziv Y, Shiloh Y et al. (2008) ATM signaling facilitates repair of DNA double-strand breaks associated with heterochromatin. Mol Cell 31(2): 167-177.

Huen MS, Grant R, Manke I, Minn K, Yu X et al. (2007) RNF8 transduces the DNA-damage signal via histone ubiquitylation and checkpoint protein assembly. Cell 131(5): 901-914.

Jackson SP, Bartek J (2009) The DNA-damage response in human biology and disease. Nature 461(7267): 1071-1078.

Kakarougkas A, Ismail A, Katsuki Y, Freire R, Shibata A et al. (2013) Co-operation of BRCA1 and POH1 relieves the barriers posed by 53BP1 and RAP80 to resection. Nucleic Acids Res.

Kolas NK, Chapman JR, Nakada S, Ylanko J, Chahwan R et al. (2007) Orchestration of the DNA-damage response by the RNF8 ubiquitin ligase. Science 318(5856): 1637-1640.

Lee JH, Goodarzi AA, Jeggo PA, Paull TT (2010) 53BP1 promotes ATM activity through direct interactions with the MRN complex. Embo J 29(3): 574-585.

Lou Z, Minter-Dykhouse K, Franco S, Gostissa M, Rivera MA et al. (2006) MDC1 maintains genomic stability by participating in the amplification of ATM-dependent DNA damage signals. Mol Cell 21(2): 187-200.

Mailand N, Bekker-Jensen S, Faustrup H, Melander F, Bartek J et al. (2007) RNF8 ubiquitylates histones at DNA double-strand breaks and promotes assembly of repair proteins. Cell 131(5): 887-900.

Mallette FA, Mattiroli F, Cui G, Young LC, Hendzel MJ et al. (2012) RNF8- and RNF168-dependent degradation of KDM4A/JMJD2A triggers 53BP1 recruitment to DNA damage sites. Embo J 31(8): 1865-1878.

Mattiroli F, Vissers JH, van Dijk WJ, Ikpa P, Citterio E et al. (2012) RNF168 ubiquitinates K13-15 on H2A/H2AX to drive DNA damage signaling. Cell 150(6): 1182-1195.

Melander F, Bekker-Jensen S, Falck J, Bartek J, Mailand N et al. (2008) Phosphorylation of SDT repeats in the MDC1 N terminus triggers retention of NBS1 at the DNA damage-modified chromatin. J Cell Biol 181(2): 213-226.

Noon AT, Shibata A, Rief N, Lobrich M, Stewart GS et al. (2010) 53BP1-dependent robust localized KAP-1 phosphorylation is essential for heterochromatic DNA double-strand break repair. Nat Cell Biol 12(2): 177-184.

Rogakou EP, Pilch DR, Orr AH, Ivanova VS, Bonner WM (1998) DNA double-stranded breaks induce histone H2AX phosphorylation on serine 139. J Biol Chem 273(10): 5858-5868.

Shiotani B, Zou L (2009) Single-stranded DNA orchestrates an ATM-to-ATR switch at DNA breaks. Mol Cell 33(5): 547-558.

Stewart GS, Panier S, Townsend K, Al-Hakim AK, Kolas NK et al. (2009) The RIDDLE syndrome protein mediates a ubiquitin-dependent signaling cascade at sites of DNA damage. Cell 136(3): 420-434.

Stucki M, Clapperton JA, Mohammad D, Yaffe MB, Smerdon SJ et al. (2005) MDC1 directly binds phosphorylated histone H2AX to regulate cellular responses to DNA double-strand breaks. Cell 123(7): 1213-1226.

Wang J, Gong Z, Chen J (2011) MDC1 collaborates with TopBP1 in DNA replication checkpoint control. J Cell Biol 193(2): 267-273.

Ziv Y, Bielopolski D, Galanty Y, Lukas C, Taya Y et al. (2006) Chromatin relaxation in response to DNA double-strand breaks is modulated by a novel ATM- and KAP-1 dependent pathway. Nat Cell Biol 8(8): 870-876.

5.7 Figure Legends

Figure 1:

(A) 2BN hTert (XLF-deficient) human fibroblasts were immunostained 15 min after irradiation (1 Gy) with the indicated antibodies, using EdU as cell cycle marker to distinguish G1- from G2-phase cells (Geuting et al. 2013) **(B)** A549 tumor cells treated with BRCA2 siRNA were irradiated with 1 Gy (0.5h) or 2 Gy (8 h) and immunostained with the indicated antibodies. BRCA2 siRNA was used in this analysis to accumulate resected DSBs **(C-E)** Focal intensities of 53BP1, MDC1 and FK2 were measured using ImageJ software as previously described in *Geuting et al 2013.* **(F)** γH2AX focal intensities from the measurements (C-E). In (C-F), at least 250 foci from 3 independent experiments were analyzed for each point. Box plots were used with a maximum whisker-length of 1.5fold the inter-quartile range; the lower and upper "x" indicated the 1% or 99% margin of the data respectively. *P* values were obtained by an one-sided *t*-test and represent a comparison of all cells analyzed in the indicated cell populations (***: $p<0.001$).

Figure 2:

(A-C) 2BN hTert (XLF-deficient) human fibroblasts were analyzed 2 h post IR with 1 Gy. Cells were stained against 53BP1, FK2 or MDC1, stained with RAD51 respectively. 53BP1, FK2 and MDC1 foci intensities were measured at RAD51-foci-positive or RAD51-foci-negative foci. XLF deficient cells were used in this analysis to prevent repair of EC DSBs during the time needed for resection of HC DSBs. At least 250 foci from 3 independent experiments were analyzed for each point. Box plots were used with a maximum whisker-length of 1.5fold the inter-quartile range; the lower and upper "x" indicated the 1% or 99% margin of the data respectively. *P* values were obtained by an one-sided *t*-test and represent a comparison of all cells analyzed in the indicated cell populations (***: $p<0.001$).

Figure 3:

(A) HeLa tumor cells were stransfected with GFP tagged MDC1-wt or phosphomimic MDC1-3E (T699E, T719E and T752E). γH2AX foci were analyzed only in GFP-positive G2-irradiated cells **(B)** SCEs were analyzed in mitotic HeLa tumor cells at 8 h post 2 Gy.

Cells were treated with caffeine and colcemid at 5 h post IR to abolish the G2 checkpoint and collect cells in mitosis. The addition of caffeine does not affect homologous recombination levels as assessed by SCE formation (Conrad et al. 2011). As cell cycle marker, cells were labeled with EdU and only EdU-negative cells (i.e. cells in G2 at the time of irradiation) were included in the analysis. At least 30 metaphases were analyzed per data point and experiment (mean ± SEM from ≥3 experiments). **(C)** HR frequencies (gene conversion) after I-SceI expression in HeLa pGC cells carrying an integrated reporter system. **(D)** γH2AX foci analysis in G2-irradiated A549 cells. **(E)** Model of focus formation at unresected and resected DSBs: At unresected breaks, ATM phosphorylates H2AX, which is bound by MDC1.and additional posphorylates MDC1 to allow RNF8 binding. RNF8 and RNF168 ubiquitinate H2A and JMJD2A. Ubiquitinated JMJD2A is degraded and allows 53BP1 binding at H4K20me2, which is needed for pATM retention at the DSB site. At resected breaks, ATR phosphorylates H2AX, but not MDC1. Thus RNF8 and 168 do not ubiquitinate JMJD2A. So JMJD2A binds to H4K20me2 and blocks 53BP1 binding.(A) and (D) G1- and G2-irradiated cells were distinguished as previously described (Geuting et al. 2013).At least 30 cells were analyzed per data point and experiment (mean ± SEM from ≥3 experiments). Background foci are subtracted. *P* values were obtained by an one-sided *t*-test and represent a comparison of all cells analyzed in the indicated cell populations (***: p<0.001).

5.8 Supporting Information

Supplementary Figure 1:

(A) Riddle hTert +HA/+RNF168 human fibroblasts were immunostained 15 min after irradiation (1 Gy) with the indicated antibodies. G1- and G2-irradiated cells were distinguished as previously described (Geuting et al. 2013) **(B)** A549 tumor cells treated with BRCA2 siRNA were irradiated with 1 Gy (0.5h) or 2 Gy (8 h) and immunostained against FK2 and γH2AX.

Supplementary Figure 2: (A) γH2AX foci analysis in G1-irradiated A549 cells. **(B)** and **(C)** Chromatid breaks and chromatid fusions measured in mitotic HeLa cells shown in Fig. 3B **(D)** HeLa tumor cells were transfected with GFP tagged MDC1 wt or phosphomimic MDC1 3D (T699E, T719E and T752E). γH2AX foci were analyszed in GFP-positive G1-irradiated

cells. (A) and (D)At least 30 cells were analyzed per data point and experiment (mean ± SEM from ≥3 experiments). Background foci are subtracted. *P* values were obtained by an one-sided *t*-test and represent a comparison of all cells analyzed in the indicated cell populations (***: $p<0.001$)

5.9 Figures

Figure 1

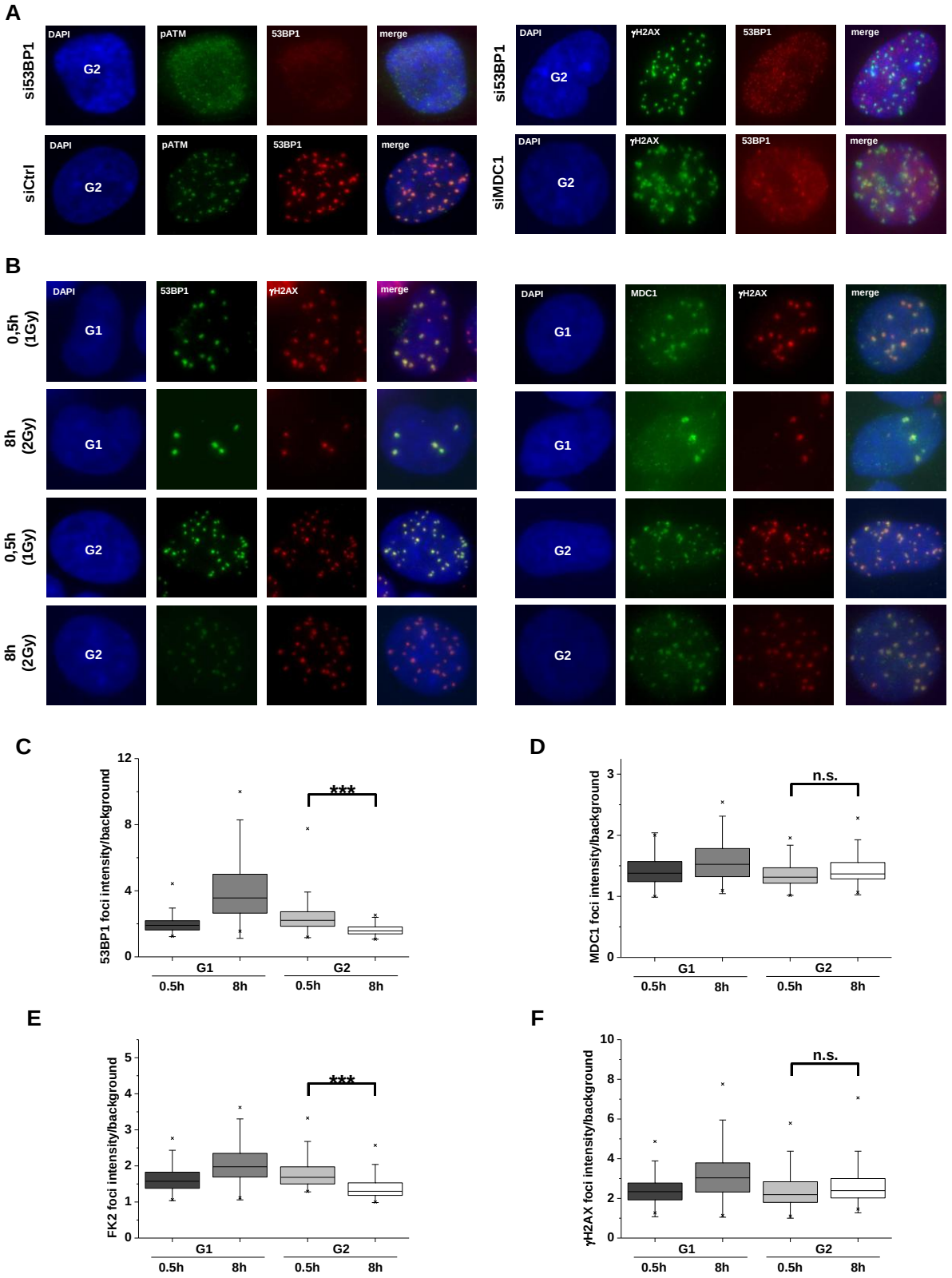

Figure 2

A

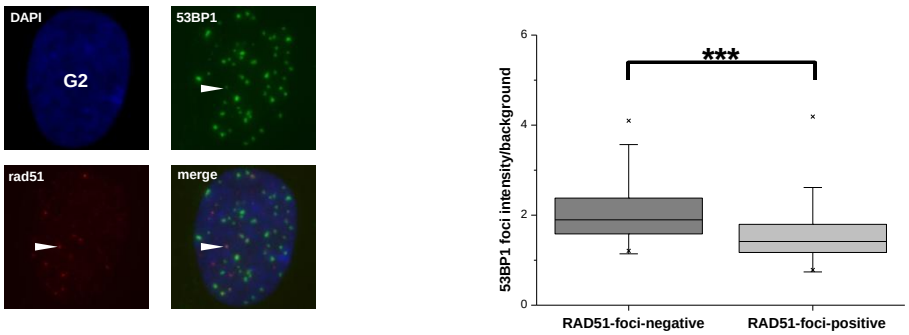
DAPI
G2
53BP1
rad51
merge
***
53BP1 foci intensity/background
0
2
4
6
RAD51-foci-negative
RAD51-foci-positive

B

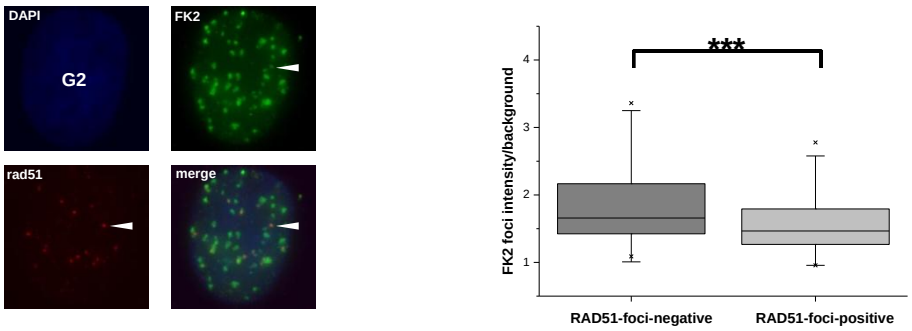
DAPI
G2
FK2
rad51
merge
***
FK2 foci intensity/background
1
2
3
4
RAD51-foci-negative
RAD51-foci-positive

C

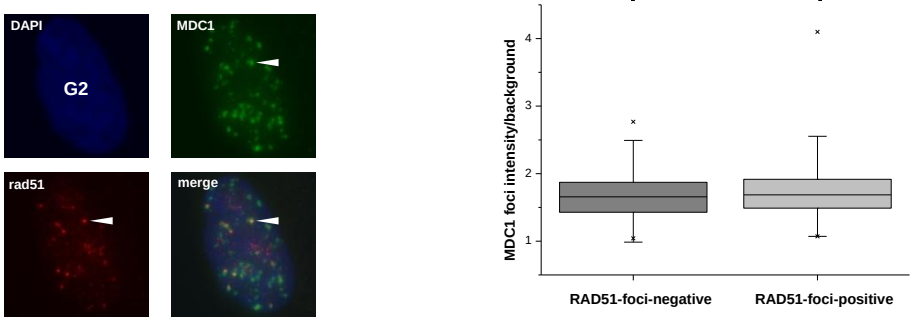
DAPI
G2
MDC1
rad51
merge
n.s.
MDC1 foci intensity/background
1
2
3
4
RAD51-foci-negative
RAD51-foci-positive

Figure 3

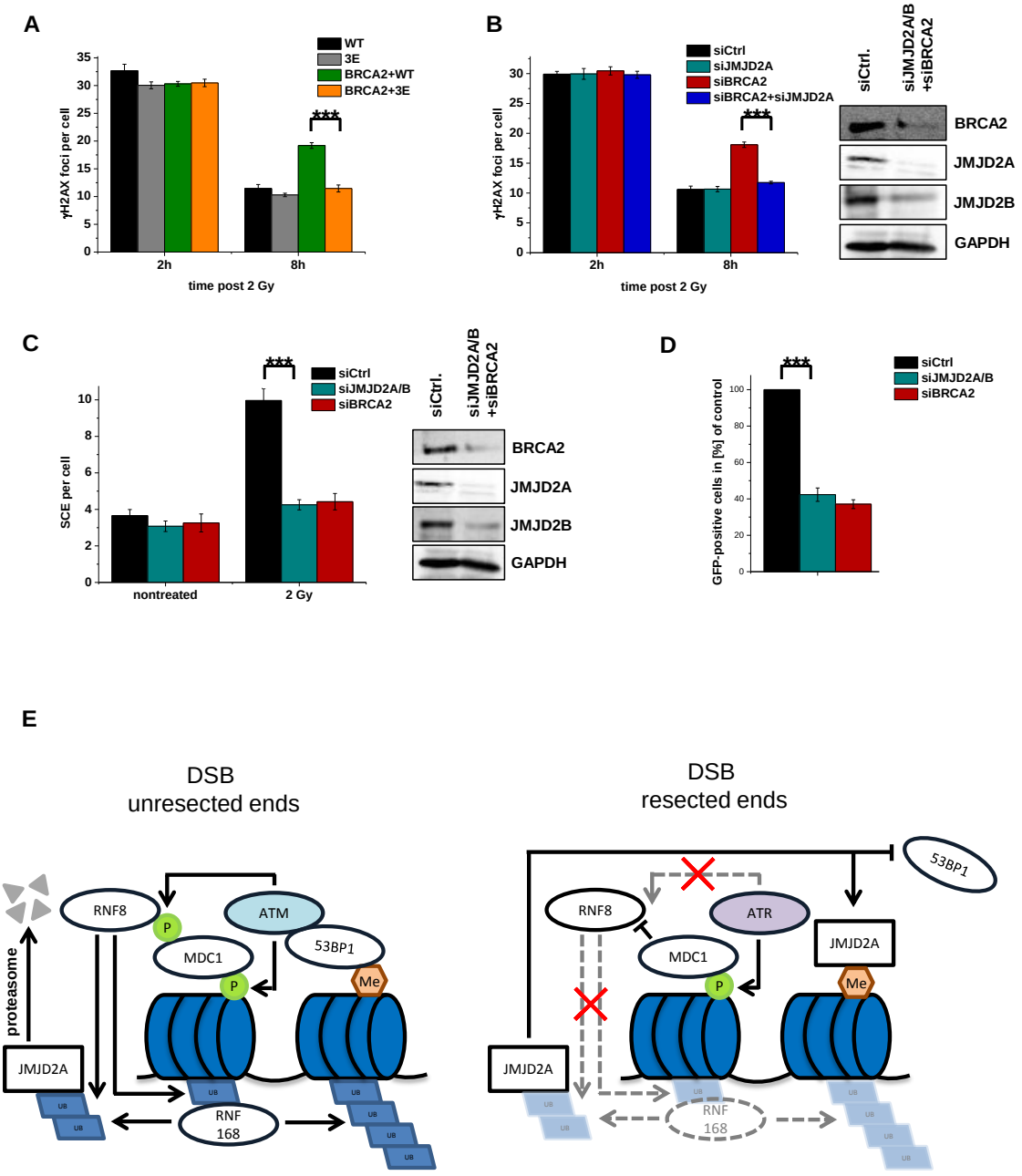
A
WT
3E
BRCA2+WT
BRCA2+3E
γH2AX foci per cell
2h
8h
time post 2 Gy
***
B
siCtrl
siJMJD2A
siBRCA2
siBRCA2+siJMJD2A
siCtrl.
siJMJD2A/B +siBRCA2
BRCA2
JMJD2A
JMJD2B
GAPDH
C
SCE per cell
nontreated
2 Gy
siJMJD2A/B
D
GFP-positive cells in [%] of control
E
DSB unresected ends
DSB resected ends
RNF8
ATM
ATR
P
MDC1
53BP1
Me
JMJD2A
proteasome
RNF 168
UB

Supplementary Figure 1

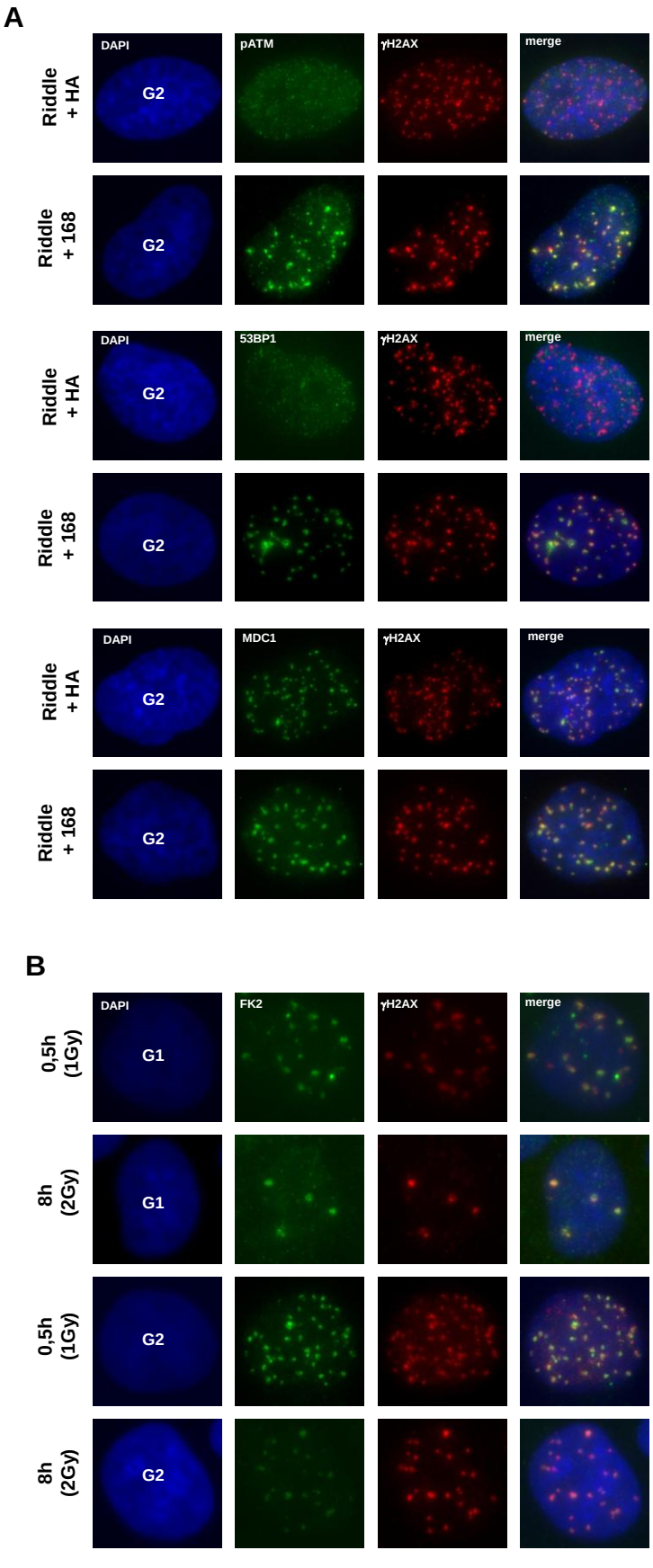

Supplementary Figure 2

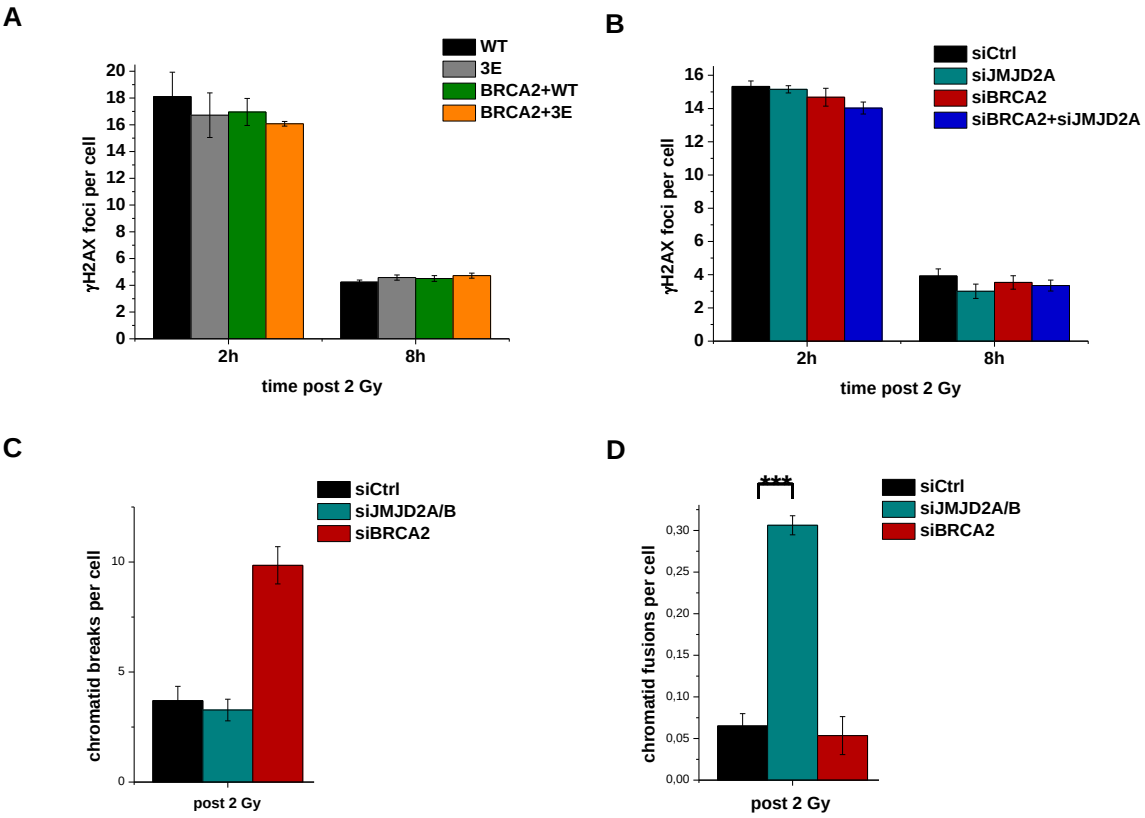

5.10 Declaration of own achievements within the publication

I designed and performed all experiments, analyzed the results and developed the model of the mechanistic reason of an ATM release at resected DSBs in collaboration with Dr. Verena Geuting and Prof. Markus Löbrich. I wrote the paper self dependent.

6 Discussion

C-NHEJ and HR are the main repair pathways in the G2-phase of the cell cycle. Both pathways and their interplay are subject of current research. The influence of the DSB surrounding chromatin on the DSB repair as well as the interplay between binding, retention and removal of repair factors and chromatin remodelers get more attention in the field.

HR involves DSB end-resection, whereas c-NHEJ works without resection. We investigated HR more precisely and found that pATM, which initially assembles and forms foci at DSBs, is released during extendend-resection. Furthermore, in the following study, we could show that the release of pATM is a consequence of the release of 53BP1, which is essential for pATM focus formation and retention. The release of 53BP1 at resected DSBs is caused by decreased RNF8/168 activity, whose activity is needed to allow 53BP1 focus formation. One target of RNF8/168 is JMJD2A, which is ubiquitinated and degraded to allow 53BP1 binding. We suggest that JMJD2A replaces 53BP1 at resected DSBs due to its higher affinity to H4K20me2 (Mallette et al. 2012). This suggestion should be verified by depletion of JMJD2A/B and measuring foci intensities at resected DSBs. If 53BP1 is replaced mainly by JMJD2A and rarely from JMJD2B, a JMJD2A/B depletion should prevent a decrease in 53BP1 foci intensities at resected DSBs. Also the amount of chromatin bound JMJD2A could be analyzed by immunoprecipitation against γH2AX before extended resection and after extended resection has taken place. If JMJD2A replaces 53BP1, the amount of coimmunoprecipitated 53BP1 should decrease from early to late times post IR, consistent to the foci data, and JMJD2A should exhibit an opposing trend.

RNF8/168 activity to allow 53BP1 binding is dependent on an ATM dependent phosphorylation of MDC1. Due to the switch from ATM to ATR activation at resected DSBs, the decreased RNF8/168 activity is a consequence of the inability of ATR to phosphorylate MDC1.

The consequence of this cascade and finally the pATM release of resected heterochromatic DSBs is a decreased KAP-1 phosphorylation at the DSB site. A decreased KAP-1 phosphorylation causes the reconstitution of the heterochromatin structure that commits resected DSBs to be repaired by HR. A direct inhibition of the heterochromatin reconstitution

by a KAP-1 depletion or using a phosphomimic form of KAP-1, causes a constantly relaxed heterochromatin structure and abolishes the commitment of resected DSBs to HR. In this case, we could show that DSBs are repaired by an alt-NHEJ mechanism that requires continous heterochromatin relaxation.

Instead of using a phosphomimic form of KAP-1, our approach was to retain ATM at the resected DSB to allow heterochromatin relaxation. The factors JMJD2A and JMJD2B compete against 53BP1 for H4K20me2 binding and are removed in a RNF8/168 dependent manner after DNA damage. Depletion of JMJD2A and JMJD2B allows RNF8/168 independent retention of 53BP1 at resected DSBs. Therefore ATM retains at resected DSBs to relax the heterochromatin structure, which abolishes the commitment of resected DSBs to HR. ATM retention at resected breaks and overcoming the commitment of resected DSBs to HR can also be achieved by expressing a phosphomimic form of MDC1. This form of MDC1 overcomes the inability of ATR to phosphorylate the ATM dependent phosphorylation site on MDC1 that RNF8/168 activity is not decreased at resected DSBs and 53BP1 and ATM are not released.

6.1 ATM release at resected DSBs is a consequence of a decrease in RNF8/168 activity

ATM has a major role in the repair of DSBs, including signaling processes and chromatin modifications. Counterintuitive to this major role, it was previously shown, that ATM is dispensable for the majority of DSBs in the G1- and the G2-phase of the cell cycle (Beucher et al. 2009). But the repair of heterochromatic DSBs is strongly dependent on ATM: in G1 by c-NHEJ and in G2 by HR (Goodarzi et al. 2008; Beucher et al. 2009). In G1 ATM phosphorylates KAP-1 continously to relax the heterochromatin and allows repair of heterochromatic DSBs (Goodarzi et al. 2011). Suprisingly, ATM was released from resected DSBs in G2, independently from the role of ATM to initiate DSB end-resection (Geuting et al. 2013). Beside the consequences of the ATM release on repair, we investigated the mechanistic reason of this release.

One of the major roles of ATM is the phosphorylation of H2AX (Rogakou et al. 1998), but we could show that the phosphorylation of H2AX at resected DSBs is independent of ATM and DNA-PK_{cs} and strongly dependent on ATR (Geuting et al. 2013). Consistent with our findings, an activation of ATM at blunt DNA ends and a switch to ATR at DNA ends with long ssDNA overhangs, as it occurs after resection, has been described in *Shiotani and Zou 2009*. The reason of an ATM release following resection is not due to a lack of γH2AX. In G1-phase cells, it has been decribed that the factors MDC1, RNF168 and 53BP1 are also essential for pATM focus formation (Noon et al. 2010). In G2 initially after IR MDC1, FK2 (as a product of RNF8 and RNF168 activity), 53BP1 and pATM form foci equal to G1-phase cells. Also the dependency, that MDC1 is needed for RNF8/168 mediated FK2 focus formation, RNF168 for 53BP1 focus formation and 53BP1 for pATM focus formation is the same for G2- and G1-phase (Mailand et al. 2007; Noon et al. 2010). Thus, after DSB induction IRIFs form with the same cascade and dependency in G1 and G2.

We could show that at resected DSBs MDC1 is not released. This is in agreement with the description, that MDC1 binds directly to the phosphate of γH2AX (Stucki et al. 2005) and γH2AX is still present due to its phosphorylation by ATR. So the reason of an ATM release at resected DSBs has to be downstream of MDC1 binding. To elucidate this, we analyzed the behavior of the product of RNF8/168 activity (FK2), which is essential for 53BP1 focus formation, which in turn accumulates ATM at the DSB site. The observed diminished FK2 and 53BP1 focus intensity is consistent with published data, where by high resolution microscopy a displacement of 53BP1 and FK2 to the periphery of the focus and a release at the resected core is shown (Chapman et al. 2012; Kakarougkas et al. 2013). An apparent conflict of both declarations can be resolved by comparing the different microscopy equipments and their results. We measured the overall intensity of a focus, whereas *Chapman et al.* and *Kakarougkas et al.* measured the distribution of the intensities within a focus. But a decrease in the core of a focus goes along with an overall decrease of focus intensity, so that both results are consistent. We could show that a potential remaining activity of pATM at the edge of a focus does not influence the heterochromatin reconstitution on a large scale to facilitate HR. This will be discussed later in detail.

6.2 Inability of ATR to phosphorylate MDC1 facilitates decrease in RNF8/168 activity

MDC1 persists at resected DSBs whereas its downstream factors 53BP1 and ATM are released. Thus, we questioned, if a modification of MDC1 might be responsible for their release. ATM phosphorylates MDC1 in its T-Q-X-F cluster to enhance RNF8 binding to start the cascade for pATM focus formation (Kolas et al. 2007; Mailand et al. 2007). But after a switch from ATM to ATR activity at resected DSBs (Shiotani and Zou 2009), the release of MDC1 downstream factors provide evidence for an inabilitiy of ATR to phosphorylate the T-Q-X-F cluster on MDC1. That means ATR can phosphorylate H2AX to allow MDC1 binding, but ATR cannot trigger the subsequent cascade. To overcome this limitation, we created a phosphomimic form of MDC1, the MDC1-3E mutant (T699E, T719E, T752E), which should be capable of triggering the cascade also at resected DSBs. By this, the release of the MDC1 downstream factors should be avoided. It was not possible to measure variations in focal intensities of 53BP1, FK2 or ATM, due to the fact that cells expressing a transfected construct already show a broad range of different foci sizes and intensities under wildtype conditions. So we used an indirect method to measure the capability of the MDC1-3E mutant to trigger the cascade and avoid the release of its downstream factors at resected DSBs. We know that one important function of assembled pATM is the phosphorylation of KAP-1 to allow efficient repair in G1. Additionally, a phosphomimic form of KAP-1 (S824D) overcomes a BRCA2 repair defect and allows repair by alt-NHEJ. Instead of a modification of KAP-1, the expression of the MDC1-3E mutant should lead to the accumulation of pATM at resected DSBs. The accumulated pATM should phosphorylate KAP-1 to allow the repair of heterochromatic DSBs in BRCA2 deficient cells by alt-NHEJ as described in *Geuting et al. 2013*. As expected, the MDC1-3E mutant overcomes the BRCA2 repair defect. We support a model, where ATR cannot phosphorylate MDC1, leading to a release of RNF8/168, 53BP1 and pATM that causes a heterochromatin reconstitution which facilitates HR.

6.3 ATM release at resected DSBs commits to HR

Cells deficient or defective in the HR factors BRCA2, XRCC3 or RAD51 have unrepaired DSBs in G2. This is remarkable, because in the G2-phase of the cell cycle, both repair pathways, NHEJ and HR, are available. A possible explanation is the incapability of NHEJ to repair DSBs with long strands of ssDNA, so that DSB end-resection commits to HR (Shibata et al. 2011).

As we further investigated resected DSBs, we could show that a downregulation of the heterochromatin building factor KAP-1 overcomes a repair defect caused by BRCA2-, XRCC3- or RAD51-deficiency and this results in normal repair kinetics. The same is observed using a phosphomimic form of KAP-1, which mimics a constitutive phosphorylation in the ATM dependent phosphorylation site, which is not phosphorylated at resected DSBs in wt cell, because ATM is released. Also, a co-depletion of JMJD2A and JMJD2B that has been described to restore 53BP1 focus formation in RNF8/168 deficient cells (Mallette et al. 2012), rescues a BRCA2 repair defect. In this case, KAP-1 is not artificially modified to a phosphomimic form, but pATM is retained at resected DSBs because 53BP1 is not released. The same effect is used by rescuing the BRCA2 repair defect by a MDC1-3E mutant that overcomes the inability of ATR to phosphorylate MDC1.

In summary, these results give a deeper insight into the repair pathway choice in the G2 phase of the cell cycle. It is not the resection step *per se* or the created ssDNA overhang, which commits the DSBs to HR. The heterochromatin reconstitution at resected DSBs commits DSBs to HR and prevents a usage of NHEJ. This constitution is a consequence of the loss of KAP-1 phosphorylation due to the ATM release at resected DSBs.

6.4 Error-prone alt-NHEJ can back-up for HR

Unrepaired DSBs in G2, caused by a depletion of BRCA2, are rescued by an additional depletion of KAP-1 or JMJD2A/B or using a phosphomimic form of KAP-1 or MDC1. They exhibit normal repair kinetics, but this is no evidence which repair pathway is used.

Due to the BRCA2 deficiency, the cells cannot repair by HR, so that a normal repair kinetic suggests a repair via an end-joining pathway. Moreover, cells depleted in BRCA2 and KAP-1 exhibit the same amount of RPA foci as wt cells, suggesting succsessful resection. The used end-joining pathway has to handle resected DSBs and a potential repair pathway could be alt-NHEJ, which has been described to use resection for DSB repair (McVey and Lee 2008). We were able to show that the rescue of a BRCA2 repair defect by KAP-1 siRNA is dependent on the alt-NHEJ factors PARP1, XRCC1 and DNA ligase I/III, but independent of the c-NHEJ factor XLF and Ku80. We also observed an enhanced number of chromosomal translocations, indicating alt-NHEJ (Simsek et al. 2011), after rescuing the BRCA2 repair defect by KAP-1 depletion. So we concluded that alt-NHEJ functions as a back-up mechanism for HR. But this back-up can only work if the heterochromatin is relaxed as it is after a KAP-1 knockdown. Also, codepletion of JMJD2A and JMJD2B rescues a BRCA2 repair defect and exhibits more chromosomal fusion events, a marker for alt-NHEJ repair. We suggest a codepletion of JMJD2A and JMJD2B prevents the ATM release from resected DSBs, so that ATM can still phosphorylate KAP-1 to relax heterochromatin structure and allow alt-NHEJ repair.

In summary, BRCA2 deficient but KAP-1 proficient cells show a repair defect that cannot be compensated by alt-NHEJ repair, because alt-NHEJ needs a relaxed heterochromatin structure, that is not present after ATM release at resected DSBs. In contrast, modifications like a phosphomimic form of KAP-1, that allows heterochromatin relaxation, will lead to a repair of DSBs by alt-NHEJ instead of HR.

6.5 KAP-1 dependent heterochromatin facilitates HR

We could show that the DSB repair pathway choice is strongly dependent on the chromatin organization/structure. It might be surprising why HR is abolished in cells, which are proficient in HR factors, but have a relaxed heterochromatin structure by KAP-1 depletion or preventing the ATM release at resected DSBs by JMJD2A and JMJD2B codepletion. Due to the dependency on PARP1, XRCC1, DNA ligase I and III, also these HR proficient cells use alt-NHEJ for the repair of heterochromatic DSBs, if the heterochromatin structure is relaxed. Furthermore, this shows that the cells cannot repair heterochromatic DSBs by HR in the absence of KAP-1. Consistent with our findings, it was shown that a knockdown of KAP-1 or HP1α leads to lower gene conversion frequencies using a HR reporter assay (Baldeyron et al. 2011). Furthermore, KAP-1 and HP1α are recruited to DSBs generated by laser- or X-irradiation (Luijsterburg et al. 2009; Zarebski et al. 2009). Taken together, heterochromatin itself is not only a barrier for c-NHEJ or alt-NHEJ repair as it is described for G1-phase cells (Goodarzi et al. 2008), moreover the heterochromatin itself even facilitates HR.

How heterochromatin facilitates HR is not clear. We support a model, where the reduced spatial distance between the sister chromatids in heterochromatic regions facilitates homology search during HR repair. Our evidence for supporting this model is the analysis of the average distance of two sister chromatids in interphase cells using FISH probes, specific for a heterochromatic region or specific for a euchromatic region. The average distance between the sister chromatids in a G2 cell is larger in euchromatic regions than in heterochromatic regions (Geuting et al., unpublished data). Furthermore, cohesin proteins, which can promote DSB repair by HR have been suggested to facilitate HR by establishing a close proximity between sister chromatids to promote the step of homology search (Watrin and Peters 2006). Another role of the heterochromatin is to exclude resected DSBs to be repaired by error-prone alt-NHEJ instead of error-free HR. Normally the heterodimer of Ku70 and Ku80 prevents the usage of alt-NHEJ (Mansour et al. 2010). After the resection step, it is likely that Ku70/80 is released from the DSB. So the cell has to prevent the usage of error-prone alt-NHEJ independently of Ku70/80. We suggest that the heterochromatin reconstitution adopts the function of Ku70/80 to prevent alt-NHEJ and to facilitate HR.

Whether the promotion of HR by facilitation of homology search or the prevention of error-prone alt-NHEJ repair is the main function of heterochromatin reconstitution or if both are equally important is yet unclear.

6.6 Consequences of the ATM release on the G2/M checkpoint

The G2/M checkpoint initiates within minutes after irradiation to prevent cells progressing into mitosis with unrepaired DSBs (Shibata et al. 2010). However, the G2/M checkpoint is abrogated, even though 10-20 DSBs are unrepaired (Deckbar et al. 2007). The mechanistic reason of this release is still unclear.

Due to the kinetics of DSB repair in G2, it is most likely that DSBs are within the process of HR repair, when the G2/M checkpoint is abrogated. The release of ATM might also affect the maintenance of the G2/M checkpoint. ATM has an important role in phosphorylation of CHK2 to initiate and maintain the checkpoint (Deckbar et al. 2011). Resection occurs in the first hours after DSB induction, leading to a switch from ATM to ATR activation and a release of chromatin bound ATM (Shiotani and Zou 2009; Geuting et al. 2013). All unresected DSBs are repaired within the first hours and this will also lead to an inactivation of ATM at the repaired DSB site. So it is most likely that in a cell at a certain time point nearly no active ATM is existent to phosphorylate and activate CHK2. It is described, that CHK2 is essential for G2/M checkpoint maintenance (Shibata et al. 2010), so that a release of ATM at resected DSBs leads to a progression of cells into mitosis with unrepaired DSBs.

Taken together, the mechanistic theory would be that ATM is activated at all DSBs, thus initiating the G2/M checkpoint and the resection of heterochromatic DSBs. Due to resection, ATR is activated and at this time ATM and ATR maintain the G2/M checkpoint over CHK1 and CHK2. Within the next hours the euchromatic DSBs are repaired and the heterochromatic DSBs are fully resected and ATM is released. This leads to an inactivation of CHK2 and the G2/M checkpoint is abrogated, due to the inability of CHK1 to maintain the G2/M checkpoint without CHK2. The cells will now progress into mitosis whether the process of HR is finished or not, which can lead to chromosomal abberations.

7 References

Acs K, Luijsterburg MS, Ackermann L, Salomons FA, Hoppe T et al. (2011) The AAA-ATPase VCP/p97 promotes 53BP1 recruitment by removing L3MBTL1 from DNA double-strand breaks. Nat Struct Mol Biol 18(12): 1345-1350.

Ahmad A, Robinson AR, Duensing A, van Drunen E, Beverloo HB et al. (2008) ERCC1-XPF endonuclease facilitates DNA double-strand break repair. Mol Cell Biol 28(16): 5082-5092.

Allen HF, Wade PA, Kutateladze TG (2013) The NuRD architecture. Cell Mol Life Sci 70(19): 3513-3524.

Bakkenist CJ, Kastan MB (2003) DNA damage activates ATM through intermolecular autophosphorylation and dimer dissociation. Nature 421(6922): 499-506.

Baldeyron C, Soria G, Roche D, Cook AJ, Almouzni G (2011) HP1alpha recruitment to DNA damage by p150CAF-1 promotes homologous recombination repair. J Cell Biol 193(1): 81-95.

Barnes DE, Stamp G, Rosewell I, Denzel A, Lindahl T (1998) Targeted disruption of the gene encoding DNA ligase IV leads to lethality in embryonic mice. Curr Biol 8(25): 1395-1398.

Bennardo N, Cheng A, Huang N, Stark JM (2008) Alternative-NHEJ is a mechanistically distinct pathway of mammalian chromosome break repair. PLoS Genet 4(6): e1000110.

Beucher A, Birraux J, Tchouandong L, Barton O, Shibata A et al. (2009) ATM and Artemis promote homologous recombination of radiation-induced DNA double-strand breaks in G2. Embo J 28(21): 3413-3427.

Blomen VA, Boonstra J (2007) Cell fate determination during G1 phase progression. Cell Mol Life Sci 64(23): 3084-3104.

Botuyan MV, Lee J, Ward IM, Kim JE, Thompson JR et al. (2006) Structural basis for the methylation state-specific recognition of histone H4-K20 by 53BP1 and Crb2 in DNA repair. Cell 127(7): 1361-1373.

Boulton SJ, Jackson SP (1996) Saccharomyces cerevisiae Ku70 potentiates illegitimate DNA double-strand break repair and serves as a barrier to error-prone DNA repair pathways. Embo J 15(18): 5093-5103.

Chapman JR, Sossick AJ, Boulton SJ, Jackson SP (2012) BRCA1-associated exclusion of 53BP1 from DNA damage sites underlies temporal control of DNA repair. J Cell Sci 125(Pt 15): 3529-3534.

Chen H, Lisby M, Symington LS (2013) RPA coordinates DNA end resection and prevents formation of DNA hairpins. Mol Cell 50(4): 589-600.

Conrad S, Kunzel J, Lobrich M (2011) Sister chromatid exchanges occur in G2-irradiated cells. Cell Cycle 10(2): 222-228.

Corneo B, Wendland RL, Deriano L, Cui X, Klein IA et al. (2007) Rag mutations reveal robust alternative end joining. Nature 449(7161): 483-486.

Daley JM, Kwon Y, Niu H, Sung P (2013) Investigations of Homologous Recombination Pathways and Their Regulation. Yale J Biol Med 86(4): 453-461.

de Jager M, van Noort J, van Gent DC, Dekker C, Kanaar R et al. (2001) Human Rad50/Mre11 is a flexible complex that can tether DNA ends. Mol Cell 8(5): 1129-1135.

Deckbar D, Jeggo PA, Lobrich M (2011) Understanding the limitations of radiation-induced cell cycle checkpoints. Crit Rev Biochem Mol Biol 46(4): 271-283.

Deckbar D, Birraux J, Krempler A, Tchouandong L, Beucher A et al. (2007) Chromosome breakage after G2 checkpoint release. J Cell Biol 176(6): 749-755.

Decottignies A (2007) Microhomology-mediated end joining in fission yeast is repressed by pku70 and relies on genes involved in homologous recombination. Genetics 176(3): 1403-1415.

DeFazio LG, Stansel RM, Griffith JD, Chu G (2002) Synapsis of DNA ends by DNA-dependent protein kinase. Embo J 21(12): 3192-3200.

Della-Maria J, Zhou Y, Tsai MS, Kuhnlein J, Carney JP et al. (2011) Human Mre11/human Rad50/Nbs1 and DNA ligase IIIalpha/XRCC1 protein complexes act together in an alternative nonhomologous end joining pathway. J Biol Chem 286(39): 33845-33853.

Doil C, Mailand N, Bekker-Jensen S, Menard P, Larsen DH et al. (2009) RNF168 binds and amplifies ubiquitin conjugates on damaged chromosomes to allow accumulation of repair proteins. Cell 136(3): 435-446.

Feldmann E, Schmiemann V, Goedecke W, Reichenberger S, Pfeiffer P (2000) DNA double-strand break repair in cell-free extracts from Ku80-deficient cells: implications for Ku serving as an alignment factor in non-homologous DNA end joining. Nucleic Acids Res 28(13): 2585-2596.

Frank KM, Sekiguchi JM, Seidl KJ, Swat W, Rathbun GA et al. (1998) Late embryonic lethality and impaired V(D)J recombination in mice lacking DNA ligase IV. Nature 396(6707): 173-177.

Gell D, Jackson SP (1999) Mapping of protein-protein interactions within the DNA-dependent protein kinase complex. Nucleic Acids Res 27(17): 3494-3502.

Geuting V, Reul C, Lobrich M (2013) ATM release at resected double-strand breaks provides heterochromatin reconstitution to facilitate homologous recombination. PLoS Genet 9(8): e1003667.

Goodarzi AA, Jeggo PA (2013) The repair and signaling responses to DNA double-strand breaks. Adv Genet 82: 1-45.

Goodarzi AA, Kurka T, Jeggo PA (2011) KAP-1 phosphorylation regulates CHD3 nucleosome remodeling during the DNA double-strand break response. Nat Struct Mol Biol 18(7): 831-839.

Goodarzi AA, Noon AT, Deckbar D, Ziv Y, Shiloh Y et al. (2008) ATM signaling facilitates repair of DNA double-strand breaks associated with heterochromatin. Mol Cell 31(2): 167-177.

Grewal SI, Elgin SC (2007) Transcription and RNA interference in the formation of heterochromatin. Nature 447(7143): 399-406.

Hall E, Giccia A (2006) Radiobiology for the Radiologist. Lippincott Williams & Wilkins.

Hammel M, Rey M, Yu Y, Mani RS, Classen S et al. (2011) XRCC4 protein interactions with XRCC4-like factor (XLF) create an extended grooved scaffold for DNA ligation and double strand break repair. J Biol Chem 286(37): 32638-32650.

Huen MS, Grant R, Manke I, Minn K, Yu X et al. (2007) RNF8 transduces the DNA-damage signal via histone ubiquitylation and checkpoint protein assembly. Cell 131(5): 901-914.

Iliakis G (2009) Backup pathways of NHEJ in cells of higher eukaryotes: cell cycle dependence. Radiother Oncol 92(3): 310-315.

Iliakis G, Wang Y, Guan J, Wang H (2003) DNA damage checkpoint control in cells exposed to ionizing radiation. Oncogene 22(37): 5834-5847.

Jackson SP, Bartek J (2009) The DNA-damage response in human biology and disease. Nature 461(7267): 1071-1078.

Kaidi A, Jackson SP (2013) KAT5 tyrosine phosphorylation couples chromatin sensing to ATM signalling. Nature 498(7452): 70-74.

Kakarougkas A, Ismail A, Katsuki Y, Freire R, Shibata A et al. (2013) Co-operation of BRCA1 and POH1 relieves the barriers posed by 53BP1 and RAP80 to resection. Nucleic Acids Res.

Kastan MB, Lim DS (2000) The many substrates and functions of ATM. Nat Rev Mol Cell Biol 1(3): 179-186.

Koff A, Giordano A, Desai D, Yamashita K, Harper JW et al. (1992) Formation and activation of a cyclin E-cdk2 complex during the G1 phase of the human cell cycle. Science 257(5077): 1689-1694.

Kolas NK, Chapman JR, Nakada S, Ylanko J, Chahwan R et al. (2007) Orchestration of the DNA-damage response by the RNF8 ubiquitin ligase. Science 318(5856): 1637-1640.

Lee JH, Goodarzi AA, Jeggo PA, Paull TT (2010) 53BP1 promotes ATM activity through direct interactions with the MRN complex. Embo J 29(3): 574-585.

Lou Z, Minter-Dykhouse K, Franco S, Gostissa M, Rivera MA et al. (2006) MDC1 maintains genomic stability by participating in the amplification of ATM-dependent DNA damage signals. Mol Cell 21(2): 187-200.

Luijsterburg MS, Dinant C, Lans H, Stap J, Wiernasz E et al. (2009) Heterochromatin protein 1 is recruited to various types of DNA damage. J Cell Biol 185(4): 577-586.

Mailand N, Bekker-Jensen S, Faustrup H, Melander F, Bartek J et al. (2007) RNF8 ubiquitylates histones at DNA double-strand breaks and promotes assembly of repair proteins. Cell 131(5): 887-900.

Mallette FA, Mattiroli F, Cui G, Young LC, Hendzel MJ et al. (2012) RNF8- and RNF168-dependent degradation of KDM4A/JMJD2A triggers 53BP1 recruitment to DNA damage sites. Embo J 31(8): 1865-1878.

Mansour WY, Rhein T, Dahm-Daphi J (2010) The alternative end-joining pathway for repair of DNA double-strand breaks requires PARP1 but is not dependent upon microhomologies. Nucleic Acids Res 38(18): 6065-6077.

Mattiroli F, Vissers JH, van Dijk WJ, Ikpa P, Citterio E et al. (2012) RNF168 ubiquitinates K13-15 on H2A/H2AX to drive DNA damage signaling. Cell 150(6): 1182-1195.

Mazon G, Mimitou EP, Symington LS (2010) SnapShot: Homologous recombination in DNA double-strand break repair. Cell 142(4): 646, 646 e641.

McVey M, Lee SE (2008) MMEJ repair of double-strand breaks (director's cut): deleted sequences and alternative endings. Trends Genet 24(11): 529-538.

Meek K, Douglas P, Cui X, Ding Q, Lees-Miller SP (2007) trans Autophosphorylation at DNA-dependent protein kinase's two major autophosphorylation site clusters facilitates end processing but not end joining. Mol Cell Biol 27(10): 3881-3890.

Melander F, Bekker-Jensen S, Falck J, Bartek J, Mailand N et al. (2008) Phosphorylation of SDT repeats in the MDC1 N terminus triggers retention of NBS1 at the DNA damage-modified chromatin. J Cell Biol 181(2): 213-226.

Mimitou EP, Symington LS (2009) DNA end resection: many nucleases make light work. DNA Repair (Amst) 8(9): 983-995.

Mladenov E, Iliakis G (2011) Induction and repair of DNA double strand breaks: the increasing spectrum of non-homologous end joining pathways. Mutat Res 711(1-2): 61-72.

Noon AT, Shibata A, Rief N, Lobrich M, Stewart GS et al. (2010) 53BP1-dependent robust localized KAP-1 phosphorylation is essential for heterochromatic DNA double-strand break repair. Nat Cell Biol 12(2): 177-184.

Panier S, Durocher D (2013) Push back to respond better: regulatory inhibition of the DNA double-strand break response. Nat Rev Mol Cell Biol 14(10): 661-672.

Riballo E, Kuhne M, Rief N, Doherty A, Smith GC et al. (2004) A pathway of double-strand break rejoining dependent upon ATM, Artemis, and proteins locating to gamma-H2AX foci. Mol Cell 16(5): 715-724.

Rogakou EP, Pilch DR, Orr AH, Ivanova VS, Bonner WM (1998) DNA double-stranded breaks induce histone H2AX phosphorylation on serine 139. J Biol Chem 273(10): 5858-5868.

Rothkamm K, Kruger I, Thompson LH, Lobrich M (2003) Pathways of DNA double-strand break repair during the mammalian cell cycle. Mol Cell Biol 23(16): 5706-5715.

Ryan RF, Schultz DC, Ayyanathan K, Singh PB, Friedman JR et al. (1999) KAP-1 corepressor protein interacts and colocalizes with heterochromatic and euchromatic HP1 proteins: a potential role for Kruppel-associated box-zinc finger proteins in heterochromatin-mediated gene silencing. Mol Cell Biol 19(6): 4366-4378.

Sartori AA, Lukas C, Coates J, Mistrik M, Fu S et al. (2007) Human CtIP promotes DNA end resection. Nature 450(7169): 509-514.

Savic V, Yin B, Maas NL, Bredemeyer AL, Carpenter AC et al. (2009) Formation of dynamic gamma-H2AX domains along broken DNA strands is distinctly regulated by ATM and MDC1 and dependent upon H2AX densities in chromatin. Mol Cell 34(3): 298-310.

Shibata A, Barton O, Noon AT, Dahm K, Deckbar D et al. (2010) Role of ATM and the damage response mediator proteins 53BP1 and MDC1 in the maintenance of G(2)/M checkpoint arrest. Mol Cell Biol 30(13): 3371-3383.

Shibata A, Conrad S, Birraux J, Geuting V, Barton O et al. (2011) Factors determining DNA double-strand break repair pathway choice in G2 phase. Embo J 30(6): 1079-1092.

Shiotani B, Zou L (2009) Single-stranded DNA orchestrates an ATM-to-ATR switch at DNA breaks. Mol Cell 33(5): 547-558.

Simsek D, Brunet E, Wong SY, Katyal S, Gao Y et al. (2011) DNA ligase III promotes alternative nonhomologous end-joining during chromosomal translocation formation. PLoS Genet 7(6): e1002080.

Singleton BK, Torres-Arzayus MI, Rottinghaus ST, Taccioli GE, Jeggo PA (1999) The C terminus of Ku80 activates the DNA-dependent protein kinase catalytic subunit. Mol Cell Biol 19(5): 3267-3277.

Stewart GS, Panier S, Townsend K, Al-Hakim AK, Kolas NK et al. (2009) The RIDDLE syndrome protein mediates a ubiquitin-dependent signaling cascade at sites of DNA damage. Cell 136(3): 420-434.

Stucki M, Clapperton JA, Mohammad D, Yaffe MB, Smerdon SJ et al. (2005) MDC1 directly binds phosphorylated histone H2AX to regulate cellular responses to DNA double-strand breaks. Cell 123(7): 1213-1226.

van Gent DC, van der Burg M (2007) Non-homologous end-joining, a sticky affair. Oncogene 26(56): 7731-7740.

Walker JR, Corpina RA, Goldberg J (2001) Structure of the Ku heterodimer bound to DNA and its implications for double-strand break repair. Nature 412(6847): 607-614.

Wang J, Gong Z, Chen J (2011) MDC1 collaborates with TopBP1 in DNA replication checkpoint control. J Cell Biol 193(2): 267-273.

Wang M, Wu W, Wu W, Rosidi B, Zhang L et al. (2006) PARP-1 and Ku compete for repair of DNA double strand breaks by distinct NHEJ pathways. Nucleic Acids Res 34(21): 6170-6182.

Ward JF (1988) DNA damage produced by ionizing radiation in mammalian cells: identities, mechanisms of formation, and reparability. Prog Nucleic Acid Res Mol Biol 35: 95-125.

Watrin E, Peters JM (2006) Cohesin and DNA damage repair. Exp Cell Res 312(14): 2687-2693.

Weinstock DM, Brunet E, Jasin M (2007) Formation of NHEJ-derived reciprocal chromosomal translocations does not require Ku70. Nat Cell Biol 9(8): 978-981.

Wilson TE, Grawunder U, Lieber MR (1997) Yeast DNA ligase IV mediates non-homologous DNA end joining. Nature 388(6641): 495-498.

Wu L, Hickson ID (2003) The Bloom's syndrome helicase suppresses crossing over during homologous recombination. Nature 426(6968): 870-874.

Wyatt HD, Sarbajna S, Matos J, West SC (2013) Coordinated actions of SLX1-SLX4 and MUS81-EME1 for holliday junction resolution in human cells. Mol Cell 52(2): 234-247.

Xiao TZ, Bhatia N, Urrutia R, Lomberk GA, Simpson A et al. (2011) MAGE I transcription factors regulate KAP1 and KRAB domain zinc finger transcription factor mediated gene repression. PLoS One 6(8): e23747.

You Z, Chahwan C, Bailis J, Hunter T, Russell P (2005) ATM activation and its recruitment to damaged DNA require binding to the C terminus of Nbs1. Mol Cell Biol 25(13): 5363-5379.

Zarebski M, Wiernasz E, Dobrucki JW (2009) Recruitment of heterochromatin protein 1 to DNA repair sites. Cytometry A 75(7): 619-625.

Zha S, Alt FW, Cheng HL, Brush JW, Li G (2007) Defective DNA repair and increased genomic instability in Cernunnos-XLF-deficient murine ES cells. Proc Natl Acad Sci U S A 104(11): 4518-4523.

Ziv Y, Bielopolski D, Galanty Y, Lukas C, Taya Y et al. (2006) Chromatin relaxation in response to DNA double-strand breaks is modulated by a novel ATM- and KAP-1 dependent pathway. Nat Cell Biol 8(8): 870-876.

8 Appendix

8.1 Publications

Geuting V, Reul C and Löbrich M (2013) ATM Release at Resected Double-Strand Breaks Provides Heterochromatin Reconstitution to Facilitate Homologous Recombination.

PLoS Genet 9(8): e1003667. doi:10.1371/journal.pgen.1003667

8.1.1 Oral presentation

Reul C, Geuting V, and Löbrich M (2013)

ATM Release at Resected Double-Strand Breaks Provides Heterochromatin Reconstitution to Facilitate Homologous Recombination.

Ataxia-Telangiectasia Workshop, Birmingham, UK

Reul C, Geuting V, and Löbrich M (2013)

Geschlossenes Chromatin unterstützt die Homologe Rekombination

1. Projektstatusgespräch zur BMBF geförderten Nuklearen Sicherheitsforschung, Karlsruhe, Germany

Reul C, Geuting V, and Löbrich M (2011)

The impact of chromatinstatus and end-resection on double-strandbreak repair in G2-phase.

GBS Jahrestagung, Cologne, Germany

8.1.2 Poster presentation

Reul C, Geuting V, and Löbrich M (2013)

ATM Release at Resected Double-Strand Breaks Provides Heterochromatin Reconstitution to Facilitate Homologous Recombination.

EMBO Conference, Cape Sounio, Greece

Reul C, Geuting V, and Löbrich M (2013)

ATM Release at Resected Double-Strand Breaks Provides Heterochromatin Reconstitution to Facilitate Homologous Recombination.

GBS Jahrestagung, Darmstadt, Germany

Reul C, Barton O, Naumann SC, and Löbrich M (2010)

The influence of endresection by CtIP on the Artemis dependent DNA double-strand break repair pathway in G1 and G2 phase

GBS Jahrestagung, Hamburg, Germany

8.1.3 Awards

Poster Award for

Reul C, Geuting V, and Löbrich M (2013)

ATM Release at Resected Double-Strand Breaks Provides Heterochromatin Reconstitution to Facilitate Homologous Recombination.

GBS Jahrestagung, Darmstadt, Germany

Travelling stipendium for

Reul C, Geuting V, and Löbrich M (2011)

The impact of chromatinstatus and end-resection on double-strandbreak repair in G2-phase.

GBS Jahrestagung, Cologne, Germany

8.2 Curriculum vitae

Name	Christian Reul
Birthday	29.03.1985
Birthplace	Frankfurt/Main

Graduation

Since 04/2010	TU Darmstadt
	Radiation Biology and DNA Repair In the group of Prof. Löbrich
Since 04/2011	Fellow in Graduate college 1657, including retreats and oral presentations

Study

10/2005-01/2010	TU Darmstadt
	Discipline: Biology
	Graduation: Diplom

School

08/1995-06/2004	Liebigschule Frankfurt
	Graduation: Abitur
07/1991-07/1995	Franckeschule Frankfurt